AD NUMBER

AD872815

NEW LIMITATION CHANGE

TO

Approved for public release, distribution unlimited

FROM

Distribution authorized to U.S. Gov't. agencies and their contractors; Critical Technology; APR 1970. Other requests shall be referred to Army Aviation Materiel Laboratory, Fort Eustis, VA 23604.

AUTHORITY

usaamrdl, ltr, 18 jun 1971

AD

USAAVLABS TECHNICAL REPORT 70-24

AN INVESTIGATION OF THE STRUCTURAL DYNAMICS
OF HELICOPTER ROTORS

By

Raymond A. Piziali

AUG 17 1970

April 1970

U. S. ARMY AVIATION MATERIEL LABORATORIES
FORT EUSTIS, VIRGINIA

CONTRACT DAAJ02-67-C-0099

CORNELL AERONAUTICAL LABORATORY, INC.

BUFFALO, NEW YORK

129

Disclaimers

The findings in this report are not to be construed as an official Department of the Army position unless so designated by other authorized documents.

When Government drawings, specifications, or other data are used for any purpose other than in connection with a definitely related Government procurement operation, the United States Government thereby incurs no responsibility nor any obligation whatsoever; and the fact that the Government may have formulated, furnished, or in any way supplied the said drawings, specifications, or other data is not to be regarded by implication or otherwise as in any manner licensing the holder or any other person or corporation, or conveying any rights or permission, to manufacture, use, or sell any patented invention that may in any way be related thereto.

Disposition Instructions

Destroy this report when no longer needed. Do not return it to the originator.

DISCLAIMER NOTICE
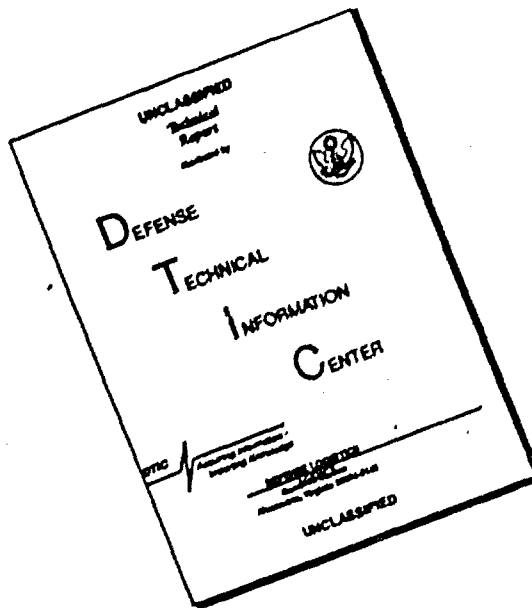
THIS DOCUMENT IS BEST QUALITY AVAILABLE. THE COPY FURNISHED TO DTIC CONTAINED A SIGNIFICANT NUMBER OF PAGES WHICH DO NOT REPRODUCE LEGIBLY.

DEPARTMENT OF THE ARMY
HEADQUARTERS US ARMY AVIATION MATERIEL LABORATORIES
FORT EUSTIS. VIRGINIA 23604

This report has been reviewed by the U. S. Army Aviation Materiel Laboratories and is considered to be technically sound. The report is published for the dissemination of information and consideration in future rotary-wing research and development.

AN INVESTIGATION OF THE STRUCTURAL DYNAMICS
OF HELICOPTER ROTORS

Final Report

By
Raymond A. Piziali

Prepared by
Cornell Aeronautical Laboratory, Inc.
Buffalo, New York

for

U. S. ARMY AVIATION MATERIEL LABORATORIES
FORT EUSTIS, VIRGINIA

ABSTRACT

An analysis and computational procedure has been developed for predicting the natural vibration modes and frequencies of rotor blade and hub systems. This method is capable of treating rotor systems which are of a general configuration and of including configuration variables which are normally neglected.

An experimental apparatus and a testing technique have been developed for obtaining the experimental data necessary to verify the analytical procedure. This apparatus and the technique are capable of determining the natural vibration modes and frequencies of two-bladed rotor systems of a very general configuration while operating in the absence of aerodynamic loads. An initial test program with the apparatus was conducted to determine the adequacy of the equipment. The tests not only demonstrated the capability of the equipment and test procedure but also revealed a problem with extrinsic excitation of the test rotor at frequencies other than the shaking frequency. Recommendations are made for modifications to the system and the techniques in order to reduce the levels of these extraneous excitations and to minimize their effects.

The computed and measured spanwise moment distributions and the corresponding natural frequencies are presented for six of the natural vibration modes of the test rotor at several rotational speeds. The theoretical and experimental results are compared, and their differences are discussed.

The model rotor used in these initial tests was intended to be so simple as to be representable by the classical uniform uncoupled beam. Because the theory for this classical configuration is well established, the differences between the measured and computed results were to be assigned to the experiment. However, the results of the tests indicate that the test rotor could not be adequately represented by the classical uniform uncoupled beam, especially in the higher frequency natural vibration modes.

iii

FOREWORD

The technical effort reported herein was conducted at Cornell Aeronautical Laboratory, Inc., during the period June 1967 to October 1969. Mr. Raymond A. Piziali was the project engineer. The program was sponsored by the U. S. Army Aviation Materiel Laboratories and was administered by Mr. William E. Nettles. The authority for this effort was DA Task 1F162204A13904.

TABLE OF CONTENTS

TABLE OF CONTENTS (Cont'd)

LIST OF ILLUSTRATIONS

LIST OF SYMBOLS

A — effective area of blade cross section for carrying axial tension

A_1, A_2, A_3 — coefficients in equations for oscillating moments

A, B, C — constants used in expressions for elastic restoring moments

a_x, a_y, a_z — components of the absolute acceleration of a mass point

a_{ij} — element of $[a]$ matrix

C_{ij} — element of $[C]$ matrix

$x.z.$ — axis of built-in twist

C_o — distance of pitch axis above x_z-axis or vertical offset of pitch axis

C_y, C_z — the y and z coordinates of the center of mass of section in undeformed blade

D_1, D_2, D_3 — coefficients in equations for oscillatory moments

D_q, D_r — coefficients of $\dot{\beta}_z$ in Equation (21)

c_y, c_z — the y and z coordinates of the local axis of built-in twist of the undeformed blade

d_1, d_2 — components perpendicular and parallel to the chord of the distance from the blade z-axis to the built-in twist axis

ds — infinitesimal distance along an elementary beam fiber

E — Young's modulus of elasticity

E_1, E_2 — coefficients used for determining components of deflections of elastic axis due to torsion

E_{ij} — element of elastic matrix $[E]$

EA — axial stiffness of blade

EB_1, EB_2 — section stiffness constants

x

EI_1, EI_2	bending stiffnesses about axes which pass through the centroid and are parallel and perpendicular to the blade chord respectively
e_A	distance of centroid forward of elastic center
e_D	distance of lead-lag hinge forward of x_2-axis
e_{DP}	distance of pitch hinge axis forward of x_3-axis
e_P	$\equiv e_D + e_{DP}$
e_t	distance of built-in twist axis forward of elastic center
e_y, e_z	y and z coordinates of elastic center for the undeformed blade condition or for a condition including steady deformations
e_1, e_2	components of local elastic axis position measured perpendicular to and parallel to blade chord
e.c.	elastic center
F_i	element of column matrix $\{F\}$
$F_p, F_q, \ldots$	coefficients of $\dot{\beta}_F$ in Equation (21)
F_{ij}	element of mass matrix $[F]$
GJ	torsional stiffness
k_A	polar radius of gyration about the elastic axis of cross-sectional area effective in carrying tensile stresses
k	polar radius of gyration of mass about elastic axis $(k^2 = k_1^2 + k_2^2)$
k_1, k_2	mass radii of gyration about the chord and about an axis perpendicular to the chord and passing through the elastic axis
l	length of blade spanwise segment or bay
M_1	flapwise bending moment (positive when it tends to compress upper fibers)

xi

M_2	chordwise bending moment about an axis passing through elastic axis (positive when it tends to compress fibers at leading edge)
m	blade mass per unit span (also used for mass of a blade segment or bay)
mK	polar moment of inertia per unit span about x-axis (undeformed blade)
mK_1, mK_2	mass moments of inertia of undeformed blade section about the local section y- and z-axes respectively
mH	product of inertia of undeformed blade section with respect to the local section y- and z-axes
$\bar{P}_x$, $\bar{P}_y$, $\bar{P}_z$	components of the total load acting on the outboard end of a blade segment
$\bar{P}_a$, $\bar{P}_b$	force components on outboard end of segment normal and parallel to chord respectively
p, q, r	angular velocity components of the xyz system in the x, y and z directions respectively
p_i, q_i, r_i	angular velocity components of the $O_i x_i y_i z_i$ system in the x_i, y_i, z_i directions respectively
$\bar{p}_x$, $\bar{p}_y$, $\bar{p}_z$	components of combined steady and oscillatory blade inertia force loadings per unit span (referred to axes parallel to the blade reference system which have been displaced along the x-axis to the blade section)
$\bar{p}_a$, $\bar{p}_b$	components of inertia force loading which are perpendicular and parallel to undeformed blade chord respectively
Q	torque about elastic axis
$\bar{Q}_x$, $\bar{Q}_y$, $\bar{Q}_z$	components of the total applied moment on section at outboard end of bay (referred to axes obtained by translating reference system along x-axis to section)

$\bar{Q}_a, \bar{Q}_b$	moment components obtained by resolving $\bar{Q}_y$ and $\bar{Q}_y$ into components which are parallel and perpendicular to the blade chord
$\bar{Q}_{x(r)}, \bar{Q}_{y(r)}, \bar{Q}_{3(r)}$	components of applied moments within bay
$\tilde{Q}_a, \tilde{Q}_b, \tilde{Q}_x$	components of the steady moment on the outboard end of a blade segment acting respectively about the blade chord (positive aft), the normal to the blade chord which passes through the elastic axis (positive up), and an axis parallel to the x-axis which passes through the intersection of the blade chord and the elastic axis
$\bar{\dot{q}}_x, \bar{q}_y, \bar{q}_3$	component of total inertia moment loading per unit span referred to a local axis system which is parallel to the $xy3$ system and whose origin is in the blade section
$\bar{q}_a, \bar{q}_b$	components of inertia moment loading per unit span obtained by resolving $\bar{q}_y$ and $\bar{q}_y$ into components parallel and perpendicular to blade chord
R_{ij}	element of transformation matrix $[R]$
r	$\equiv r_p + x_o$ (approximate radial distance from rotor shaft to blade section)
r_D	$\equiv r_F + r_{FD}$ (approximate radial offset of lead-lag hinge)
r_p	$\equiv r_F + r_{FD} + r_{DP}$ (approximate distance from shaft to origin of blade axis system)
r_F	flapping hinge offset
r_{DP}	distance of origin of blade reference axis system outboard of lead-lag hinge
r_{FD}	distance of lead-lag hinge outboard of flapping hinge
S_p, S_q	coefficients of Ω in Equation (21)
s	distance inboard of outboard end of a bay
T	total tension load in blade

$\dot{u}, \dot{v}, \dot{w}$	translational velocity components of the origin of the xyz system in the x, y, and z directions respectively
$\dot{u}_i, \dot{v}_i, \dot{w}_i$	linear velocity components of the origin of the ith coordinate system in the x_i, y_i, z_i directions
V_x, V_y, V_z	components of the absolute velocity of a mass point in the x, y, and z directions respectively
u	displacement of the centroid of a section in the x direction
v, w	displacement of elastic center in y and z directions respectively due to bending of blade
v_z, w_z	displacement of elastic center in y and z directions respectively due to the combined effect of bending and torsional deformations
x, y, z	coordinates relative to blade reference axes
x_i, y_i, z_i	coordinates relative to i^{th} coordinate system
α_{ij}	element of $[\alpha]$ matrix which relates root and tip variables
β	built-in twist angle of blade for unloaded condition or twist angle including steady deformations
β_D	blade lead-lag angle
β_F	flapping angle
β_P	blade root pitch angle
$\{\Delta\}$	column matrix of variables
$\Delta y, \Delta z$	y and z displacements of elastic axis due to torsional deformation
δ_1, δ_2	components of elastic axis deflection due to bending deformation measured perpendicular and parallel to blade chord
$\delta_{1_t}, \delta_{2_t}$	components of total elastic axis deflection measured perpendicular and parallel to blade chord (includes combined effects of bending and torsion)

ϵ	longitudinal tensile strain in fiber
$\epsilon_T = \frac{T}{EA}$	strain due to tension
ζ	distance of point in blade section above and perpendicular to blade chord
η	$= e_t + \tilde{\eta}$ = distance forward of elastic center
$\tilde{\eta}$	distance of point in blade section forward of axis of twist
η_c	distance of center of mass of section forward of elastic center
θ_A	azimuth angle of the x-axis in the $x_5 y_5 z_5$ system
θ_E	elevation angle of the x-axis in the $x_5 y_5 z_5$ system
$\lambda_1, \lambda_2, \lambda_3$	coefficients in equations for oscillatory moments
ρ	local mass density of blade
r_{ij}	element in the matrix $[\, r \,]$ relating vectors in the xyz and $x_5 y_5 z_5$ systems
ϕ	torsional displacement of blade section
ψ	azimuth angle
Ω	constant rotational speed
$\overline{(\,)}$	$\equiv \hat{(\,)} + (\,) =$ total value of a variable
	$(\,)$ oscillatory component of a variable
	$\hat{(\,)}$ nonoscillatory or steady component of a variable (the caret symbol is also used to indicate dummy variables in some definite integrals)
$(\,)'$	$= \frac{d(\,)}{d x_o}$ (primes denote differentiation with respect to x_o)
$\dot{(\,)}$	$= \frac{d(\,)}{dt}$ (dots denote derivatives with respect to time)

xv

$( )_o$ subscript o denotes the value of a quantity in the unloaded condition prior to deformation of the blade

$( )^i$ superscript i indicates the value of a parameter in the bay inboard of $r = r^i$

$( )_{oscil.}$ the subscript $oscil.$ is used for the oscillatory component of a variable. This subscript is omitted in the latter part of the development.

INTRODUCTION

The structural dynamic characteristics of helicopter rotors have a significant influence on the vibratory loadings experienced by the rotor, the control system, the fuselage, and fuselage contents. Thus, the ability of the designer to predict adequately these dynamic characteristics is essential for minimization of the vibratory loads experienced by the aircraft and its components.

The many configuration variables and physical parameters of the blade and rotor system apparently provide the designer with a great latitude to the layout of a new rotor for satisfying the various performance and structural integrity requirements. In practice, however, the uncertainties involved in the predictions of the aerodynamic loads and structural characteristics encourage an extremely conservative approach in which maximum use is made of features which have previously proved to be satisfactory to the particular manufacturer.

Extremely conservative practices with regard to rotor design have been justified on the grounds that changes to the geometry or elastic characteristics of the rotor would change the aerodynamic forces in an unpredictable way. Consequently, radical departures from established successful rotor systems have been avoided. A fair amount of evidence suggests that this judgment has been correct. Recent developments in the aerodynamic theory of rotor blades and the beginning of an understanding of tip effects suggest that aerodynamic forces are now sufficiently predictable to encourage a more precise approach to blade layout. There is a corresponding need, however, for the establishment of a validated structural dynamics theory that will permit the combining of the new developments in aerodynamics with reliable structural and stability analyses to arrive at rotor designs that satisfy a number of simultaneously imposed constraints. The effort reported herein is the first phase of a program initiated to develop and validate a reliable method for predicting the structural dynamics of rotor systems.

At the present time, blade articulation is largely a matter of individual company practice, and the particular methods of attachment and hinge arrangement have evolved from cut- and-try procedures. The distribution of structural material reflects stress-level estimates, and the resulting blade designs tend to have some variations in the mass and elastic characteristics which are generally ignored in current vibration analyses. For example, the use of bonded doubler skins, particularly in the vicinity of the blade root, can introduce shifts in the elastic-axis location. Also, point forces, such as those introduced through a pitch-control horn, usually are neglected in the estimation of rotor and blade dynamic characteristics. Finally, there are virtually no quantitative data which would permit the evaluation of structural dynamic analysis methods of rotor and blades under the ideal condition assumed in their development--that is, in the absence of all aerodynamic loads.

1

One purpose of this effort, then, was to develop an analytical procedure for predicting the natural vibration modes and frequencies of representative helicopter rotor systems (operating in the absence of aerodynamic loads) of general configuration. The other purpose of this effort was to develop an experimental apparatus and a test techniq e for obtaining data to verify the analytical method.

The analytical procedure which has been developed is a generalization of the associated matrix analysis technique (reported, for example, in References 1 and 2). The theoretical effort was largely devoted to the derivation of expressions for the inertia loadings and elastic restoring moments (used to define the elements of the mass and elastic matrices) for a rotor and blade of a very general configuration. The analytical procedure includes the effects of the following rotor parameters:

1. Nonuniform mass and torsional inertia distributions.

2. Nonuniform flapwise, edgewise, and torsional stiffness distributions.

3. Built-in twist.

4. Mean bent shape.

5. Noncoincident and nonstraight cross-section c.g., centroid, and elastic axes which do not pass through the rotor axis of rotation.

6. Details of articulation including:

   a. Root fixities.

   b. Radial and chordwise hinge offsets.

   c. Hinge inclinations.

   d. Pitch-horn location (point forces).

   e. Pitch-axis offset and inclination.

The experimental effort was largely devoted to the design, fabrication, and installation in a vacuum tank of a rotating shaker system and rotor drive and support system. The initial experimental investigation reported herein was intended primarily to establish the adequacy of the apparatus. This was to be accomplished by measuring the natural vibration modes and frequencies of a model rotor system intended to be simple enough to be adequately represented by the classical uniform uncoupled beam. Because the theory for the dynamic response of this classical configuration is sufficiently well established,

2

any differences between the measured and computed results could presumably be assigned to the experiment.   The results of these tests and comparisons with the simple theory are presented and discussed.

THEORETICAL DEVELOPMENT

INTRODUCTION

It is the purpose of this analysis to develop a method for predicting the natural vibration modes and frequencies (in the absence of aerodynamic loads) of rotor blades which are of a general configuration. The analysis will allow for the combined elastic and rigid body motions of the blades, arbitrary offsets of the root hinges, and noncoincidence of the blade twist axis, elastic axis, and centroidal axis. Furthermore, these three axes need not be straight and need not pass through the center of rotation. The elastic description of the blade includes flapwise bending, chordwise bending and blade torsion, while the rigid body degrees of freedom are flapping, lead-lag, and rigid body pitching.

The basic nomenclature used in the analysis are defined in the list of symbols.

The second section is concerned with the elastic behavior of a twisted blade, and formulas are developed for the elastic restoring moments as functions of blade deformations. Expressions are also given for the deflection of a mass point in the blade relative to a blade reference axis system which rotates with the blade. The treatment of the elastic behavior of the blade has been based, to a large extent, on concepts developed by Houbolt and Brooks (Reference 3) in considering a simpler blade representation without rigid body degrees of freedom. In particular, the axial stresses due to centrifugal forces are treated as if the blade acted as a collection of longitudinal fibers.

Expressions for the inertia forces acting on the blade are required in the procedure developed for finding the blade dynamic motions and natural frequencies. These are obtained by finding the acceleration of a differential mass in the blade, multiplying by the mass to determine the inertia force, and then carrying out the appropriate integrations.

The problem of determining inertia forces is complicated because of the generality of the configuration which has been allowed and the need for determining absolute accelerations relative to an inertial frame. The derivation of the blade inertial loadings is somewhat lengthy but is carried out by a series of straightforward steps. Successive sections treat: (1) the motion of coordinate systems by a series of transformations, (2) the derivation of the absolute acceleration of a mass point of the blade from the accelerations relative to moving coordinates, and (3) the integration of the blade inertial forces to obtain blade inertial loadings per unit span referred to the blade reference axis system. Finally, the inertial loading is transformed to moments about the local elastic axis and the major and minor axes of the blade section. Equations are then derived for the total force and moment components acting on a section of the blade.

4

The analysis has been simplified by dropping terms in the course of the development which would lead to nonlinear terms in the oscillatory variables in the final equations. It has also been assumed that the mean values of the nondimensional structural deformations and the mean flapping, lead-lag and pitching angles are all small quantities, so that their squares and products can be neglected when they occur in the coefficients of the oscillatory variables.

General differential equations for studying the vibrations of a nonuniform, twisted, rotating helicopter blade including elastic and rigid body motions could be obtained by combining the expressions for the blade elastic behavior and the expressions for the blade inertial loadings and acting bending and torsional moments. Such a development would be analogous to the one used in Reference 3 . However, the resulting differential equations would be so complicated (even though linearized) that some type of approximate method would be required to solve for the vibration characteristics of the blade.

A different type of procedure was developed in the present investigation for determining natural frequencies which is an extension of Targoff's associated matrix technique (References 1 and 2). In this procedure the blade is represented by a number of spanwise segments or bays, and the inertial loadings on each bay are assumed to be concentrated and to act at the center of the bay. Each bay is then divided into two parts--one outboard and one inboard of the concentrated mass. The half bays are treated as if weightless, with the concentrated mass being located at the junction between them. The elastic properties are assumed to be constant within the outboard and inboard halves of the bay (but not necessarily the same on each). The built-in blade twist is incorporated in the model by permitting angle changes at the junction between bays.

The variables in the vibration problem include the forces and moments acting at the ends of each bay; the elastic deformations at the ends of the bays; and the flapping, lead-lag, and pitching angles. The variations of these quantities along the span are related by matrices. Expressions for the elements of these matrices are derived in successive sections of this chapter by application of the results for the elastic behavior of the blade and the blade loadings obtained in preceding sections. The transformation matrix gives the changes in the variables at a section where there is an abrupt change in built-in twist. Elastic matrices for the inner and outer parts of a bay give the changes in the variables across the inner and outer sections of the bays respectively. Finally, a section is devoted to the mass matrix which gives the changes in the variables from a position just outboard to a position just inboard of a concentrated weight at the middle of a bay.

Relationships can be obtained between the variables at the tip and at the root of the blade by multiplying the matrices for all the blade segments together. In the final section of the chapter a discussion is given of how a solution for the vibration characteristics of the blade can be obtained from these relationships and the application of appropriate boundary conditions.

5

ELASTIC BEHAVIOR OF A TWISTED BLADE

In this section, the elastic restoring moment components of a cross section of a twisted blade are expressed in terms of deformations. The development is made following the principles of engineering beam theory similar to the one given by Houbolt and Brooks in Reference 3 . The blade effective cross section may change gradually along the span but is assumed symmetric about the chord. The axis of built-in twist (a.t.), the elastic center (e.c.) and the centroid are all on the chord. In the treatment of the elastic behavior, the present analysis differs from the analysis of Houbolt and Brooks principally in that the axis of built-in twist and the elastic axis of the undeformed blade are not assumed to be coincident and aligned with the z axis. Due to the built-in twist, the blade angle β varies with z and the distances e_y, e_γ, e_t and e_A shown on Figure 1 may also change gradually along the span.
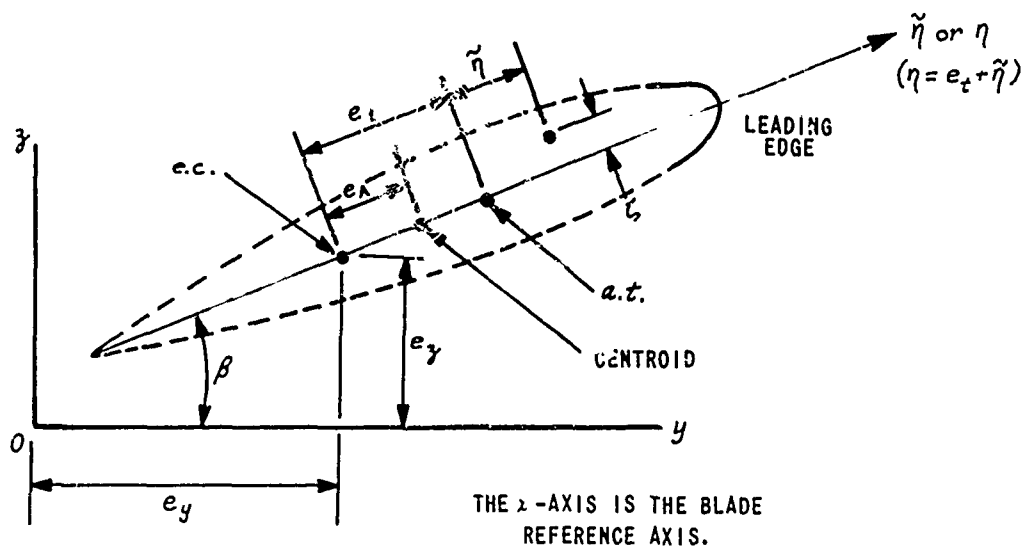
Figure 1. DIAGRAM DEFINING BLADE STRUCTURAL AXES
AND POINTS IN BLADE SECTION.

The x, y, z reference axes for the blade are fixed relative to the blade root. Equations are first obtained for the displacement of a general point in the blade relative to these axes assuming that plane sections remain plane as the blade deflects. The longitudinal fiber strains and corresponding stresses at any point in a cross section can then be derived from the equations for the displacements, and finally, expressions can be obtained for the contribution of these stresses to the internal elastic moments.

Before the occurrence of any deformation, let there be a point in a blade section at $z = x_o$ with the coordinates $y = y_o$ and $z = z_o$. Then, from the sketch on Figure 1,

$$y_o = e_y + (e_t + \tilde{\eta}) \cos \beta - \zeta \sin \beta \tag{1}$$

$$z_o = e_z + (e_t + \tilde{\eta}) \sin \beta + \zeta \cos \beta . \tag{2}$$

When the blade is under loading, let ϕ be the torsional displacement of the section originally at x_o, let u be the displacement in the x-direction of the centroid of this section and let v and w be the displacements due to bending of the elastic center of the same section in the y- and z-directions, respectively. Then, the original point (x_o, y_o, z_o) will have the following new coordinates:

$$x = x_o + u - v' \left\{ (e_t - e_A + \tilde{\eta}) \cos(\beta + \phi) - \zeta \sin(\beta + \phi) \right\}$$

$$- w' \left\{ (e_t - e_A + \tilde{\eta}) \sin(\beta + \phi) + \zeta \cos(\beta + \phi) \right\}$$

$$y = e_y - \int_0^{x_o} (e_z - \hat{e}_z) \frac{d\phi}{d\hat{x}_o} d\hat{x}_o + v$$

$$+ (e_t + \tilde{\eta}) \cos(\beta + \phi) - \zeta \sin(\beta + \phi)$$

$$z = e_z + \int_0^{x_o} (e_y - \hat{e}_y) \frac{d\phi}{d\hat{x}_o} d\hat{x}_o + w$$

$$+ (e_t + \tilde{\eta}) \sin(\beta + \phi) + \zeta \cos(\beta + \phi)$$

where $\hat{e}_z$ or $\hat{e}_y$ is the value of e_z or e_y, respectively, of a section originally at $\hat{x}_o$. Here a prime is used to indicate differentiation with respect to x_o, such that

$$v' = \frac{dv}{dx_o} , \quad w'' = \frac{d^2 w}{dx_o} , \quad etc.$$

7

The quantities Δ_y and Δ_{ζ} are defined as

$$\Delta y \equiv \int_0^{x_o} (e_{\zeta} - \hat{e}_{\zeta}) \frac{d\phi}{d\hat{x}_o} d\hat{x}_o$$

and

$$\Delta \zeta \equiv \int_0^{x_o} (e_y - \hat{e}_y) \frac{d\phi}{d\hat{x}_o} d\hat{x}_o$$

and give the linear displacements of the elastic axis at $x = x_o$ arising from torsional deflection at more inboard stations. When torsional displacements are small, it can be assumed that $\cos\phi = 1$, $\sin\phi = \phi$ and $v'\phi = w'\phi = 0$, and the preceding expressions for x, y, and ζ become

$$x = x_o + u - v'(y_o - e_y - e_A \cos\beta)$$

$$- w'(\zeta_o - e_{\zeta} - e_A \sin\beta) \tag{3}$$

$$y = y_o + v - (\zeta_o - e_{\zeta})\phi - \Delta_y \tag{4}$$

$$\zeta = \zeta_o + w + (y_o - e_y)\phi + \Delta_{\zeta} \quad . \tag{5}$$

Since, with $\phi = 0$ at $x_o = 0$,

$$\Delta_y = e_{\zeta}\phi - \int_0^{x_o} e_{\zeta}\phi' dx_o$$

and

$$\Delta_{\zeta} = e_y \phi - \int_0^{x_o} e_y \phi' dx_o \quad ,$$

it is clear that

$$\Delta'_y = e'_{\zeta}\phi \quad \text{and} \quad \Delta'_{\zeta} = e'_y \phi \quad .$$

8

Thus,

$$x' = 1 + u' - v''(y_o - e_y - e_A \cos\beta)$$

$$- w''(z_o - e_z - e_A \sin\beta)$$

$$- v'(y_o' - e_y' - e_A' \cos\beta + e_A \beta' \sin\beta)$$

$$(6)$$

$$- w'(z_o' - e_z' - e_A' \sin\beta - e_A \beta' \cos\beta)$$

$$y' = y_o' + v' - (z_o - e_z)\phi' - z_o' \phi$$

$$(7)$$

$$z' = z_o' + w' + (y_o - e_y)\phi' + y_o' \phi$$

$$(8)$$

where y_o' and z_o' are evaluated for constant $\tilde{\eta}$ and ζ . By differentiating (1) and (2), it is found that

$$y_o' = e_y' - \beta'(z_o - e_z) + e_t' \cos\beta$$

$$z_o' = e_z' + \beta'(y_o - e_y) + e_t' \sin\beta$$

and, hence, Equation (6) becomes

9

$$x = 1 + u' - v'(y_0 - e_y - e_A \cos\beta)$$

$$- w''(z_0 - e_z - e_A \sin\beta)$$

$$+ v'\beta'(z_0 - e_z - e_A \sin\beta)$$

$$- w'\beta'(y_0 - e_y - e_A \cos\beta)$$

$$- (e_z' - e_A')(v'\cos\beta + w'\sin\beta).$$

Now, by taking any product of v, w, ϕ, v', w', ϕ', v'' and w'' equal to zero, it follows that

$$(x')^2 - (y')^2 - (z')^2$$

$$= 1 - (y_0')^2 + (z_0')^2 + 2u'$$

$$- 2v'(y_0 - e_y - e_A \cos\beta) - 2w''(z_0 - e_z - e_A \sin\beta)$$

$$- 2v'(e_A \cos\beta - e_A \beta' \sin\beta + e_y') \tag{9}$$

$$+ 2w'(e_A \sin\beta + e_A \beta' \cos\beta + e_z')$$

$$+ 2\phi'\Bigg[(y_0 - e_y)(e_z' + e_z' \sin\beta)$$

$$- (z_0 - e_z)(e_y' + e_z' \cos\beta)$$

$$- \left\{ (y_0 - e_y)^2 - (z_0 - e_z)^2 \right\} \beta' \Bigg].$$

10

· Let ds_o and ds be the lengths of an elementary fiber before and after deformation.* Then,

$$\left(\frac{ds_o}{dx_o}\right)^2 = 1 + (y_o')^2 + (z_o')^2$$

$$\left(\frac{ds}{dx_o}\right)^2 = (x')^2 + (y')^2 + (z')^2$$

and the longitudinal (tensile) strain of the fiber is

$$\epsilon = \frac{ds - ds_o}{ds_o} = \sqrt{\left(\frac{ds}{dx_o}\right)^2 \bigg/ \left(\frac{ds_o}{dx_o}\right)^2} - 1$$

$$= \left\{1 + \frac{(x')^2 + (y')^2 + (z')^2 - 1 - (y_o')^2 - (z_o')^2}{1 + (y_o')^2 + (z_o')^2}\right\}^{1/2} - 1$$

$$= \frac{1}{2} \frac{(x')^2 + (y')^2 + (z')^2 - 1 - (y_o')^2 - (z_o')^2}{1 + (y_o')^2 + (z_o')^2}$$

where the last step follows because ds/ds_o is approximately equal to unity. When Equation (9) is substituted into this expression and it is assumed that $(y_o')^2 + (z_o')^2 \ll 1$, the following equation for ϵ is obtained:

---

*The end points of an elementary fiber in the two adjacent sections are taken to have the same $\tilde{\eta}$ and the same ζ.

11

$$\epsilon = \frac{1}{2}\left\{ (x')^2 + (y')^2 + (z')^2 - 1 - (y_o')^2 - (z_o')^2 \right\}$$

$$= u' - v''(y_o - e_y - e_A \cos\beta) - w''(z_o - e_z - e_A \sin\beta)$$

$$+ v'\left(e_y' + e_A' \cos\beta - e_A \beta' \sin\beta \right)$$

$$+ w'\left(e_z' + e_A' \sin\beta + e_A \beta' \cos\beta \right)$$

$$+ \phi'\left[(y_o - e_y)(e_z' + e_t' \sin\beta) \right.$$

$$- (z_o - e_z)(e_y' + e_t' \cos\beta)$$

$$\left. + \left\{ (y_o - e_y)^2 + (z_o - e_z)^2 \right\} \beta' \right] \quad .$$

The expression given below for ϵ is obtained by letting

$$\eta = e_t + \tilde{\eta}$$

and by using Equations (1) and (2) to eliminate y_o and z_o .

12

$$\epsilon = u' - (\eta - e_A)(v'' \cos\beta + w'' \sin\beta)$$

$$- \zeta (w'' \cos\beta - v'' \sin\beta) + e'_y \, v' + e'_z \, w'$$

$$+ e'_A (v' \cos\beta + w' \sin\beta) + \beta' e_A (w' \cos\beta - v' \sin\beta) \quad (10)$$

$$+ \phi' \left\{ \eta (e'_z \cos\beta - e'_y \sin\beta) - \zeta (e'_y \cos\beta + e'_z \sin\beta + e'_t) \right.$$

$$\left. + (\eta^2 + \zeta^2) \beta' \right\} \quad .$$

The following elastic properties of the section will be used in the subsequent development:

$$EA \equiv \int_A E \, dA$$

$$e_A \equiv \frac{1}{EA} \int_A \eta \, E \, dA$$

$$\int_A \zeta E \, dA = 0$$

Figure 2. CROSS-SECTION SYMMETRY.

$$k_A^2 \equiv \frac{1}{EA} \int_A (\eta^2 + \zeta^2) E \, dA$$

$$EI_1 \equiv \int_A \zeta^2 E \, dA$$

$$EI_2 \equiv \int_A (\eta - e_A)^2 E \, dA = \int_A \eta (\eta - e_A) E \, dA$$

$$EB_2 \equiv \int_A \eta (\eta^2 + \zeta^2 - k_A^2) E \, dA$$
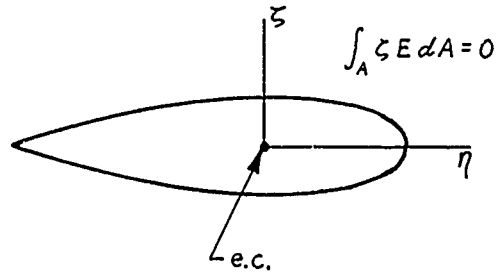
$$= \int_A (\eta^2 + \zeta^2)(\eta - e_A) E \, dA$$

13

$$EB_1 = \int_A (\eta^2 - \zeta^2)(\eta^2 + \zeta^2 - k_A^2) E \, dA$$

$$GJ \equiv \text{conventional torsional rigidity}$$

The total tension load applied to the blade section in the x-direction is denoted by T and is given by

$$T = \int_A E \, \epsilon \, dA \ .$$

The substitution of ϵ from Equation (10) into this expression yields

$$u = \epsilon_- - e_y' v - e_z' w' - e_A' (v' \cos\beta + w' \sin\beta)$$

$$- \epsilon' e_A (w' \cos\beta - v' \sin\beta)$$

$$- \phi \left\{ e_A (e_y' \cos\beta - e_y' \sin\beta) + k_A^2 \beta' \right\} \ .$$

Where the average tensile strain is defined by $\epsilon_\tau = \dfrac{T}{EA}$. This expression can be used to eliminate u' from Equation (10), giving

$$\epsilon = \epsilon_\tau - (\eta - e_A)(v'' \cos\beta + w'' \sin\beta)$$

$$- \zeta (w'' \cos\beta - v'' \sin\beta)$$

$$+ \phi \left\{ (\eta - e_A)(e_y' \cos\beta - e_y' \sin\beta) \right.$$

$$\left. - \zeta (e_y \cos\beta + e_z \sin\beta + e_t) + (\eta^2 + \zeta^2 - k_A^2) \beta' \right\} \ . \tag{11}$$

Let M_1 be the flapwise bending moment, M_2 be the chordwise bending moment, and Q be the torque, all referred to axes passing through the elastic center of the section. M_1 is positive when it tends to compress the upper surface, M_2 is positive when it tends to compress the leading edge. and Q is positive when the torque applied to the inboard side of the section tends to make the leading edge move up. The bending moments are found by multiplying the stress by appropriate moment arms and integrating over the section, giving

$$M_1 = -\int_A \zeta E \epsilon \, dA \tag{12}$$

14

$$M_2 = -\int_A \eta \, E \, \epsilon \, dA \quad . \tag{13}$$

It may be noted that the tensile stress $E\epsilon$ of a fiber has components equal to

$$- E \, \epsilon \, \zeta \, (\beta' + \phi)$$

and

$$E \, \epsilon \left\{ (\eta - e_t) \, \beta' + \eta \, \phi' \right\}$$

acting in the η- and ζ- directions, respectively, on the inboard portion of the blade at a given section. The torsional moment due to these components must be added to the St. Venant type torsional term $G J \phi'$, giving

$$Q = G J \phi' + \int_A \zeta E \, \epsilon \, \zeta \, (\beta' + \phi') \, dA$$

$$+ \int_A \eta \, E \, \epsilon \left\{ (\eta - e_t)\beta' + \eta \, \phi' \right\} dA \quad . \tag{14}$$

By substituting Equation (11) into Equations (12), (13), and (14) and using the sectional elastic properties defined in the last paragraph, the following results are obtained:

$$M_1 = E I_1 \left\{ w'' \cos\beta - v'' \sin\beta \right.$$

$$\left. + \phi'(e'_y \cos\beta + e'_z \sin\beta + e'_t) \right\} \tag{15}$$

$$M_2 = E I_2 \left\{ v'' \cos\beta + w'' \sin\beta - \phi'(e'_z \cos\beta - e'_y \sin\beta) \right\} \tag{16}$$

$$- T e_A - E B_2 \, \beta' \phi'$$

15

$$Q = \left\{ GJ + T k_A^2 + (e'_{\not{z}} \cos\beta - e'_y \sin\beta)(E B_2 - e_t \, E I_2)\beta' \right.$$

$$\left. + (EB_1 - e_t \, EB_2)(\beta')^2 \right\} \phi' + T(k_A^2 - e_t \, e_A)\beta'$$

$$- (EB_2 - e_t \, EI_2)\beta' \left(v'' \cos\beta + w'' \sin\beta \right) . \tag{17}$$

Let d_y and $d_{\not{z}}$ be the y- and $\not{z}$- coordinates of the local axis of built-in thrust of the undeformed blade. Then,

$$e_y = d_y - e_t \cos\beta \quad \text{and} \quad e_{\not{z}} = d_{\not{z}} - e_t \sin\beta .$$

Hence,

$$e'_y \cos\beta + e'_{\not{z}} \sin\beta + e'_t = d'_y \cos\beta + d'_{\not{z}} \sin\beta$$

$$e'_{\not{z}} \cos\beta - e'_y \sin\beta = d'_{\not{z}} \cos\beta - d'_y \sin\beta - e_t \beta'$$

and Equations (15), (16), and (17) may be written as

$$M_1 = E I_1 \left\{ w'' \cos\beta - v'' \sin\beta + \phi'(d'_y \cos\beta + d'_{\not{z}} \sin\beta) \right\} \tag{18}$$

$$M_2 = E I_2 \left\{ v'' \cos\beta + w'' \sin\beta - \phi'(d'_{\not{z}} \cos\beta - d'_y \sin\beta) \right\} \tag{19}$$

$$- T e_A - (EB_2 - e_t \, EI_2)\beta' \phi'$$

and

16

$$Q = \left\{ GJ + T k_A^2 + (d_z' \cos\beta - d_y' \sin\beta)(EB_2 - e_t EI_2)\beta' \right.$$

$$+ (EB_1 - 2e_t EB_2 + e_t^2 EI_2)(\beta')^2 \left. \right\} \phi'$$

$$+ T(k_A^2 - e_t e_A)\beta'$$

$$- (EB_2 - e_t EI_2)\beta'(v'' \cos\beta + w'' \sin\beta) \ .$$

(20)

If the axis of built-in twist is a straight line parallel to the blade reference axis, $d_y' = d_z' \equiv 0$, and several terms are zero in the above equations. When the two axes are also coincident ($e_t = 0$), the above expressions reduce to those given by Houbolt and Brooks (Reference 3).

MOTION OF COORDINATE SYSTEMS

In the present analysis, equations of motion are developed for a rotating blade by finding the inertial forces acting on mass elements of the blade in terms of the motions about the flapping, lead-lag, and pitching axes as well as the blade elastic deformations. The expressions for blade motions caused by rotations about these axes are very complex, particularly when possible offsets of the various axes are taken into account. The required expressions for these motions are derived in this section by a series of transformations, each showing the effect of a particular rotation and/or a translation of the origin of the axis system.

The first six coordinate systems which are used in finding all the blade motions exclusive of elastic deformations are shown on Figure 3. Two additional transformations will be described later which give the orientation of the blade reference axes relative to those shown. The $O_I \, x_I \, y_I \, z_I$ system shown on the figure is an inertial system. Ω is the constant rotational speed of the rotor about the z_I- or z_1-axis, in radians per second. The $O_1 x_1 \, y_1 \, z_1$ system rotates with the rotor. Let U_i, V_i, W_i be the linear velocity components of the origin O_i in the x_i, y_i, z_i directions and p_i, q_i, r_i be the angular velocity components of the $O_i \, x_i y_i \, z_i$ system in the x_i, y_i, z_i directions ($i = 1$, 2, 3, 4, or 5). Then,

$$U_1 = V_1 = W_1 = p_1 = q_1 = 0 \ ,$$

$$r_1 = \Omega \ .$$

17

Figure 3. COORDINATE SYSTEMS.

18

The $O_2\, x_2\, y_2\, z_2$ system is obtained by rotating the $O_1\, x_1\, y_1\, z_1$ system about the negative y_2-axis (which is parallel to the y_1-axis and located at $x_1 = r_F$). This rotation angle, β_F, is the flapping angle of the blade, and it can be seen that

$$U_2 = W_2 = 0, \qquad\qquad V_2 = \Omega\, r_F \ ,$$

$$p_2 = \Omega\, \sin \beta_F \ , \qquad\qquad q_2 = -\dot\beta_F \ , \qquad\qquad r_2 = \Omega\, \cos \beta_F \ .$$

The $O_3\, x_3\, y_3\, z_3$ system is obtained by rotating the $O_2\, x_2\, y_2\, z_2$ system about the z_2-axis through angle β_D, the blade lead angle, and then translating the origin in the $x_2 y_2$-plane to $x_2 = r_{FD}$ and $y_2 = e_D$, so that

$$p_3 = p_2\, \cos \beta_D + q_2\, \sin \beta_D$$

$$= \Omega\, \sin \beta_F\, \cos \beta_D - \dot\beta_F\, \sin \beta_D$$

$$q_3 = q_2\, \cos \beta_D - p_2\, \sin \beta_D$$

$$= -\Omega\, \sin \beta_F\, \sin \beta_D - \dot\beta_F\, \cos \beta_D$$

$$r_3 = r_2 + \dot\beta_D = \Omega\, \cos \beta_F + \dot\beta_D$$

$$U_3 = U_2\, \cos \beta_D + V_2\, \sin \beta_D - r_2\, (e_D\, \cos \beta_D - r_{FD}\, \sin \beta_D)$$

$$= \Omega \left\{ r_F\, \sin \beta_D - (e_D\, \cos \beta_D - r_{FD}\, \sin \beta_D)\, \cos \beta_F \right\}$$

$$V_3 = V_2\, \cos \beta_D - U_2\, \sin \beta_D + r_2\, (e_D\, \sin \beta_D + r_{FD}\, \cos \beta_D)$$

$$= \Omega \left\{ r_F\, \cos \beta_D + (e_D\, \sin \beta_D + r_{FD}\, \cos \beta_D)\, \cos \beta_F \right\}$$

$$W_3 = W_2 - p_2\, e_D - q_2\, r_{FD} = \Omega\, e_D\, \sin \beta_F + \dot\beta_F\, r_{FD} \quad .$$

The $O_4\, x_4\, y_4\, z_4$ system is obtained by translating the origin of the $O_3\, x_3\, y_3\, z_3$ system to $x_3 = r_{DP}$, $y_3 = e_{DP}$ and $z_3 = C_p$, so that

19

$$p_4 = p_3 = \Omega \sin \beta_F \cos \beta_D - \dot{\beta}_F \sin \beta_D$$

$$q_4 = q_3 = -\Omega \sin \beta_F \sin \beta_D - \dot{\beta}_F \cos \beta_D$$

$$r_4 = r_3 = \Omega \cos \beta_F + \dot{\beta}_D$$

$$U_4 = U_3 + q_3 \, C_P - r_3 \, e_{DP}$$

$$= \Omega \left\{ (r_F - C_P \sin \beta_F) \sin \beta_D - (e_{DP} + e_D \cos \beta_D - r_{FD} \sin \beta_D) \cos \beta_F \right\}$$

$$- \dot{\beta}_F \, C_P \cos \beta_D - \dot{\beta}_D \, e_{DP}$$

$$V_4 = V_3 + r_3 \, r_{DP} - p_3 \, C_P$$

$$= \Omega \left\{ (r_F - C_P \sin \beta_F) \cos \beta_D + (r_{DP} + e_D \sin \beta_D + r_{FD} \cos \beta_D) \cos \beta_F \right\}$$

$$+ \dot{\beta}_F \, C_P \sin \beta_D + \dot{\beta}_D \, r_{DP}$$

$$W_4 = W_3 + p_3 \, e_{DP} - q_3 \, r_{DP}$$

$$= \Omega (e_D + e_{DP} \cos \beta_D + r_{DP} \sin \beta_D) \sin \beta_F + \dot{\beta}_F (r_{FD} + r_{DP} \cos \beta_D - e_{DP} \sin \beta_D).$$

The $x_5 \, y_5 \, z_5$ system is obtained by rotating the $0_4 \, x_4 \, y_4 \, z_4$ system about the x_4-axis through an angle β_P, the blade root pitch angle, so that

$$U_5 = U_4$$

$$= \Omega \left\{ (r_F + r_{FD} \cos\beta_F - C_P \sin\beta_F) \sin\beta_D \right.$$

$$\left. - (e_{DP} + e_D \cos\beta_D) \cos\beta_F \right\}$$

$$- \dot\beta_F \, C_P \cos\beta_D - \dot\beta_D \, e_{DP}$$

$$V_5 = V_4 \cos\beta_P + W_4 \sin\beta_P$$

$$= \Omega \left[\left\{ (r_F + r_{FD} \cos\beta_F - C_P \sin\beta_F) \cos\beta_D \right. \right.$$

$$\left. + (r_{DP} + e_D \sin\beta_D) \cos\beta_F \right\} \cos\beta_P$$

$$\left. + (e_D + e_{DP} \cos\beta_D + r_{DP} \sin\beta_D) \sin\beta_F \sin\beta_P \right]$$

$$+ \dot\beta_F \left\{ C_P \sin\beta_D \cos\beta_P + (r_{FD} + r_{DP} \cos\beta_D - e_{DP} \sin\beta_D) \sin\beta_P \right\}$$

$$+ \dot\beta_D \, r_{DP} \cos\beta_P$$

$$W_5 = W_4 \cos\beta_P - V_4 \sin\beta_P$$

$$= \Omega \left[(e_D + e_{DP} \cos\beta_D + r_{DP} \sin\beta_D) \sin\beta_F \cos\beta_P \right.$$

$$- \left\{ (r_F + r_{FD} \cos\beta_F - C_P \sin\beta_F) \cos\beta_D \right.$$

$$\left. + (r_{DP} + e_D \sin\beta_D) \cos\beta_F \right\} \sin\beta_P \left. \right] - \dot\beta_D \, r_{DP} \sin\beta_P$$

$$+ \dot\beta_F \left\{ (r_{FD} + r_{DP} \cos\beta_D - e_{DP} \sin\beta_D) \cos\beta_P - C_P \sin\beta_D \sin\beta_P \right\}$$

$$p_5 = p_4 + \dot\beta_P$$

$$= \Omega \sin\beta_F \cos\beta_D - \dot\beta_F \sin\beta_D + \dot\beta_P$$

$$q_5 = q_4 \cos \beta_p + r_4 \sin \beta_p$$

$$-\Omega \left(\sin \beta_F \sin \beta_D \cos \beta_p - \cos \beta_F \sin \beta_p \right)$$

$$- \dot{\beta}_F \cos \beta_D \cos \beta_p + \dot{\beta}_D \sin \beta_p$$

$$r_5 = r_4 \cos \beta_p - q_4 \sin \beta_p$$

$$= \Omega \left(\cos \beta_F \cos \beta_p + \sin \beta_F \sin \beta_D \sin \beta_p \right)$$

$$+ \dot{\beta}_F \cos \beta_D \sin \beta_p - \dot{\beta}_D \cos \beta_p$$

These six relations may be written in matrix form as

$$
\begin{bmatrix} p_5 \\ q_5 \\ r_5 \\ u_5 \\ v_5 \\ w_5 \end{bmatrix}
=
\begin{bmatrix}
S_v & F_p & 0 & 1 \\
S_q & F_q & D_q & 0 \\
S_r & F_r & D_r & 0 \\
S_u & F_u & D_u & 0 \\
S_v & F_v & D_v & 0 \\
S_w & F_w & D_w & 0
\end{bmatrix}
\begin{Bmatrix} \Omega \\ \dot{\beta}_F \\ \dot{\beta}_D \\ \dot{\beta}_p \end{Bmatrix}
\tag{21}
$$

where

$$S_p = \sin \beta_F \cos \beta_D$$

$$S_q = \cos \beta_F \sin \beta_p - \sin \beta_F \sin \beta_D \cos \beta_p$$

$$S_r = \cos \beta_F \cos \beta_p - \sin \beta_F \sin \beta_D \sin \beta_p$$

$$S_U = (r_F + r_{FD} \cos \beta_F - C_P \sin \beta_F) \sin \beta_D - (e_{DP} + e_D \cos \beta_D) \cos \beta_F$$

$$S_V = \left\{ (r_F + r_{FD} \cos \beta_F - C_P \sin \beta_F) \cos \beta_D + (r_{DP} + e_D \sin \beta_D) \cos \beta_F \right\} \cos \beta_P$$
$$+ (e_D + e_{DP} \cos \beta_D + r_{DP} \sin \beta_D) \sin \beta_F \sin \beta_P$$

$$S_W = -\left\{ (r_F + r_{FD} \cos \beta_F - C_P \sin \beta_F) \cos \beta_D + r_{DP} + e_D \sin \beta_D) \cos \beta_F \right\} \sin \beta_P$$
$$+ (e_D + e_{DP} \cos \beta_D + r_{DP} \sin \beta_D) \sin \beta_F \cos \beta_P$$

$$F_p = -\sin \beta_D$$

$$F_q = -\cos \beta_D \cos \beta_P$$

$$F_r = \cos \beta_D \sin \beta_P$$

$$F_U = -C_P \cos \beta_D$$

$$F_V = (r_{FD} + r_{DP} \cos \beta_D - e_{DP} \sin \beta_D) \sin \beta_P + C_P \sin \beta_D \cos \beta_P$$

$$F_W = (r_{FD} + r_{DP} \cos \beta_D - e_{DP} \sin \beta_D) \cos \beta_P - C_P \sin \beta_D \sin \beta_P$$

$$D_q = \sin \beta_P \qquad D_r = \cos \beta_P \qquad (D_p = 0)$$

$$D_U = -e_{DP} \qquad D_V = r_{DP} \cos \beta_P \qquad D_W = -r_{DP} \sin \beta_P$$

It follows from the preceding matrix, e.g., noting $\dot{D}_u = 0$, that

$$
\left\{
\begin{array}{c}
\dot{p}_s \\
\dot{\varphi}_s \\
\dot{r}_s \\
\dot{u}_s \\
\dot{v}_s \\
\dot{w}_s
\end{array}
\right\}
=
\left[
\begin{array}{ccc}
F_p & 0 & 1 \\
F_q & D_q & 0 \\
F_r & D_r & 0 \\
F_u & D_u & 0 \\
F_v & D_v & 0 \\
F_w & D_w & 0
\end{array}
\right]
\left\{
\begin{array}{c}
\ddot{\beta}_F \\
\ddot{\beta}_D \\
\ddot{\beta}_P
\end{array}
\right\}
+
\left[
\begin{array}{ccc}
\dot{S}_p & \dot{F}_r & 0 \\
\dot{S}_q & \dot{F}_q & \dot{D}_q \\
\dot{S}_r & \dot{F}_r & \dot{D}_r \\
\dot{S}_u & \dot{F}_u & 0 \\
\dot{S}_v & \dot{F}_v & \dot{D}_v \\
\dot{S}_w & \dot{F}_w & \dot{D}_w
\end{array}
\right]
\left\{
\begin{array}{c}
\Omega \\
\dot{\beta}_F \\
\dot{\beta}_D
\end{array}
\right\}
\qquad (22)
$$

As mentioned previously, the final equations of motion which are obtained for finding natural vibration frequencies and mode shapes of rotating helicopter blades are simplified by the omission of terms of negligible importance. These equations could be obtained by first working out exact equations and then linearizing them. However, a considerable simplification can be obtained in the analysis if terms are dropped in the course of the derivation when it becomes clear that they will lead to negligible terms in the final equations.

The first time derivatives of the blade flapping, lead-lag, and pitching angles (i.e., $\dot{\beta}_F$, $\dot{\beta}_D$, and $\dot{\beta}_P$) appear explicitly on the right-hand sides of Equations (21) and (22) and also enter implicitly through the time derivatives, $\dot{S}_p$, $\dot{F}_p$, $\dot{S}_q$, $\dot{F}_q$, $\dot{D}_q$, etc. The ratios of these time derivatives to the rotor angular velocity are assumed to be quantities of first order which are small compared to one. This assumption might be justified, for example, by assuming sinusoidal oscillation of the blade at a frequency of 10Ω which involved a blade root flapping motion of $\beta_F = 0.5$ deg. $= 0.00872$ rad. In this case, $\dot{\beta}_F/\Omega = (10\Omega)(0.0087)/\Omega = .087$. Lower values of this ratio would be obtained at lower oscillation frequencies and amplitudes of vibration.

If Equations (21) and (22) were used in deriving expressions for the absolute accelerations of a mass point in a blade, a number of terms would be obtained involving products of $\dot{\beta}_F$, $\dot{\beta}_D$, and $\dot{\beta}_P$. These products could be neglected because they would give higher-order terms in $\dot{\beta}_F/\Omega$, $\dot{\beta}_D\,\Omega$, and $\dot{\beta}_P\,\Omega$ if the expressions were written in a suitable nondimensional form. Some additional terms would be found in the expressions for the absolute accelerations in which $\dot{\beta}_F$, $\dot{\beta}_D$, and $\dot{\beta}_P$ would enter linearly. These terms could be identified as Coriolis accelerations.

The Coriolis forces acting on a rotating blade produce couplings between vibration modes which are uncoupled when the blade is not rotating. These intermodal couplings are unusual in that they are proportional to the time rate of change of the variables ($\dot{\beta}_F$, $\dot{\beta}_D$, and $\dot{\beta}_P$)

24

and they are unsymmetrical. An interesting consequence of couplings of this type is that the exact solutions for the "natural vibration modes" of the rotating system would give motion in which all parts of the elastic body would not move exactly in or out of phase. However, these effects are small in the case of rotor blades and can be safely neglected when computing their vibration frequencies and mode shapes.

It follows that the terms involving $\dot{\beta}_F$, $\dot{\beta}_D$, and $\dot{\beta}_P$ in Equations (21) and (22) will have a negligible effect in the final equations and can be omitted in the following derivation. Thus, Equations (21) and (22) are simplified as shown below:

$$
\begin{Bmatrix} p_5 \\ q_5 \\ r_5 \\ U_5 \\ V_5 \\ W_5 \end{Bmatrix} = \begin{Bmatrix} S_p \\ S_q \\ S_r \\ S_U \\ S_V \\ S_W \end{Bmatrix} \Omega \quad ; \tag{23}
$$

$$
\begin{Bmatrix} \dot{p}_5 \\ \dot{q}_5 \\ \dot{r}_5 \\ \dot{U}_5 \\ \dot{V}_5 \\ \dot{W}_5 \end{Bmatrix} = \begin{Bmatrix} F_p\,\ddot{\beta}_F + \ddot{\beta}_P \\ F_q\,\ddot{\beta}_F + D_q\,\ddot{\beta}_D \\ F_r\,\ddot{\beta}_F + D_r\,\ddot{\beta}_D \\ F_U\,\ddot{\beta}_F + D_U\,\ddot{\beta}_D \\ F_V\,\ddot{\beta}_F + D_V\,\ddot{\beta}_D \\ F_W\,\ddot{\beta}_F + D_W\,\ddot{\beta}_D \end{Bmatrix} . \tag{24}
$$

The (x_1, y_1, γ_1), (x_2, y_2, γ_2), (x_3, y_3, γ_3), (x_4, y_4, γ_4), and (x_5, y_5, γ_5) axes systems have been introduced in order to define the linear and angular motions of the blade due to shaft rotation and motion about the flapping, lead-lag, and pitching axes. The $x\,y\,\gamma$ axes system which is used as a reference system for the blade has a fixed orientation relative to the $x_5 y_5 \gamma_5$ axes system, as indicated on Figure 4.
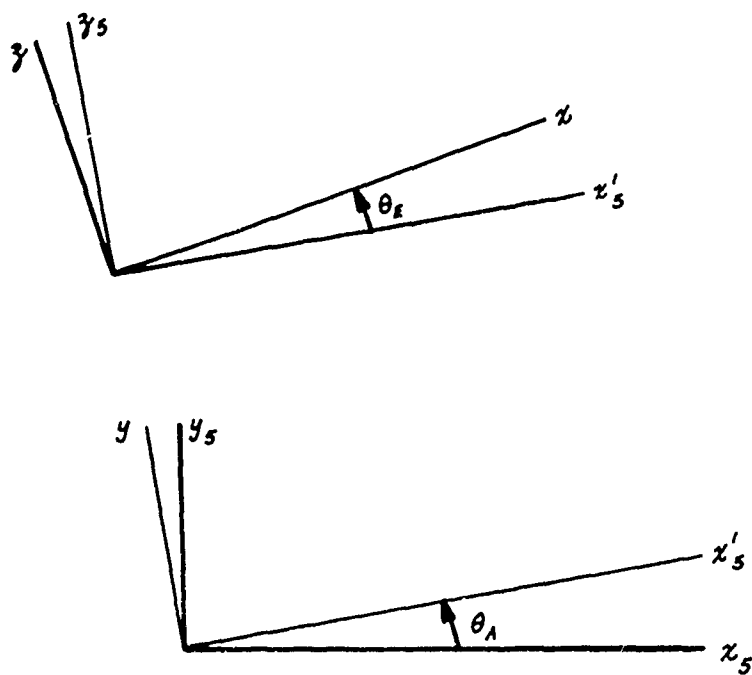
Figure 4. ORIENTATION OF xyz-AXES (BLADE REFERENCE SYSTEM) RELATIVE TO $x_s y_s z_s$-AXES SYSTEM.

The $xy\zeta$ system (with the x-axis being the blade reference axis) is obtained by rotating the $x_s y_s \zeta_s$ system first about the ζ_s-axis through an azimuth angle θ_A and then about the negative y- axis through an elevation angle θ_E. Thus, the rotational velocity components of the $xy\zeta$ system in the x-, y- , and ζ- directions are:

$$p = (p_s \cos \theta_A + q_s \sin \theta_A) \cos \theta_E + r_s \sin \theta_E$$

$$q = q_s \cos \theta_A - p_s \sin \theta_A$$

$$r = r_s \cos \theta_E - (p_s \cos \theta_A + q_s \sin \theta_A) \sin \theta_E$$

They may be written as follows using Equation (23):

$$\begin{Bmatrix} p \\ q \\ r \end{Bmatrix} = \begin{bmatrix} \gamma \end{bmatrix} \begin{Bmatrix} p_s \\ q_s \\ r_s \end{Bmatrix} = \begin{bmatrix} \gamma \end{bmatrix} \begin{Bmatrix} S_p \\ S_q \\ S_r \end{Bmatrix} \Omega$$

where $\begin{bmatrix} \gamma \end{bmatrix}$ is a 3-x-3 matrix with the following elements:

$$\gamma_{11} = \cos \theta_A \cos \theta_E \qquad \gamma_{12} = \sin \theta_A \cos \theta_E \qquad \gamma_{13} = \sin \theta_E$$

$$\gamma_{21} = -\sin \theta_A \qquad \gamma_{22} = \cos \theta_A \qquad (\gamma_{23} = 0)$$

$$\gamma_{31} = -\cos \theta_A \sin \theta_E \qquad \gamma_{32} = -\sin \theta_A \sin \theta_E \qquad \gamma_{33} = \cos \theta_E$$

Similarly, the translational velocity components of the origin of the $xy\zeta$ system in the x- , y- and ζ- directions are given by:

$$\begin{Bmatrix} U \\ V \\ W \end{Bmatrix} = \begin{bmatrix} \gamma \end{bmatrix} \begin{Bmatrix} U_s \\ V_s \\ W_s \end{Bmatrix} = \begin{bmatrix} \gamma \end{bmatrix} \begin{Bmatrix} S_U \\ S_V \\ S_W \end{Bmatrix} \Omega$$

27

The xyz components of the angular accelerations of the xyz system and the linear acceleration components of the origin of the xyz system can be obtained from the $x_s y_s z_s$ components by the same transformation, giving

$$\begin{Bmatrix} \dot{p} \\ \dot{q} \\ \dot{r} \end{Bmatrix} = \begin{bmatrix} \tau \end{bmatrix} \begin{Bmatrix} \dot{p}_s \\ \dot{q}_s \\ \dot{r}_s \end{Bmatrix} = \begin{bmatrix} \tau \end{bmatrix} \begin{Bmatrix} F_p \ddot{\beta}_F + \ddot{\beta}_P \\ F_q \ddot{\beta}_F + D_q \ddot{\beta}_D \\ F_r \ddot{\beta}_F + D_r \ddot{\beta}_D \end{Bmatrix}$$

and

$$\begin{Bmatrix} \dot{U} \\ \dot{V} \\ \dot{W} \end{Bmatrix} = \begin{bmatrix} \tau \end{bmatrix} \begin{Bmatrix} \dot{U}_s \\ \dot{V}_s \\ \dot{W}_s \end{Bmatrix} = \begin{bmatrix} \tau \end{bmatrix} \begin{Bmatrix} F_U \ddot{\beta}_F + D_U \ddot{\beta}_D \\ F_V \ddot{\beta}_F + D_V \ddot{\beta}_D \\ F_W \ddot{\beta}_F + D_W \ddot{\beta}_D \end{Bmatrix}$$

The total flapping angle and flapping acceleration can be written as

$$\beta_F = (\beta_F)_{oscil.} + \hat{\beta}_F$$

$$\ddot{\beta}_F = (\ddot{\beta}_F)_{oscil.}$$

where $\hat{\beta}_F$ is the steady or average flapping angle and $(\beta_F)_{oscil.}$ is the oscillatory component of the flapping angle. A similar breakdown into steady and oscillatory components can be made of β_D and β_P and the elastic deformations. It is required that final vibration equations be linear in the oscillatory variables. This will always be a reasonable approximation for sufficiently small oscillations.

In addition, the mean angles $\hat{\beta}_F$, $\hat{\beta}_D$, and $\hat{\beta}_P$, the azimuth angle (θ_A) and the elevation angle (θ_E) are considered to be small which leads to simplifications in the equations for the acceleration components obtained in the next section. Although these constant quantities are not considered to be as small as the oscillatory quantities, they are assumed to be small enough so that their squares and products can be neglected when they appear in the coefficients of the oscillatory variables. When the expressions for p, q, r, etc., and simplified accordingly, for use in the next section, they take the following form:

28

$$p = \Omega \, (\theta_E + \beta_F)$$

$$q = \Omega \, \beta_P$$

$$r = \Omega$$

$$U = \Omega \, (r_D \beta_D + r_P \theta_A - e_P)$$

$$V = \Omega \, (e_P \theta_A + r_P + e_D \beta_D - C_P \beta_F)$$

$$W = \Omega \, (e_P \theta_E + e_P \beta_F - r_P \beta_P)$$

$$\dot{p} = -\ddot{\beta}_F \, (\theta_A + \beta_D) + \ddot{\beta}_D \, \theta_E + \ddot{\beta}_P$$

$$\dot{q} = -\ddot{\beta}_F + \ddot{\beta}_D \, \beta_P - \ddot{\beta}_P \, \theta_A$$

$$\dot{r} = \ddot{\beta}_F \, \beta_P + \ddot{\beta}_D - \ddot{\beta}_P \, \theta_E$$

$$\dot{U} = -\ddot{\beta}_F \, \left\{ C_P - (r_P - r_F) \theta_E \right\} + \ddot{\beta}_D \, (-e_{DP} + r_{DP} \, \theta_A)$$

$$\dot{V} = \ddot{\beta}_F \, \left\{ C_P (\theta_A + \beta_D) + (r_P - r_F) \beta_P \right\} + \ddot{\beta}_D \, (e_{DP} \theta_A + r_{DP})$$

$$\dot{W} = \ddot{\beta}_F \, (C_P \theta_E + r_P - r_F - e_{DP} \beta_D) + \ddot{\beta}_D \, (e_{DP} \theta_E - r_{DP} \beta_P)$$

$$\left. \right\} \quad (25)$$

The blade is a beam in the xyz system cantilevered at $x = 0$. Consequently, a mass point in it can move relative to the xyz system as described in the section on the elastic behavior of a twisted beam. This motion will be taken into account in addition to the velocities and accelerations given by Equation (25) in finding the inertia forces acting on a mass point in the blade.

The absolute velocity and acceleration components of a mass point referred to a moving coordinate system are given by the classical expressions

$$v_x = \dot{x} + U + qz - ry$$

$$v_y = \dot{y} + V + rx - pz$$

$$v_z = \dot{z} + W + py - qx \qquad (26)$$

$$a_x = \dot{v}_x + q v_z - r v_y$$
$$= \ddot{x} + \dot{U} + \dot{q}z - \dot{r}y + 2(q\dot{z} - r\dot{y}) - qW - rV$$
$$- p(qy + rz) - (q^2 - r^2)x$$

$$a_y = \dot{v}_y + r v_x - p v_z$$
$$= \ddot{y} + \dot{V} + \dot{r}x - \dot{p}z - 2(r\dot{x} - p\dot{z}) - rU - pW$$
$$+ q(rz - px) - (r^2 - p^2)y$$

$$a_z = \dot{v}_z + p v_y - q v_x$$
$$= \ddot{z} + \dot{W} + \dot{p}y - \dot{q}z - 2(p\dot{y} - q\dot{x}) - pV - qU$$
$$- r(px + qy) - (p^2 - q^2)z \qquad (27)$$

In the present case the xyz axes are the reference system for the blade. In the section on the motion of coordinate systems, expressions were derived for the xyz components of the linear velocity of the origin of the xyz system and for the components of the angular velocity of the xyz system. Expressions were also obtained for the time derivatives of these components. The approximate forms of these expressions for $p,\ldots,W$, given in Equation (25) are to be substituted into Equation (27). Equations (3), (4), and (5) derived in the section on the elastic behavior of a twisted blade express the coordinates of a mass point of the blade in terms of the elastic deformations. These expressions for x, y, and z are also to be substituted into Equation (27).

The underlined terms in Equation (27) represent Coriolis accelerations associated with the velocities of a mass point relative to the xyz system arising from elastic deformations of the blade. As discussed earlier, the inertia couplings produced by Coriolis forces have only a small influence on the vibration frequencies and mode shapes of rotating helicopter blades and can be neglected.

Some new notation and some changes in notation will be made in carrying out the above-mentioned substitutions. The symbol r will no longer be used to represent the z component of angular velocity but will be defined by

$$r \cong r_o + x_o$$

The physical significance of the redefined quantity, r, can be seen most readily for the case where δ_e, $\delta_z = \delta_\rho$, θ_k, θ_k, 0, where it is the radial distance from the rotor shaft to a blade section (which is taken normal to the blade reference axis).

The deflections of the elastic axis in the y and z directions, which are produced by the total combined effects of bending and twist, are denoted respectively by

$$\cdots \simeq \Delta_r$$

$$= r_{\nu s}$$

It then follows from Equations (4) and (5) that

$$z \quad \cdots \quad \gamma \quad \cdots \quad z \qquad \cdots \quad \cdots \quad z \tag{28}$$

$$z \quad \cdots \quad z \quad \cdots \quad z \tag{29}$$

Only very small oscillatory motions of the blade about the blade steady configuration are considered. Let $\hat{v}_\zeta$, $\hat{\omega}_\zeta$, $\hat{\phi}$, $\hat{\beta}_\xi$, $\hat{\beta}_D$ and $\hat{\beta}_C$ be the steady portions of v_ζ, ω_ζ, ϕ, β_s, β_D and β_P, respectively, while the latter set of symbols will represent from now on only their oscillatory portions. (The subscript is omitted from the symbol $\beta_{P_{osc}}$ used in the previous section leaving the symbol β'_ξ for the oscillatory flapping angle.)

By making the substitutions which have been discussed on the right-hand side of Equation (27) observing that $\dot{\beta}_s \dots = \dot{\beta}_\xi = 0$, and dropping any product of the oscillatory displacements or their time derivatives, the following results are obtained

$$(50)$$

$$z_K = z_y + z_z$$

where

$$(51)$$

where

32

$$\hat{a}_y = -\Omega^2 \left[y_0 + e_P - r_P \theta_A - r_D \hat{\beta}_D + \hat{v}_t - (\tilde{y}_0 - e_y)\hat{\phi} \right.$$

$$\left. - \left\{ \tilde{y}_0 + (r - r_D)(\theta_E + \hat{\beta}_E) \right\} \hat{\beta}_P \right] \quad ,$$

and

$$\bar{a}_y = a_y + \hat{a}_y \tag{32}$$

where

$$a_y = \ddot{w} + (y_0 - e_y)\ddot{\phi}$$

$$- \left\{ r - r_c + c_P \theta_E - e_{DP} \dot{\beta}_D - (\theta_A + \beta_D) y_0 \right\} \ddot{\beta}_E$$

$$+ \left\{ (e_{DP} + y_0) \theta_E - (r - r_D) \dot{\beta}_P \right\} \ddot{\beta}_D + \left\{ (r - r_D) \theta_A + y_0 \right\} \ddot{\beta}_D$$

$$+ \Omega^2 \left\{ r \beta_E + (e_D + y_0) \beta_D \right\} - \hat{a}_y$$

$$\hat{a}_y = \Omega^2 \left\{ r(\theta_E + \hat{\beta}_E) + (e_D + y_0 + \hat{j}_D) \right\} \quad .$$

Here the total components of the absolute acceleration are denoted by $\bar{a}_x$, $\bar{a}_y$, and $\bar{a}_j$; the oscillatory components by a_x, a_y, and a_j, and the steady components due to Ω by $\hat{a}_x$, $\hat{a}_y$, and $\hat{a}_j$.

As discussed earlier, θ_A and θ_E and the steady portions of the nondimensional variables are assumed to be small quantities although not necessarily as small as the oscillatory variables. The squares or products of these quantities are neglected in the coefficients of the oscillatory quantities. However, products of these quantities have been retained in the nonoscillatory parts of the expressions which enter into the determination of the average deformations.

33

It can be readily seen that the inertia forces produced by the ϵ_z component of acceleration are essentially in the axial direction and are, in general, multiplied by oscillatory angles or moment arms in the vibration equations. Hence, after inspecting Equation (30), it appears reasonable to approximate $\bar{a}_x$ by the familiar expression

$$\bar{a}_z = \hat{a}_x = -\Omega^2 r \tag{33}$$

dropping terms already multiplied by oscillatory quantities plus a few additional small terms. These additional terms which are dropped would be much smaller than the one given above except possibly those very close to the blade root.

A similar simplification of the expressions for $\bar{a}_y$ and $\bar{a}_y$ is not possible since no single term predominates for these components and the corresponding inertia forces act normal to the blade axis. However, when the above formulas are used in obtaining the blade inertia loading later in the analysis, all the underlined terms in Equations (31) and (32) will be dropped by considering that the geometric effects of the steady deformations $\hat{v}$, $\hat{w}$, $\hat{\phi}$ and $\hat{\beta}_\rho$ on the oscillatory motions are either negligible or would be included in e_y, e_z, β, θ_A and θ_ϵ. (That is, the initial blade configuration would be defined including the steady deformations produced by centrifugal forces.)

BLADE INERTIA LOADING

The inertia force on an infinitesimal element of the blade is obtained by simply multiplying its mass times the negative of its absolute acceleration as given by the expressions in the preceding section. For convenience in the following analysis, these infinitesimal forces are integrated over a section to obtain expressions for the inertia forces and moments acting on the blade per unit span. A blade section is considered which is perpendicular to the z-axis of the blade reference system and located at $z = z_o$ in the unloaded condition. The components of inertia forces and moments per unit span acting at this blade section are first determined with respect to axes which are parallel to the blade reference system but whose origin has been displaced a distance $z = z_o$ along the z-axis. The components of the inertia forces are then found relative to axes which are parallel and perpendicular to the blade chord for the given section.

Thus, with ρ being the mass density of the blade material at an elementary cross-sectional area dA, and $\bar{a}_x$, $\bar{a}_y$, $\bar{a}_z$ being the absolute accelerations at dA, the six force and moment components per unit span are:

$$\bar{P}_x = -\int_A \bar{a}_x \, \rho \, dA$$

$$\bar{P}_y = -\int_A \bar{a}_y \, \rho \, dA$$

$$\bar{P}_z = -\int_A \bar{a}_z \, \rho \, dA$$

$$\bar{q}_x = \int_A (\bar{a}_y \, z - \bar{a}_z \, y) \, \rho \, dA$$

$$\bar{q}_y = \int_A \bar{a}_x \, z \, \rho \, dA \qquad\qquad \text{(This moment compo-}$$

$$\bar{q}_z = \int_A \bar{a}_x \, y \, \rho \, dA$$

The moment components about the elastic axes of any blade section are readily computed from these inertia force and moment loadings.

The expressions for $\bar{a}_x$, $\bar{a}_y$, and $\bar{a}_z$ given by Equations (31), (32), and (33) and the expressions for y and z given by Equations (28) and (29) are to be substituted into the above equations. and higher-order terms in the oscillatory variables are to be dropped as in the preceding section. The initial position of a blade element which appears in these expressions is then written in terms of the section coordinates indicated on Figure 1 as

$$y_o = e_y + \eta \cos\beta - \zeta \sin\beta$$

$$z_o = e_z + \eta \sin\beta + \zeta \cos\beta$$

It is convenient to define the following sectional inertia properties for use in the further development:

$$m \equiv \int_A \rho \, dA \qquad\qquad \eta_c \equiv \frac{1}{m} \int_A \eta \, \rho \, dA$$

$$k_1^2 \equiv \frac{1}{m} \int_A \zeta^2 \rho \, dA$$

35

$$k_2^2 \equiv \frac{1}{m} \int_A \eta^2 \rho \, dA \qquad\qquad k^2 \equiv k_1^2 - k_2^2$$

$$\int_A y_0 \, \rho \, dA = m(e_y + \eta_c \cos\beta)$$

$$\int_A \zeta_0 \, \rho \, dA = m(e_\zeta - \eta_c \sin\beta)$$

$$m K_1 \equiv \int_A \zeta_0^2 \, \rho \, dA = m(e_\zeta^2 + 2 e_\zeta \eta_c \sin\beta + k_2^2 \sin^2\beta + k_1^2 \cos^2\beta)$$

$$m K_2 \equiv \int_A y_0^2 \, \rho \, dA = m(e_y^2 - 2 e_y \eta_c \cos\beta + k_2^2 \cos^2\beta + k_1^2 \sin^2\beta)$$

$$m H = \int_A y_0 \, \zeta_0 \, \rho \, dA = m \left\{ e_y e_\zeta + (e_y \sin\beta + e_\zeta \cos\beta) \eta_c \right.$$
$$\left. + (k_2^2 - k_1^2) \sin\beta \cos\beta \right\}$$

$$K \equiv K_1 + K_2 = k^2 + e_y^2 + e_\zeta^2 + 2 \eta_c (e_y \cos\beta + e_\zeta \sin\beta)$$

$$K_2 - K_1 = (k_2^2 - k_1^2) \cos 2\beta + e_y^2 - e_\zeta^2 - 2 \eta_c (e_y \cos\beta - e_\zeta \sin\beta) \ .$$

Also, since the blade is assumed to be symmetric about the chord line, it follows that

$$\int_A \zeta \rho \, dA = 0, \quad \int \eta \zeta \rho \, dA = 0, \quad etc.$$

Using these properties, the sectional properties defined above and the expressions for $\bar{a}_x$, $\bar{a}_y$, and $\bar{a}_\zeta$ (excluding the underlined terms in Equations (31) and (32)), the inertia loading components become

$$\bar{p}_x = \Omega^2 m r \tag{34}$$

$$\bar{P}_y = -m\,\ddot{v}_t + m\,(\eta_c\,\sin\beta)\ddot{\phi}$$

$$-m\left(\theta_A + \hat{\beta}_D\right)\left(C_P + e_{\mathfrak{z}} + \eta_c\,\sin\beta\right)\ddot{\beta}_F$$

$$-m\left\{r - r_D + \theta_A\,e_{DP} - \theta_E\,(e_{\mathfrak{z}} + \eta_c\,\sin\beta)\right\}\ddot{\beta}_D$$

$$+m\left\{\theta_E\,(r-r_P) + e_{\mathfrak{z}} + \eta_c\,\sin\beta\right\}\ddot{\beta}_P$$

$$+\Omega^2 m\left[v_t - (\eta_c\,\sin\beta)\phi - r_D\,\beta_D - \left\{e_{\mathfrak{z}} + \eta_c\,\sin\beta + (\theta_E + \hat{\beta}_F)(r-r_P)\right\}\beta_P\right]$$

$$+\Omega^2 m\left(e_P - \theta_A\,r_P - \hat{\beta}_D\,r_D + e_y + \eta_c\,\cos\beta\right) \tag{35}$$

$$\bar{P}_{\mathfrak{z}} = -m\,\ddot{w}_t - m\,(\eta_c\,\cos\beta)\ddot{\phi}$$

$$-m\left\{r - r_F + \theta_E\,C_P - \hat{\beta}_D\,e_{DP} - (\theta_A + \hat{\beta}_D)(e_y + \eta_c\,\cos\beta)\right\}\ddot{\beta}_F$$

$$-m\,\theta_E\,(e_{DP} + e_y + \eta_c\,\cos\beta)\,\ddot{\beta}_D$$

$$-m\left\{\theta_A\,(r-r_P) + e_y + \eta_c\,\cos\beta\right\}\ddot{\beta}_P$$

$$-\Omega^2 m\left\{r\,\beta_F + (e_P + e_y + \eta_c\,\cos\beta)\,\beta_P\right\}$$

$$-\Omega^2 m\,(\theta_E + \hat{\beta}_F)\,r \tag{36}$$

$$q_z = -m(e_{\bar{z}} - r_c \sin\beta)\ddot{v}_{\bar{z}} - m(e_y + \eta_c \cos\beta)\ddot{w}_{\bar{z}} - m\left\{k^2 - \eta_c(e_y\cos\beta + e_{\bar{z}}\sin\beta)\right\}\ddot{\phi}$$

$$- m\left[(r - r_z - \theta_c r_o - \hat{\beta}_D^2 c_{DP})(e_y + \eta_c\cos\beta) - (\theta_A + \hat{\beta}_D)\left\{K + c_P(e_{\bar{z}} + \eta_c\sin\beta)\right\}\right]\ddot{\beta}_F$$

$$+ m\left[(r - r_D - \theta_A e_{DP})(e_{\bar{z}} - \eta_c\sin\beta) - \theta_E\left\{K + e_{DP}(e_y + \eta_c\cos\beta)\right\}\right]\ddot{\beta}_D$$

$$- m\left[(r - r_P)\left\{\theta_A(e_y + \eta_c\cos\beta) + \theta_E(e_{\bar{z}} + \eta_c\sin\beta)\right\} + K\right]\ddot{\beta}_P$$

$$- \Omega^2 m\left\{(\theta_E - \hat{\beta}_F)r + e_{\bar{z}} + \eta_c\sin\beta\right\}v_{\bar{z}}$$

$$- \Omega^2 m(e_P - \theta_A r_P - \hat{\beta}_D^2 r_D + e_y + \eta_c\cos\beta)w_{\bar{z}}$$

$$- \Omega^2 m\left\{(e_P - \theta_A r_P - \hat{\beta}_D^2 r_D)\eta_c\cos\beta + (k_2^2 - k_1^2)\cos 2\beta + \eta_c(e_y\cos\beta - e_{\bar{z}}\sin\beta)\right\}\phi$$

$$- \Omega^2 m\left[r(e_y - \eta_c\cos\beta)\beta_F - r_D(e_{\bar{z}} + \eta_c\sin\beta)\beta_D\right.$$

$$\left. + \left\{K_2 - K_1 + e_o(e_y - \eta_c\cos\beta) - (\theta_E + \hat{\beta}_F)(r - r_P)(e_{\bar{z}} + \eta_c\sin\beta)\right\}\beta_P\right]$$

$$- \Omega^2 m\left\{H + (e_P - \theta_A r_D - \hat{\beta}_D^2 r_D)(e_{\bar{z}} + \eta_c\sin\beta) + (\theta_E + \hat{\beta}_F)r(e_y + \eta_c\cos\beta)\right\}$$

$$\tag{37}$$

$$\bar{q}_y = -\Omega^2 mr\left\{w_{\bar{z}} + \eta_c\cos\beta\cdot\phi\right\} - \Omega^2 mr(e_{\bar{z}} + \eta_c\sin\beta) \tag{38}$$

and

$$\bar{q}_{\bar{z}} = -\Omega^2 mr\left\{v_{\bar{z}} - \eta_c\sin\beta\cdot\phi\right\} - \Omega^2 mr(e_y - \eta_c\cos\beta) \tag{39}$$

38

In the expressions for each of the components, the last term does not depend on any oscillatory displacement or its time derivative. Therefore, these are steady terms and will be designated $\hat{p}_x$, $\hat{p}_y$, $\hat{p}_j$, $\hat{q}_x$, $\hat{q}_y$, and $\hat{q}_j$ for easy reference. (Note that $\hat{p}_x = \bar{p}_x = \Omega^2 m r$.)

In the subsequent application of the associated matrix method for finding vibration characteristics, the blade is divided into spanwise segments. The treatment of individual segments employs axes which are parallel and perpendicular to the blade chord of the segment (in the unloaded condition). The figure below indicates the resolution of the loadings and deformations into components which are parallel and perpendicular to the chord at a particular segment.
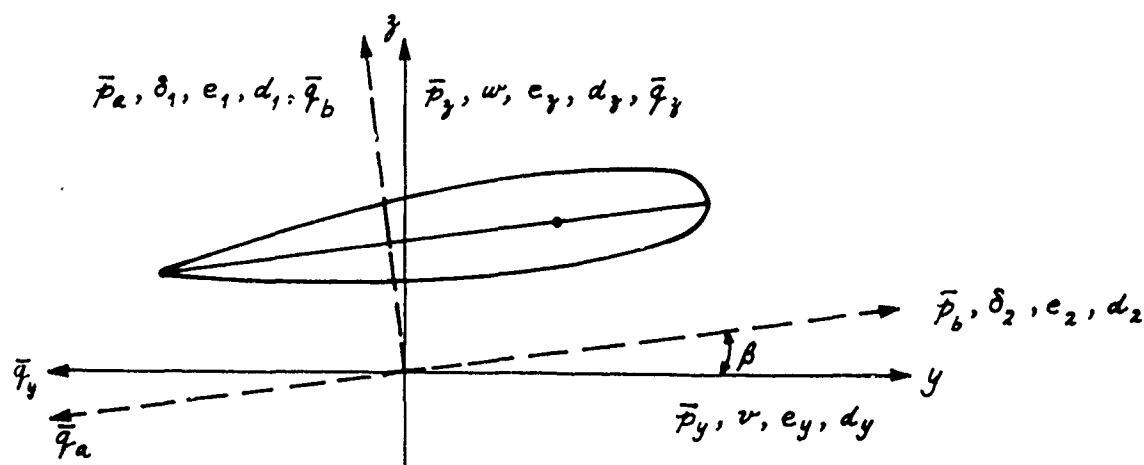
Figure 5. RESOLUTIONS OF LOADS AND DISPLACEMENTS PARALLEL AND PERPENDICULAR TO LOCAL CHORD.

The deformations of the elastic axis due to bending are denoted by δ_1 and δ_2 and the components of the total deformation due to the combination of bending and torsion by δ_{1t} and δ_{2t}. The initial coordinates of the elastic center and the axis of built-in twist are denoted by (e_1, e_2) and (d_1, d_2) respectively. These components and their derivatives with respect to x can be found from the components relative to the x-, y-, j-axes by the following transformations:

39

$$(\delta_{1t}, \; S_1, \; \delta_1', \; \text{or} \; \delta_1'') = (w_t, \; w, \; w', \; \text{or} \; w'') \cos\beta$$

$$- (v_t, \; v, \; v' \; \text{or} \; v'') \sin\beta$$

$$(\delta_{2t}, \; \delta_2, \; \delta_2' \; \text{or} \; \delta_2'') = (w_t, \; w, \; w', \; \text{or} \; w'') \sin\beta$$

$$+ (v_t, \; v, \; v', \; \text{or} \; v'') \cos\beta$$

$$(e_1 \; \text{or} \; d_1) = (e_{\jmath} \; \text{or} \; d_{\jmath}') \cos\beta - (e_y \; \text{or} \; d_y') \sin\beta$$

$$(e_2 \; \text{or} \; d_2') = (e_{\jmath} \; \text{or} \; d_{\jmath}') \sin\beta + (e_y \; \text{or} \; d_y') \cos\beta$$

$$\tag{40}$$

Expressions given below for the components of the force and moment loadings with respect to axes which are parallel and perpendicular to the blade chord are obtained by similar rotation transformations. It should be noted on the diagram that $\bar{p}_a$ and $\bar{p}_b$ are the inertia force loading components perpendicular and parallel to the chord respectively but that $\bar{q}_a$ and $\bar{q}_b$ are the moment loading components taken respectively about axes which are parallel and perpendicular to the chord.

$$\bar{p}_a = \bar{p}_{\jmath} \cos\beta - \bar{p}_y \sin\beta$$

$$= - m \, \ddot{\delta}_{1t} - m \, \eta_c \, \ddot{\phi}$$

$$- m \left\{ (r - r_F + \theta_E C_P - \hat{\beta}_D e_{DP}) \cos\beta - (\theta_A + \hat{\beta}_D)(C_P \sin\beta + e_2 + \eta_c) \right\} \ddot{\delta}_F$$

$$+ m \left\{ (r - r_D) \sin\beta - e_{DP}(\theta_E \cos\beta - \theta_A \sin\beta) - \theta_E (e_2 + \eta_c) \right\} \ddot{\beta}_D$$

$$- m \left\{ (r - r_D)(\theta_E \sin\beta + \theta_A \cos\beta) + e_2 + \eta_c \right\} \ddot{\beta}_P$$

$$- \Omega^2 m \left\{ \delta_{2t} \cos\beta \sin\beta - \delta_{1t} \sin^2\beta - (\eta_c \sin^2\beta) \phi \right\}$$

$$- \Omega^2 m r (\cos\beta) \delta_F - \Omega^2 m (r_D \sin\beta) \beta_D$$

$$- \Omega^2 m \left\{ c_P \cos\beta + (e_2 + \eta_c) \cos 2\beta - e_1 \sin 2\beta - (\theta_E + \hat{\beta}_F)(r - r_P) \sin\beta \right\} \beta_P$$

$$+ \dot{b}_{\jmath} \cos\beta - \hat{p}_y \sin\beta$$

$$\tag{41}$$

40

$$\bar{p}_b = \bar{p}_{\bar{3}}\, \sin\beta + \bar{p}_y\, \cos\beta$$

$$= -m\,\ddot{\delta}_{2t} - m\left\{(r-r_F+\theta_E\,C_P-\hat{\beta}_D\,e_{DP})\,\sin\beta + (\theta_A+\hat{\beta}_D)(C_P\cos\beta+e_1)\right\}\ddot{s}_z$$

$$-m\left\{(r-r_D)\cos\beta + e_{DP}(\theta_E\,\sin\beta+\theta_A\,\cos\beta)-\theta_E\,e_1\right\}\ddot{\beta}_D$$

$$+m\left\{(r-r_P)(\theta_E\cos\beta-\theta_A\,\sin\beta)+e_1\right\}\ddot{\beta}_P$$

$$+\Omega^2 m\left\{\delta_{2t}\cos^2\beta-\delta_{1t}\sin\beta\cos\beta-(\eta_c\,\sin\beta\cos\beta)\phi\right\}$$

$$-\Omega^2 mr\,(\sin\beta)\beta_F-\Omega^2 m(r_D\cos\beta)\beta_D$$

$$-\Omega^2 m\left\{e_P\sin\beta + (e_2+\eta_c)\,\sin 2\beta + e_1\cos 2\beta + (\theta_E+\hat{\beta}_F)(r-r_P)\cos\beta\right\}\ddot{s}_P$$

$$+\hat{p}_{\bar{3}}\,\sin\beta + \hat{p}_y\,\cos\beta \tag{42}$$

$$\bar{q}_a = \bar{q}_y\,\cos\beta - \bar{q}_{\bar{3}}\,\sin\beta$$

$$= -\Omega^2 mr\,\delta_{1t} + \hat{q}_y\,\cos\beta - \hat{q}_{\bar{3}}\,\sin\beta \tag{43}$$

$$\bar{q}_b = \bar{q}_y\,\sin\beta + \bar{q}_{\bar{3}}\,\cos\beta$$

$$= -\Omega^2 mr\,\delta_{2t} + \hat{q}_y\,\sin\beta + \hat{q}_{\bar{3}}\,\cos\beta . \tag{44}$$

When the quantities C_y and $C_{\bar{3}}$ are defined as below,

$$C_y \equiv e_y + \eta_c\,\cos\beta = (e_2+\eta_c)\cos\beta - e_1\,\sin\beta$$

$$C_{\bar{3}} \equiv e_{\bar{3}} + \eta_c\,\sin\beta = (e_2+\eta_c)\,\sin\beta + e_1\,\cos\beta ,$$

it follows that

$$\left(\begin{array}{l} C_y\cos\beta - C_{\bar{3}}\sin\beta = (e_2+\eta_c)\cos 2\beta - e_1\sin 2\beta \\[2em] C_y\sin\beta + C_{\bar{3}}\cos\beta = (e_2+\eta_c)\sin 2\beta + e_1\cos 2\beta \end{array}\right)$$

$$\bar{q}_2 = -m(e_2 + \eta_c)\ddot{\delta}_{1t} + m c_2 \ddot{\delta}_{2t} - m(k^2 + \eta_c e_2)\ddot{\phi}$$

$$-m\left\{(r - r_F + \theta_E c_p - \hat{\beta}_D c_{DP}) c_y - (\theta_A + \hat{\beta}_D)(K + c_p c_{\gamma})\right\}\ddot{\beta}_F$$

$$-m\left\{(r - r_D + \theta_A e_{DP}) c_{\gamma} - \theta_E(K + e_{DP} c_y)\right\}\ddot{\beta}_D$$

$$-m\left\{(r - r_o)(\theta_A c_y + \theta_E c_{\gamma}) + K\right\}\ddot{\beta}_P$$

$$-\Omega^2 m\left\{(e_2 + \eta_c)\cos 2\beta - e_1 \sin 2\beta\right.$$

$$\left. + (e_p - \theta_A r_p - \hat{\beta}_D r_D)\cos\beta - (\theta_E + \hat{\beta}_F) r \sin\beta\right\}\delta_{1t}$$

$$-\Omega^2 m\left\{(e_2 + \eta_c)\sin 2\beta + e_1 \cos 2\beta\right.$$

$$\left. + (e_p - \theta_A r_p - \hat{\beta}_D r_D)\sin\beta + (\theta_E + \hat{\beta}_F) r \cos\beta\right\}\delta_{2t}$$

$$-\Omega^2 m\left\{(e_p - \theta_A r_p - \hat{\beta}_D r_D)\eta_c \cos\beta + (k_2^2 - k_1^2)\cos 2\beta\right.$$

$$\left. + \eta_c (e_2 \cos 2\beta - e_1 \sin 2\beta)\right\}\phi$$

$$-\Omega^2 m r\, c_y \beta_F + \Omega^2 m r_D\, c_{\gamma}\, \beta_D$$

$$-\Omega^2 m\left\{K_2 - K_1 + e_p c_y - (\theta_E + \hat{\beta}_F)(r - r_p) c_{\gamma}\right\}\beta_P + \hat{q}_x \ . \tag{45}$$

42

$$\hat{p}_x = \bar{p}_x = \Omega^2 m\, r$$

$$\hat{p}_y = \Omega^2 m\, (e_P - \theta_A\, r_P - \hat{\beta}_D\, r_D + C_y)$$

$$\hat{p}_\delta = -\Omega^2 m\, (\theta_E + \hat{\beta}_F)\, r$$

$$\hat{q}_x = -\Omega^2 m\, \left\{ H + (e_P - \theta_A\, r_P - \hat{\beta}_D\, r_D)\, C_\gamma + (\theta_E + \beta_F)\, r\, C_y \right\}$$

$$\hat{q}_y = -\Omega^2 m\, r\, C_\gamma$$

$$\hat{q}_\delta = -\Omega^2 m\, r\, C_y$$

(46)

In the computational setup, the blade is divided into a number of short bays and the mass of each whole bay is considered to be concentrated at the mid-span of the bay. By considering m to be the mass of one bay (equal to the product of the span of the bay and the average mass per unit span of the bay), all the above expressions for the p's and q's express correctly the inertia loads of one bay.

ACTING BENDING AND TORSIONAL MOMENTS

In this section, expressions are derived for the bending and torsional moments acting at any blade section within a given spanwise segment or bay of the blade as a function of the loads applied at the outboard end of the bay and the deformations in the bay. These expressions for the acting moments are combined with expressions for the elastic restraining moments in a later section in order to obtain differential equations from which the total deformations across each bay can be determined. This solution for the deformations in an "elastic bay" is carried out considering the bay weightless because the effects of inertia forces are introduced as concentrated loads at the junctions between bays.

Consider a short bay of a blade between $r = r''^{'}$ and $r = r'' > r''^{''}$ with constant β, e_y, and e_γ. These constant geometric parameters are designated $\beta'^{'}$, $e_y'^{'}$, and $e_\gamma'^{'}$. The total load acting on the outboard end, where $r = r'^{'}$, has the force components $\bar{P}_x$, $\bar{P}_y$, and $\bar{P}_\delta$ and the moment components $\bar{Q}_x$, $\bar{Q}_y$, and $\bar{Q}_\gamma$. These six components can be found

43

respectively by integrating the inertia loadings p_x, p_y, p_y, q_x, q_y, and $\hat{p}_y$, from $r-r'^{1}$ to the tip. The pitching moment is taken about the intersection of the x-axis and the plane of the outboard end of the cross section. (As usual, $\bar{Q}_y$ is positive in the <u>negative</u> y-direction while the force components and other moment components are positive in the positive directions indicated by their subscripts.) When all terms containing any oscillatory displacement or its time derivative as a factor are dropped out, the load components are designated by $\hat{P}_x$, $\hat{P}_y$, $\hat{P}_y$, $\hat{Q}_x$, $\hat{Q}_y$ and $\hat{Q}_y$ and may be called the steady portions of $\bar{P}_x$, $\bar{P}_y$, $\bar{P}_y$, $\bar{Q}_x$, $\bar{Q}_y$, and $\bar{q}_y$, respectively.

A local coordinate system ($x(r)$, $y(r)$, $y(r)$) is introduced in considering the moments acting on a section at

$$r = r^{(j)} - s \qquad\qquad 0 < s < r^{(j)} - r^{(j-1)}.$$

The origin of this system is at the point where the elastic axis intersects the section. Let $\bar{Q}_{x(r)}$, $\bar{Q}_{y(r)}$, and $\bar{Q}_{y(r)}$ be the components of the total moment acting on the section referred to these axes. ($\bar{Q}_{x(r)}$ and $\bar{Q}_{y(r)}$ are taken positive in the positive $x(r)$ and $y(r)$-directions but $\bar{q}_{y(r)}$ is taken positive in the negative $y(r)$-direction.) It then follows that

$$\bar{Q}_{x(r)} = \bar{Q}_x + (e_y^{(j)} + \bar{w}_r)\,\bar{P}_y - (e_y^{(j)} + \bar{v}_r)\,\bar{P}_y$$

$$\bar{Q}_{y(r)} = \bar{Q}_y + (e_y^{(j)} + \bar{w}_r)\,\bar{P}_x + s\,\bar{P}_y$$

$$\bar{Q}_{y(r)} = \bar{Q}_y + (e_y^{(j)} + \bar{v}_r)\,\bar{P}_x + s\,\bar{P}_y$$

where it is understood that $\bar{P}_x$, $\bar{Q}_x$, $\bar{P}_y$, etc., are force and moment components applied at station r r'^{j}, while $\bar{v}_r$ and $\bar{w}_r$ are elastic axis deflections at station r. When second-order terms in the oscillatory variables are dropped, these equations reduce to the following:

$$\bar{Q}_{x(r)} = \bar{Q}_x + e_y^{(j)}\,\bar{P}_y + \bar{w}_r\,\hat{P}_y\quad e_y^{(j)}\,\bar{P}_y - \bar{v}_r\,\hat{P}_y$$

$$\bar{Q}_{y(r)} = \bar{Q}_y + e_y^{(j)}\,\bar{P}_x + w_r\,\hat{P}_x + s\,\bar{P}_y$$

$$\bar{Q}_{y(r)} = \bar{Q}_y + e_y^{(j)}\,\bar{P}_z + \bar{v}_r\,\hat{P}_x + s\,\bar{P}_y \quad.$$

Here the steady deflections of the elastic axis have been included in the definitions of $e_y^{(i)}$ and $e_y^{(i)}$. Since the blade section is not normal to the x-axis when there is bending deformation, and the blade chord is at an angle $(\beta^{(i)}+\phi)$ relative to the $y(r)$-axis, the above moments must be resolved accordingly. The true local flatwise bending, chordwise bending and torsional moments (which are to be equated to the elastic restoring moments $\bar{M}_1$, $\bar{M}_2$ and $\bar{Q}$) are given by

$$\bar{M}_1 = \left(\bar{Q}_{y(r)} + \bar{Q}_{x(r)} v'\right) \cos\left(\beta^{(i)} + \phi\right) - \left(\bar{Q}_{3(r)} - \bar{Q}_{x(r)} w'\right) \sin\left(\beta^{(i)} + \phi\right)$$

$$\bar{M}_2 = \left(\bar{Q}_{y(r)} + \bar{Q}_{x(r)} v'\right) \sin\left(\beta^{(i)} + \phi\right) + \left(\bar{Q}_{3(r)} - \bar{Q}_{x(r)} w'\right) \cos\left(\beta^{(i)} + \phi\right)$$

and

$$\bar{Q} = \bar{Q}_{x(r)} - \bar{Q}_{y(r)} v' + \bar{Q}_{3(r)} w'$$

respectively. After dropping small terms of second order, substituting for $\bar{Q}_{x(r)}$, $\bar{Q}_{y(r)}$, and $\bar{Q}_{3(r)}$, and using the conversion formulas in Equation (40), the above equations become

$$\bar{M}_1 = \bar{Q}_a + e_1^{(i)} \bar{P}_x + \hat{P}_x \,\bar{\delta}_{1t} + s\bar{P}_a + \tilde{Q}_x \delta_2' - (\tilde{Q}_b + s\hat{P}_b)\phi \tag{47}$$

$$\bar{M}_2 = \bar{Q}_b + e_2^{(i)} \bar{P}_x + \hat{P}_x \bar{\delta}_{2t} + s\bar{P}_b - \tilde{Q}_x \delta_1' + (\tilde{Q}_a + s\hat{P}_a)\phi \tag{48}$$

$$\bar{Q} = \bar{Q}_x + e_1^{(i)} \bar{P}_b - e_2^{(i)} \bar{P}_a + \hat{P}_b \,\bar{\delta}_{1t} - \hat{P}_a \bar{\delta}_{2t} + (\tilde{Q}_b + s\hat{P}_b)\delta_1' - (\tilde{Q}_a + s\hat{P}_a)\delta_2' \tag{49}$$

where

$$\bar{P}_a = \bar{P}_y \cos\beta^{(i)} - \bar{P}_y \sin\beta^{(i)}$$

$$\bar{P}_b = \bar{P}_y \sin\beta^{(i)} + \bar{P}_y \cos\beta^{(i)}$$

$$\bar{Q}_a = \bar{Q}_y \cos\beta^{(i)} - \bar{Q}_y \sin\beta^{(i)}$$

$$\bar{Q}_b = \bar{Q}_y \sin\beta^{(i)} + \bar{Q}_y \cos\beta^{(i)}$$

45

$$\tilde{P}_a = \hat{P}_z \cos\beta^{(i)} - \hat{P}_y \sin\beta^{(i)}$$

$$\hat{P}_b = \hat{P}_z \sin\beta^{(i)} + \hat{P}_y \cos\beta^{(i)}$$

$$\tilde{Q}_a = (\hat{Q}_y + e_z^{(i)} \hat{P}_x) \cos\beta^{(i)} - (\hat{Q}_z + e_y^{(i)} \hat{P}_x) \sin\beta^{(i)}$$

$$\tilde{Q}_b = (\hat{Q}_y + e_z^{(i)} \hat{P}_x) \sin\beta^{(i)} + (\hat{Q}_z + e_y^{(i)} \hat{P}_x) \cos\beta^{(i)}$$

$$\tilde{Q}_x = \hat{Q}_x + e_z^{(i)} \hat{P}_y - e_y^{(i)} \hat{P}_z \ .$$

It will be recalled that

$$v_r \equiv v - \Delta_y \ , \qquad w_t \equiv w + \Delta_z \ ,$$

$$\Delta_y \equiv e_z \phi - \int_o^{x_o} e_z \phi' \, d x_o \ , \qquad \text{and}$$

$$\Delta_z \equiv e_y \phi - \int_o^{x_o} e_y \phi' \, d x_o . \qquad (\phi = 0 \ \text{at} \ x_o = 0)$$

Once the shape of ϕ vs. x_o is estimated, say ϕ_{est}, the following two quantities can be computed at any desired r :

$$E_z = e_z - \frac{1}{\phi_{est}} \int_o^{x_o} e_z \, \phi'_{est} \, d x_o$$

$$E_y = e_y - \frac{1}{\phi_{est}} \int_o^{x_o} e_y \, \phi'_{est} \, d x_o$$

Then, at the desired x_o ,

$$\Delta_y = E_z \phi$$

$$\Delta_z = E_y \phi$$

$$v_t = v - E_z \phi$$

46

$$u^{\sim}_{\rho} \quad u^{\sim} + \xi_y \, \phi$$

$$\delta_{1t} = w_\xi \, \cos\beta - v_\xi \, \sin\beta = \delta_1 + E_2 \, \phi$$

$$\delta_{2t} = w_\xi \, \sin\beta + v_\xi \, \cos\beta = \delta_2 - E_1 \, \phi$$

where
$$\begin{cases} E_1 = E_\xi \, \cos\beta - E_y \, \sin\beta \\[2mm] E_2 = E_\xi \, \sin\beta + E_y \, \cos\beta \end{cases}$$

Since the steady portions of the moment components only cause steady displacements, they may be dropped when only the oscillatory displacements are being considered. Thus, the following expressions for the oscillatory moment components are obtained from Equations (47), (48), and (49):

$$M_1 = Q_a + \hat{P}_\xi \, \delta_1 + \tilde{Q}_\xi \, \delta_2' - (\tilde{Q}_b - E_2 \, \hat{P}_\xi) \, \phi + (P_a - \hat{P}_b \, \phi) \, s \tag{50}$$

$$M_2 = Q_b + \hat{P}_\xi \, \delta_2 - \tilde{Q}_\xi \, \delta_1' + (\tilde{Q}_a - E_1 \, \hat{P}_\xi) \, \phi + (P_b + \hat{P}_a \, \phi) \, s \tag{51}$$

$$Q = Q_\xi - e_1^{(1)} \, P_b - e_2^{(1)} \, P_a + \hat{P}_b \, \delta_1 - \hat{P}_a \, \delta_2 + \tilde{Q}_b \, \delta_1' - \tilde{Q}_a \, \delta_2'$$

$$+ (\hat{P}_b \, \delta_1' - \hat{P}_a \, \delta_2') \, s \tag{52}$$

where

$$P_a = \bar{P}_a - \hat{P}_a \qquad\qquad P_b = \bar{P}_b - \hat{P}_b \qquad\qquad (P_\xi = \bar{P}_\xi - \hat{P}_\xi = 0)$$

$$Q_a = \bar{Q}_a - \hat{Q}_a \qquad\qquad \left(\hat{Q}_a = \hat{Q}_y \, \cos\beta^{(1)} - \hat{Q}_\xi \, \sin\beta^{(1)} \right)$$

$$Q_b = \bar{Q}_b - \hat{Q}_b \qquad\qquad \left(\hat{Q}_b = \hat{Q}_y \, \sin\beta^{(1)} - \hat{Q}_\xi \, \cos\beta^{(1)} \right)$$

$$Q_\xi = \bar{Q}_\xi - \hat{Q}_\xi$$

... where for ... distribution ... . When there is a total number of $\mathcal{S}$ concentrated masses outboard of $r = r^{(i)}$, use of the formulas in Equation (4b) (with $m^{(i)}$ being the mass of the ith mass bay concentrated at $r = r^{(i)}$) yields

$$\hat{P}_x = \Omega^2 \sum_{i=1}^{\mathcal{S}} m^{(i)} r^{(i)} \qquad (i=1 \text{ for the tip mass bay.})$$

$$\hat{P}_a = -(\Omega^2 \cos\beta^{(j)})(\theta_E + \hat{\beta}_F)\sum_{i=1}^{\mathcal{S}} m^{(i)} r^{(i)}$$

$$-(\Omega^2 \sin\beta^{(j)})\left\{\sum_{i=1}^{\mathcal{S}} m^{(i)} C_y^{(i)} + (e_P - \theta_A r_P - \hat{\beta}_D r_D)\sum_{i=1}^{\mathcal{S}} m^{(i)}\right\}$$

$$\hat{P}_b = -(\Omega^2 \sin\beta^{(j)})(\theta_E + \hat{\beta}_F)\sum_{i=1}^{\mathcal{S}} m^{(i)} r^{(i)}$$

$$+(\Omega^2 \cos\beta^{(j)})\left\{\sum_{i=1}^{\mathcal{S}} m^{(i)} C_y^{(i)} + (e_P - \theta_A r_P - \hat{\beta}_D r_D)\sum_{i=1}^{\mathcal{S}} m^{(i)}\right\}$$

$$\tilde{Q}_x = -\Omega^2 \left\{\sum_{i=1}^{\mathcal{S}} m^{(i)} H^{(i)} + (e_P - \theta_A r_P - \hat{\beta}_D r_D)\sum_{i=1}^{\mathcal{S}} m^{(i)} C_y^{(i)}\right.$$

$$\left.+ (\theta_E + \hat{\beta}_F)\sum_{i=1}^{\mathcal{S}} m^{(i)} r^{(i)} C_y^{(i)}\right\}$$

$$+ \Omega^2 e_y^{(j)}\left\{\sum_{i=1}^{\mathcal{S}} m^{(i)} C_y^{(i)} + (e_P - \theta_A r_P - \hat{\beta}_D r_D)\sum_{i=1}^{\mathcal{S}} m^{(i)}\right\}$$

$$- \Omega^2 e_y^{(j)}(\theta_E + \hat{\beta}_F)\sum_{i=1}^{\mathcal{S}} m^{(i)} r^{(i)}$$

$$\tilde{Q}_a = -(\Omega^2 \cos\beta^{(j)})\left(\sum_{i=1}^{\mathcal{S}} m^{(i)} r^{(i)} C_y^{(i)} - e_y^{(j)}\sum_{i=1}^{\mathcal{S}} m^{(i)} r^{(i)}\right)$$

$$+(\Omega^2 \sin\beta^{(j)})\left(\sum_{i=1}^{\mathcal{S}} m^{(i)} r^{(i)} C_y^{(i)} - e_y^{(j)}\sum_{i=1}^{\mathcal{S}} m^{(i)} r^{(i)}\right)$$

and

$$\check{Q}_b = -(\Omega^2 \sin\beta^{(j)})\left(\sum_{i=1}^{\mathcal{S}} m^{(i)} r^{(i)} C_y^{(i)} - e_y^{(j)}\sum_{i=1}^{\mathcal{S}} m^{(i)} r^{(i)}\right)$$

$$-(\Omega^2 \cos\beta^{(j)})\left(\sum_{i=1}^{\mathcal{S}} m^{(i)} r^{(i)} C_y^{(i)} - e_y^{(j)}\sum_{i=1}^{\mathcal{S}} m^{(i)} r^{(i)}\right)$$

48

The vibration analysis is carried out using a model in which the blade is divided into spanwise segments or bays, each of which is considered to be a uniform beam without twist. The actual twist will be taken into account in the model by introducing discontinuities in twist at the junction between bays as indicated in the diagram below.

$$\{\Delta\}^{(i.b.)} = [R] \{\Delta\}^{(o.b.)}$$

Figure 6. ANALYTICAL REPRESENTATION OF BLADE TWIST.

49

The elements of the column matrix $\{\Delta\}$, which are displayed on Figure 6 are the flatwise and chordwise force components (F_a , P_b); the bending moments (Q_a , Q_b); the torsional moment (Q_x); the flatwise deflection and flatwise slope (δ_1 , δ_1'); the chordwise deflection and chordwise slope (δ_2 , δ_2'); the torsional deflection ϕ ; and the flapping, lead-lag, and pitching angles (β_F , β_D , β_P).

Some of these quantities will change where there is a twist continuity because the flatwise and chordwise directions are defined differently on the inboard and outboard sides of the junction. The changes in $\{\Delta\}$ across the twist discontinuity can be found by multiplying by a rotation matrix $[R]$. The nonzero elements of this 13 by 13 matrix are:

$$R_{ii} = \cos\left(\beta^{(i.b.)} - \beta^{(o.b.)}\right) = a , \qquad \text{for } i = 1 \text{ to } 8 ;$$

$$R_{15} = R_{26} = R_{37} = R_{48} = -\sin\left(\beta^{(i.b.)} - \beta^{(o.b.)}\right) = -b ;$$

$$R_{51} = R_{62} = R_{73} = R_{84} = \sin\left(\beta^{(i.b.)} - \beta^{(o.b.)}\right) = b ;$$

and

$$R_{ii} = 1 , \qquad \text{for } i = 9 \text{ to } 13 .$$

The form of the $[R]$ matrix is indicated explicitly on Figure 6.

ELASTIC MATRIX

The 13 by 13 elastic matrix $[E]$ relates column matrices for the inboard and outboard ends of an elastic bay of span ℓ according to

$$\{\Delta\}^{(i.e.)} = [E] \{\Delta\}^{(o.e.)} \tag{53}$$

where $\{\Delta\}$ is the column matrix indicated in Figure 6 . Since P_a , P_b , Q_x , β_F , β_D and β_P do not change across any elastic bay, the only nonzero elements in the 1st, 5th, 9th, 11th, 12th and 13th rows of $[E]$ are

$$E_{11} = E_{55} = E_{99} = E_{11,11} = E_{12,12} = E_{13,13} = 1 .$$

50

$$Q_a^{(ie)} = Q_a^{(oe)} + \ell P_a^{(oe)}$$

and

$$Q_b^{(ie)} = Q_b^{(oe)} + \ell P_b^{(oe)}$$

there are two nonzero elements in both the 2nd and 6th rows; they are

$$E_{22} = E_{66} = 1 \quad \text{and} \quad E_{21} = E_{65} = \ell .$$

The rest of the rows of elements depend on the elastic properties of the bay and are derived in the following paragraphs.

The differential equations for the deformations of an elastic bay are obtained by equating the acting moment components M_1, M_2 and Q, as given by Equations (50) through (52), to the corresponding restoring moment components, as given by Equation (18) through (20) of the blade elastic behavior analysis. In the latter equations, the steady terms are dropped (namely, $-Te_A$ in M_2 and $-T(\ell_A^2 - e_t e_A)\beta'$ in Q). With δ_1'', δ_2'', α_1' and α_2' as defined in Equation (40), $T = \hat{P}_x$,

$$B \equiv (E B_2 - e_t E I_2) \beta'$$

and

$$A \equiv G J + \hat{P}_x \ell_A^2 + B \alpha_1' + (E B_1 - 2 e_t E B_2 + e_t^2 E I_2)(\beta')^2 ,$$

the oscillatory restoring moment components may be written

$$M_1 = E I_1 (\delta_1'' + \alpha_2' \phi')$$

$$M_2 = E I_2 \delta_2'' - (E I_2 \alpha_1' + B) \phi'$$

$$Q = A \phi' - B \delta_2''$$

$$= \left\{ A - B \left(\alpha_1' + \frac{B}{E I_2} \right) \right\} \phi' - \frac{B}{E I_2} M_2$$

$$= C \phi' - \frac{B}{E I_2} M_2$$

51

where

$$C \equiv GJ + \dot{P}_x \, \ell_A^2 + \left(EB_1 - \frac{EB_2}{EI_2} EB_2 \right) (\beta')^2$$

It can be seen that when the expressions for M_1, M_2, and Q given in Equations (50) and (51) are substituted into the above equations, three second-order simultaneous linear differential equations for δ_1, δ_2 and ϕ are obtained in which some of the coefficients vary with s .*

In the expressions for M_1, M_2, and Q given in Equations (50) through (52), the terms containing δ_1', δ_2', δ_1, δ_2 or ϕ as a factor account for the effects of the variations of the acting moment components along the bay due to the variations of the deformations along the bay. Thus, by keeping the bay lengths short, the variations of δ_1, δ_1', δ_2, δ_2', or ϕ within each bay may be assumed to be linear in the evaluation of M_1, M_2 and Q along the bay. By using

$$\delta_{avg}' \equiv \frac{1}{\ell}\left(\delta^{(o.e.)} - \delta^{(i.e.)} \right), \qquad \delta = \delta^{(o.e.)} - \delta_{avg}' \, s \quad ;$$

$$\delta_{avg}'' \equiv \frac{1}{\ell}\left\{ (\delta')^{(o.e.)} - (\delta')^{(i.e.)} \right\}, \qquad \delta' = (\delta')^{(o.e.)} - \delta_{avg}'' \, s \quad ;$$

and

$$\phi_{avg}' \equiv \frac{1}{\ell}\left(\phi^{(o.e.)} - \phi^{(i.e.)} \right), \qquad \phi = \phi^{(o.e.)} - \phi_{avg}' \, s$$

the expressions for M_1, M_2 and Q in Equations (50) through (52) become

$$M_1 = A_1 + A_2 s + A_3 s^2$$

$$M_2 = D_1 + D_2 s - D_3 s^2$$

$$Q = \lambda_1 + \lambda_2 s - \lambda_3 s^2$$

---

* Since each elastic bay is considered to be untwisted, it follows (within each bay) that

$$\left(\delta_1', \ \delta_2' \ or \ \phi' \right) = \frac{d}{dr}\left(\delta_1, \ \delta_2, \ or \ \phi \right) = -\frac{d}{ds}\left(\delta_1, \ \delta_2, \ or \ \phi \right)$$

and

$$\left(\delta_1'' \ or \ \delta_2'' \right) = \frac{d^2}{dr^2}\left(\delta_1 \ or \ \delta_2 \right) = \frac{d^2}{ds^2}\left(\delta_1 \ or \ \delta_2 \right) .$$

52

where, with all P's and Q's understood to be $P^{(o.e.)}$'s and $Q^{(o.e.)}$'s , the coefficients are

$$A_1 = Q_a + \hat{P}_x \delta_1^{(a.e.)} + \tilde{Q}_x (\delta_2')^{(o.e.)} - (\tilde{Q}_b - E_2 \hat{P}_x) \phi^{(o.e.)}$$

$$A_2 = P_a - \hat{P}_b \phi^{(o.e.)} - \hat{P}_x \delta_{1_{avg}}' - \tilde{Q}_x \delta_{2_{avg}}'' + (\tilde{Q}_b - E_2 \hat{P}_x) \phi_{avg}'$$

$$A_3 = \hat{P}_b \phi_{avg}'$$

$$D_1 = Q_b + \hat{P}_x \delta_2^{(o.e.)} - \tilde{Q}_x (\delta_1')^{(o.e.)} + (\tilde{Q}_a - E_1 \hat{P}_x) \phi^{(o.e.)}$$

$$D_2 = P_b + \hat{P}_a \phi^{(o.e.)} - \hat{P}_x \delta_{2_{avg}}' + \tilde{Q}_x \delta_{1_{avg}}'' - (\tilde{Q}_a - E_1 \hat{P}_x) \phi_{avg}'$$

$$D_3 = \hat{P}_a \phi_{avg}''$$

$$\lambda_1 = Q_x + e_1 P_b - e_2 P_a + \hat{P}_b \delta_1^{(a.e.)} - \hat{P}_a \delta_2^{(o.e.)}$$
$$+ \tilde{Q}_b (\delta_1')^{(o.e.)} - \tilde{Q}_a (\delta_2')^{(o.e.)} + (E_1 \hat{P}_a + E_2 \hat{P}_b) \phi^{(o.e.)}$$

$$\lambda_2 = \hat{P}_b (\delta_1')^{(o.e.)} - \hat{P}_a (\delta_2')^{(o.e.)} - \hat{P}_b \delta_{1_{avg}}' + \hat{P}_a \delta_{2_{avg}}' - \tilde{Q}_b \delta_{1_{avg}}'' + \tilde{Q}_a \delta_{2_{avg}}''$$
$$- (E_1 \hat{P}_a + E_2 \hat{P}_b) \phi_{avg}'$$

and

$$\lambda_3 = \hat{P}_b \delta_{1_{avg}}'' - \hat{P}_a \delta_{2_{avg}}'' \quad .$$

53

Consequently, the desired differential equations are

$$\delta_1' = -\alpha_2\,\phi' + \frac{1}{EI_1}\left(A_1 + A_2 s + A_3 s^2\right)$$

$$\delta_2' = \left(\alpha_1' + \frac{B}{EI_2}\right)\phi' - \frac{1}{EI_2}\left(D_1 + D_2 s + D_3 s^2\right)$$

$$\phi' = \left\{\lambda_1 + \lambda_2 s - \lambda_3 s^2 + \frac{B}{EI_2}\left(D_1 + D_2 s - D_3 s^2\right)\right\}\frac{1}{C}\quad.$$

Then, by subsequent integrations and use of boundary conditions at $r = r^{(o\,e)}$ or $s = 0$, it follows that

$$\delta_1' = \left(\delta_1'\right)^{(oe)} - \alpha_2'\left(\phi - \phi^{(o.e.)}\right) - \frac{s}{EI_1}\left(A_1 + \frac{1}{2}A_2 s + \frac{1}{3}A_3 s^2\right)$$

$$\delta_1 = \delta_1^{(oe)} - \left(\delta_1'\right)^{(oe)} s - \alpha_2'\left(\int\phi\,ds - \phi^{(a.e.)}s\right)$$

$$+ \frac{s^2}{2EI_1}\left(A_1 - \frac{1}{3}A_2 s + \frac{1}{6}A_3 s^2\right)$$

$$\delta_2' = \left(\delta_2'\right)^{(oe)} + \left(\alpha_1' + \frac{B}{EI_2}\right)\left(\phi - \phi^{(a.e.)}\right)$$

$$- \frac{s}{EI_2}\left(D_1 + \frac{1}{2}D_2 s - \frac{1}{3}D_3 s^2\right)$$

$$\delta_2 = \delta_2^{(oe)} - \left(\delta_2'\right)^{(oe)} s - \left(\alpha_1' + \frac{B}{EI_2}\right)\left(\int\phi\,ds - \phi^{(o.e.)}s\right)$$

$$+ \frac{s^2}{2EI_2}\left(D_1 + \frac{1}{3}D_2 s - \frac{1}{6}D_3 s^2\right)$$

$$\phi - \phi^{(oe)} - \left\{\lambda_1 + \frac{s}{2}\lambda_2 - \frac{s^2}{3}\lambda_3 + \frac{B}{EI_2}\left(D_1 + \frac{1}{2}D_2 s - \frac{1}{3}D_3 s^2\right)\right\}\frac{s}{C}$$

$$\int\phi\,ds = \phi^{(oe)}s - \left\{\lambda_1 + \frac{s}{3}\lambda_2 - \frac{s^2}{6}\lambda_3 + \frac{B}{EI_2}\left(D_1 + \frac{1}{3}D_2 s - \frac{D_3}{6}s^2\right)\right\}\frac{s^2}{2C}\quad.$$

54

After eliminating $(\int \phi ds - \phi^{(o\,e)} s)$ in the second and fourth of these six equations by the use of the sixth, the first five yield the following five equations for the derivatives of the deformations averaged from $s = 0$ to $s = \ell$:

$$\delta_{1_{avg}}'' = -\alpha_2'\,\phi_{avg}' + \frac{1}{EI_1}\left(A_1 + \frac{\ell}{2}A_2 + \frac{\ell^2}{3}A_3\right)$$

$$\delta_{1_{avg}}' = (\delta_1')^{(o.e.)} - \frac{\ell}{2EI_1}\left(A_1 + \frac{\ell}{3}A_2 + \frac{\ell^2}{6}A_3\right)$$

$$+ \alpha_2'\left\{\lambda_1 + \frac{\ell}{3}\lambda_2 - \frac{\ell^2}{6}\lambda_3 + \frac{B}{EI_2}\left(D_1 + \frac{\ell}{3}D_2 - \frac{\ell^2}{6}D_3\right)\right\}\frac{\ell}{2C}$$

$$\delta_{2_{avg}}'' = \left(\alpha_1' + \frac{B}{EI_2}\right)\phi_{avg}' + \frac{1}{EI_2}\left(D_1 + \frac{\ell}{2}D_2 - \frac{\ell^2}{3}D_3\right)$$

$$\delta_{2_{avg}}' = (\delta_2')^{(o\,e)} - \left(\alpha_1' + \frac{B}{EI_2}\right)\frac{\ell}{2C}\left(\lambda_1 + \frac{\ell}{3}\lambda_2 - \frac{\ell^2}{6}\lambda_3\right)$$

$$- \left\{1 + \frac{B}{C}\left(\alpha_1' + \frac{B}{EI_2}\right)\right\}\frac{\ell}{2EI_2}\left(D_1 + \frac{\ell}{3}D_2 - \frac{\ell^2}{6}D_3\right)$$

$$\phi_{avg}' = \left\{\lambda_1 + \frac{\ell}{2}\lambda_2 - \frac{\ell^2}{3}\lambda_3 + \frac{B}{EI_2}\left(D_1 + \frac{\ell}{2}D_2 - \frac{\ell^3}{3}D_3\right)\right\}\frac{1}{C}$$

When the expressions for A_2, A_3, D_2, D_3, λ_2, and λ_3 are substituted into the above five equations, they can be written in the form

$$[\alpha]\left\{\begin{array}{c} -\delta_{1_{avg}}'' \\[6pt] -\delta_{1_{avg}}' \\[6pt] -\delta_{2_{avg}}'' \\[6pt] -\delta_{2_{avg}}' \\[6pt] -\phi_{avg}' \end{array}\right\} = \left\{\begin{array}{c} F_1 \\[6pt] F_2 \\[6pt] F_3 \\[6pt] F_4 \\[6pt] F_5 \end{array}\right\} \qquad (54)$$

55

where

$$F_1 = -\frac{1}{EI_1}\left\{A_1 + \frac{\ell}{2}\left(P_a - \hat{P}_b\,\phi^{(o.e.)}\right)\right\}$$

$$F_2 = -(\delta_1')^{(o.e.)} + \frac{\ell}{2EI_1}\left\{A_1 + \frac{\ell}{3}\left(P_a - \hat{P}_b\,\phi^{(o.e.)}\right)\right\}$$

$$-\,d_2'\,\frac{\ell}{2C}\left[\lambda_1 + \frac{B}{EI_2}\left\{B_1 + \frac{\ell}{3}\left(P_b + \hat{P}_a\,\phi^{(o.e.)}\right)\right\} + \frac{\ell}{3}\left\{\hat{P}_b(\delta_1')^{(o.e.)} - \hat{P}_a(\delta_2')^{(o.e.)}\right\}\right]$$

$$F_3 = -\frac{1}{EI_2}\left\{B_1 + \frac{\ell}{2}\left(P_b + \hat{P}_a\,\phi^{(o.e.)}\right)\right\}$$

$$F_4 = -(\delta_2')^{(o.e.)} + \left(d_1' + \frac{B}{EI_2}\right)\,\frac{\ell}{2C}\left[\lambda_1 + \frac{\ell}{3}\left\{\hat{P}_b(\delta_1')^{(o.e.)} - \hat{P}_a(\delta_2')^{(o.e.)}\right\}\right]$$

$$+\left\{1 + \frac{B}{C}\left(d_1' + \frac{B}{EI_2}\right)\right\}\,\frac{\ell}{2EI_2}\left\{B_1 + \frac{\ell}{3}\left(P_b + \hat{P}_a\,\phi^{(o.e.)}\right)\right\}$$

$$F_5 = -\frac{1}{C}\left[\lambda_1 + \frac{B}{EI_2}\left\{B_1 + \frac{\ell}{2}\left(P_b + \hat{P}_a\,\phi^{(o.e.)}\right)\right\} + \frac{\ell}{2}\left\{\hat{P}_b(\delta_1')^{(o.e.)} - \hat{P}_a(\delta_2')^{(o.e.)}\right\}\right]$$

and $[a]$ is a 5 by 5 matrix with its elements as listed below:

$$a_{11} = 1$$

$$a_{12} = \frac{\ell}{2EI_1}\,\hat{P}_x$$

$$a_{13} = \frac{\ell}{2EI_1}\,\check{Q}_x$$

56

$$a_{14} = 0$$

$$a_{15} = -\frac{\ell}{2EI_1}\left(\tilde{Q}_b + \frac{2\ell}{3}\hat{P}_b - E_2\hat{P}_x\right) + d_2'$$

$$a_{21} = d_2'\frac{\ell^2}{6C}\left(\tilde{Q}_b - \frac{B}{EI_2}\tilde{Q}_x + \frac{\ell}{2}\hat{P}_b\right)$$

$$a_{22} = 1 - \frac{\ell^2}{6EI_1}\hat{P}_x + d_2'\frac{\ell^2}{6C}\hat{P}_b$$

$$a_{23} = -\frac{\ell^2}{6EI_1}\tilde{Q}_x - d_2'\frac{\ell^2}{6C}\left(\tilde{Q}_a + \frac{\ell}{2}\hat{P}_a\right)$$

$$a_{24} = -d_2'\frac{\ell^2}{6C}\left(\hat{P}_a - \frac{B}{EI_2}\hat{P}_x\right)$$

$$a_{25} = \frac{\ell^2}{6EI_1}\left(\tilde{Q}_b + \frac{\ell}{2}\hat{P}_b - E_2\hat{P}_x\right)$$

$$+ d_2'\frac{\ell^2}{6C}\left\{\frac{B}{EI_2}\left(\tilde{Q}_a + \frac{\ell}{2}\hat{P}_a - E_1\hat{P}_x\right) + E_1\hat{P}_a + E_2\hat{P}_b\right\}$$

$$a_{31} = -\frac{\ell}{2EI_2}\tilde{Q}_x$$

$$a_{32} = 0$$

$$a_{33} = 1$$

$$a_{34} = \frac{\ell}{2EI_2}\hat{P}_x$$

$$a_{35} = \frac{\ell}{2EI_2}\left(\breve{Q}_a + \frac{2\ell}{3}\hat{P}_a - E_1\hat{P}_x\right) - \left(d_1' + \frac{B}{EI_2}\right)$$

$$a_{41} = \left\{\,\cdot\, + \frac{B}{C}\left(d_1' + \frac{B}{EI_2}\right)\right\}\frac{\ell^2}{6EI_2}\tilde{Q}_x - \left(d_1' + \frac{B}{EI_2}\right)\frac{\ell^2}{6C}\left(\tilde{Q}_b + \frac{\ell}{2}\hat{P}_b\right)$$

$$a_{42} = -\left(d_1' + \frac{B}{EI_2}\right)\frac{\ell^2}{6C}\hat{P}_b$$

$$a_{43} = \left(d_1 + \frac{B}{EI_2}\right)\frac{\ell^2}{6C}\left(\tilde{Q}_a + \frac{\ell}{2}\hat{P}_a\right)$$

$$a_{44} = \cdot -\left\{1 + \frac{B}{C}\left(d_1' + \frac{B}{EI_2}\right)\right\}\frac{\ell^2}{6EI_2}\hat{P}_x + \left(d_1' + \frac{B}{EI_2}\right)\frac{\ell^2}{6C}\hat{P}_a$$

$$a_{45} = -\left\{1 + \frac{B}{C}\left(d_1 + \frac{B}{EI_2}\right)\right\}\frac{\ell^2}{6EI_2}\left(\tilde{Q}_a + \frac{\ell}{2}\hat{P}_a - E_1\hat{P}_x\right)$$

$$\qquad - \left(d_1' + \frac{B}{EI_2}\right)\frac{\ell^2}{6C}\left(E_1\hat{P}_a + E_2\hat{P}_b\right)$$

$$a_{51} = \frac{\ell}{2C}\left(\breve{Q}_b - \frac{B}{EI_2}\tilde{Q}_x + \frac{2\ell}{3}\hat{P}_b\right)$$

$$a_{52} = \frac{\ell}{2C}\,\hat{P}_b$$

$$a_{53} = -\frac{\ell}{2C}\left(\tilde{Q}_a + \frac{2\ell}{3}\hat{P}_a\right)$$

$$a_{54} = -\frac{\ell}{2C}\left(\hat{P}_a - \frac{B}{EI_2}\hat{P}_x\right)$$

$$a_{55} = 1 + \frac{\ell}{2C}\left\{\frac{B}{EI_2}\left(\tilde{Q}_a + \frac{2\ell}{3}\hat{P}_a - E_1\hat{P}_x\right) + E_1\hat{P}_a + E_2\hat{P}_b\right\}\cdot$$

By substituting the expressions for A_1, D_1 and λ_1 in the expressions for the F_k's, the latter expressions may be written

$$
\ell \left\{ \begin{array}{c} F_1 \\ F_2 \\ F_3 \\ F_4 \\ F_5 \end{array} \right\} = \begin{bmatrix} C \end{bmatrix} \left\{ \begin{array}{c} P_a \\ Q_a \\ \delta_1' \\ \delta_1 \\ P_b \\ Q_b \\ \delta_2' \\ \delta_2 \\ Q_x \\ \phi \end{array} \right\}^{(o.e.)}
\tag{55}
$$

where $\begin{bmatrix} C \end{bmatrix}$ is a 5-x-10 matrix with the following elements:

$$
C_{11} = -\frac{\ell^2}{2EI_1}
$$

$$
C_{12} = -\frac{\ell}{EI_1}
$$

$$
C_{13} = 0
$$

$$
C_{14} = -\frac{\ell}{EI_1} \, \hat{P}_x
$$

$$C_{15} = C_{16} = 0$$

$$C_{17} = - \frac{\ell}{EI_1} \, \tilde{Q}_x$$

$$C_{18} = C_{19} = 0$$

$$C_{1,10} = \frac{\ell}{EI_1} \left(\tilde{Q}_b + \frac{\ell}{2} \hat{P}_b - E_2 \hat{P}_x \right)$$

$$C_{21} = \frac{\ell^3}{6EI_1} + d_2' \frac{\ell^2}{2C} e_2$$

$$C_{22} = \frac{\ell^2}{2EI_1}$$

$$C_{23} = -\ell - d_2' \frac{\ell^2}{2C} \left(\tilde{Q}_b - \frac{B}{EI_2} \tilde{Q}_x + \frac{\ell}{3} \hat{P}_b \right)$$

$$C_{24} = \frac{\ell^2}{2EI_1} \hat{P}_x - d_2' \frac{\ell^2}{2C} \hat{P}_b$$

$$C_{25} = - d_2' \frac{\ell^2}{2C} \left(e_1 + \frac{\ell}{3} \frac{B}{EI_2} \right)$$

$$C_{26} = - d_2' \frac{\ell^2}{2C} \frac{B}{EI_2}$$

$$C_{17} = \frac{\ell^2}{2EI_1} \tilde{Q}_x + d_2' \frac{\ell^2}{2C} \left(\tilde{Q}_a + \frac{\ell}{3} \hat{P}_a \right)$$

$$C_{28} = d_2' \frac{\ell^2}{2C} \left(\hat{P}_a - \frac{B}{EI_2} \hat{P}_x \right)$$

$$C_{29} = - d_2' \frac{\ell^2}{2C}$$

$$C_{2,10} = -\frac{\ell^2}{2EI_1}\left(\tilde{Q}_b + \frac{\ell}{3}\hat{P}_b - E_2\hat{P}_x\right)$$

$$- d_2' \frac{\ell^2}{2C}\left\{\frac{B}{EI_2}\left(\tilde{Q}_a + \frac{\ell}{3}\hat{P}_a - E_1\hat{P}_x\right) + E_1\hat{P}_a + E_2\hat{P}_b\right\}$$

$$C_{31} = C_{32} = 0$$

$$C_{33} = \frac{\ell}{EI_2}\tilde{Q}_x$$

$$C_{34} = 0$$

$$C_{35} = -\frac{\ell^2}{2EI_2}$$

$$C_{36} = -\frac{\ell}{EI_2}$$

$$C_{37} = 0$$

$$C_{38} = -\frac{\ell}{EI_2}\hat{P}_x$$

$$C_{39} = 0$$

$$C_{3,10} = -\frac{\ell}{EI_2}\left(\tilde{Q}_a + \frac{\ell}{2}\hat{P}_a - E_1\hat{P}_x\right)$$

$$C_{41} = -\left(d_1' + \frac{B}{EI_2}\right)\frac{\ell^2}{2C}e_2$$

$$C_{42} = 0$$

$$C_{43} = -\left\{1 + \frac{3}{C}\left(d_1 - \frac{B}{EI_2}\right)\right\} \frac{\ell^2}{2EI_2} \tilde{Q}_x + \left(d_1' + \frac{B}{EI_2}\right) \frac{\ell^2}{2C}\left(\tilde{Q}_b + \frac{\ell}{3}\hat{P}_b\right)$$

$$C_{44} = \left(d_1' + \frac{B}{EI_2}\right) \frac{\ell^2}{2C} \hat{P}_b$$

$$C_{45} = \left\{1 + \frac{3}{C}\left(d_1' + \frac{3}{EI_2}\right)\right\} \frac{\ell^3}{6EI_2} + \left(d_1' + \frac{B}{EI_2}\right) \frac{\ell^2}{2C} e_1$$

$$C_{46} = \left\{1 + \frac{B}{C}\left(d_1' - \frac{B}{EI_2}\right)\right\} \frac{\ell^2}{2EI_2}$$

$$C_{47} = -\ell - \left(d_1' + \frac{B}{EI_2}\right) \frac{\ell^2}{2C}\left(\tilde{Q}_a + \frac{\ell}{3}\hat{P}_a\right)$$

$$C_{48} = \left\{1 + \frac{B}{C}\left(d_1' + \frac{B}{EI_2}\right)\right\} \frac{\ell^2}{2EI_2} \hat{P}_x - \left(d_1' + \frac{B}{EI_2}\right) \frac{\ell^2}{2C} \hat{P}_a$$

$$C_{49} = \left(d_1' + \frac{B}{EI_2}\right) \frac{\ell^2}{2C}$$

$$C_{4,10} = \left\{1 + \frac{B}{C}\left(d_1' + \frac{B}{EI_2}\right)\right\} \frac{\ell^2}{2EI_2}\left(\tilde{Q}_a + \frac{\ell}{3}\hat{P}_a - E_1\hat{P}_x\right)$$

$$+ \left(d_1' + \frac{B}{EI_2}\right) \frac{\ell^2}{2C}\left(E_1\hat{P}_a + E_2\hat{P}_b\right)$$

$$C_{51} = \frac{\ell}{C} e_2$$

$$C_{52} = 0$$

$$C_{53} = -\frac{\ell}{C}\left(\tilde{Q}_b - \frac{B}{EI_2}\tilde{Q}_x + \frac{\ell}{2}\hat{P}_b\right)$$

$$C_{54} = -\frac{\ell}{C}\hat{P}_b$$

$$C_{55} = -\frac{\ell}{C}\left(e_1 + \frac{\ell}{2}\ \frac{B}{EI_2}\right)$$

$$C_{56} = -\frac{\ell}{C}\ \frac{B}{EI_2}$$

$$C_{57} = \frac{\ell}{C}\left(\tilde{Q}_a + \frac{\ell}{2}\ \hat{P}_a\right)$$

$$C_{58} = \frac{\ell}{C}\left(\hat{P}_a' - \frac{B}{EI_2}\ \hat{P}_x\right)$$

$$C_{59} = -\frac{\ell}{C}$$

$$C_{5,10} = -\frac{\ell}{C}\left\{\frac{B}{EI_2}(\tilde{Q}_a + \frac{\ell}{2}\ \hat{P}_a - E_1\ \hat{P}_x) + E_1\ \hat{P}_a + E_2\ \hat{P}_b\right\}$$

The following matrix equation is obtained by combining Equations (54) and (55):

$$\begin{Bmatrix} -\delta_{1_{avg}}'' \ell \\ -\delta_{1_{avg}}' \ell \\ -\delta_{2_{avg}}'' \ell \\ -\delta_{2_{avg}}' \ell \\ -\phi_{avg}' \ell \end{Bmatrix} = \begin{bmatrix} a \end{bmatrix}^{-1} \begin{bmatrix} C \end{bmatrix} \begin{Bmatrix} P_a \\ Q_a \\ \delta_1' \\ \delta_1 \\ P_b \\ Q_b \\ \delta_2' \\ \delta_1' \\ Q_x \\ \phi \end{Bmatrix}^{(o.e.)} \tag{56}$$

Let $\left[\,d\,\right]$ denote the 5-x-10 matrix obtained by the product

$$\left[\,d\,\right] = \left[\,a\,\right]^{-1} \left[\,C\,\right] \; .$$

Then the relations

$$(\delta')^{(i.e)} = (\delta')^{(o.e)} - \delta''_{avg} \, \ell$$

$$\delta^{(i.e)} = \delta^{(o.e)} - \delta'_{avg} \, \ell$$

$$\phi^{(i.e)} = \phi^{(o.e)} - \phi'_{avg} \, \ell$$

lead to the following expressions for the nonzero elements in the 3rd, 4th, 7th, 8th, and 10th rows of the elastic matrix:

$$E_{3h} = d_{1h} \qquad\qquad (h = 1, 2, \text{ and } 4, 5, \ldots 10)$$

$$E_{33} = 1 + d_{13}$$

$$E_{4h} = d_{2h} \qquad\qquad (h = 1, 2, 3, \text{ and } 5, 6, \ldots 10)$$

$$E_{44} = 1 + d_{24}$$

$$E_{7h} = d_{3h} \qquad\qquad (h = 1, 2, \ldots 6, \text{ and } 8, 9, 10)$$

$$E_{77} = 1 + d_{37}$$

$$E_{8h} = d_{4h} \qquad (h = 1, 2, 7, \text{ and } 9, 10)$$

$$E_{88} = 1 + d_{48}$$

$$E_{10,h} = d_{5h} \qquad (h = 1, 2, \ldots 9)$$

$$E_{10,10} = d_{5,10} \quad .$$

The explicit form of the elastic matrix $[E]$ is indicated below:

$$[E] =$$

$$
\begin{bmatrix}
1 \\
\ell & 1 \\
d_{11} & d_{12} & 1+d_{13} & d_{14} & d_{15} & d_{16} & d_{17} & d_{18} & d_{19} & d_{1,10} \\
d_{21} & d_{22} & d_{23} & 1+d_{24} & d_{25} & d_{26} & d_{27} & d_{28} & d_{29} & d_{2,10} \\
 & & & & 1 \\
 & & & & \ell & 1 \\
d_{31} & d_{32} & d_{33} & d_{34} & d_{35} & d_{36} & 1+d_{37} & d_{38} & d_{39} & d_{3,10} \\
d_{41} & d_{42} & d_{43} & d_{44} & d_{45} & d_{46} & d_{47} & 1+d_{48} & d_{49} & d_{4,10} \\
 & & & & & & & 1 \\
d_{51} & d_{52} & d_{53} & d_{54} & d_{55} & d_{56} & d_{57} & d_{58} & d_{59} & 1+d_{5,10} \\
 & & & & & & & & 1 \\
 & & & & & & & & & 1 \\
 & & & & & & & & & & 1
\end{bmatrix}
$$

MASS MATRIX

The 13 by 13 mass matrix, $[F]$, relates the column matrices for positions just inboard and just outboard of an assumed concentrated mass, such that

$$\left\{\Delta\right\}^{(in.)} = \left[F\right]\left\{\Delta\right\}^{(out.)} \qquad . \qquad (57)$$

The column matrix $\left\{\Delta\right\}$ is the same one discussed previously which has the matrix elements shown on Figure 6 .

Expressions for the elements in the $[F]$ matrix can be derived from the expressions for $\bar{p}_a$, $\bar{p}_b$, $\bar{q}_a$, $\bar{q}_b$, and $\bar{q}_x$ which are given by Equations (41) through (45) in the section on blade inertia loading. When Equations (41) through (45) are used for this purpose, the mass m appearing in them is considered to be the total mass of a segment of the blade rather than the mass per unit length. These equations are for the combined oscillatory and nonoscillatory loadings; but recognizing that $p_a = \bar{p}_a - \hat{p}_a$, $p_b = \bar{p}_b - \hat{p}_b$, etc., it is easy to separate the oscillatory parts of the equations. Steady components of the inertia loadings which remain in the coefficients of the oscillatory variables can be expressed in terms of basic mass parameters by using Equation (46).

Also, for sinusoidal oscillations at frequency ω , the second time derivatives of the oscillatory variables can be replaced as follows,

$$\ddot{\delta}_{1t} = -\omega^2 \delta_{1t} = -\omega^2 \left(\delta_1 + E_2 \phi\right)$$

$$\ddot{\delta}_{2t} = -\omega^2 \left(\delta_2 - E_1 \phi\right) \qquad \text{(see page 47)}$$

$$\left(\ddot{\phi}, \ddot{\beta}_F, \ddot{\beta}_D, \text{ or } \ddot{\beta}_P\right) = -\omega^2 \left(\phi, \beta_F, \beta_D, \text{ or } \beta_P\right)$$

When Equations (41) through (45) have been modified as discussed above, the elements of the $[F]$ matrix are

$$F_{ii} = \prime \qquad \left(i = 1, 2, \ldots, 13\right)$$

$$F_{14} = m \left(\omega^2 + \Omega^2 \sin^2 \beta\right)$$

$$F_{18} = -m \Omega^2 \cos \beta \sin \beta$$

$$F_{1,10} = m\,\eta_c\,(\omega^2 + \Omega^2 \sin^2\beta) + E_2\,F_{14} - E_1\,E_{18}$$

$$F_{1,11} = m\,\omega^2 \left\{ (r - r_F + \theta_E\,C_P - \hat{\beta}_D\,e_{DP})\cos\beta - (\theta_A + \hat{\beta}_D)(C_P\,\sin\beta + e_2 + \eta_c) \right\}$$

$$- m\,\Omega^2\,r\,\cos\beta$$

$$F_{1,12} = m\,\omega^2 \left\{ (r - r_D)\sin\beta - e_{DP}(\theta_E\,\cos\beta - \theta_A\,\sin\beta) - \theta_E\,(e_2 + \eta_c) \right\}$$

$$+ m\,\Omega^2\,r_D\,\sin\beta$$

$$F_{1,13} = m\,\omega^2 \left\{ (r - r_P)(\theta_E\,\sin\beta + \theta_A\,\cos\beta) + e_2 + \eta_c \right\}$$

$$- m\,\Omega^2 \left\{ e_P\,\cos\beta - (\theta_E + \hat{\beta}_F)(r - r_P)\,\sin\beta \right.$$

$$\left. + (e_2 + \eta_c)\,\cos 2\beta - e_1\,\sin 2\beta \right\}$$

$$F_{24} = -m\,\Omega^2\,r$$

$$F_{2,10} = -m\,\eta_c\,\Omega^2\,r + E_2\,F_{24}$$

$$F_{54} = F_{18} = -m\,\Omega^2\,\sin\beta\,\cos\beta$$

$$F_{58} = m\,(\omega^2 + \Omega^2\,\cos^2\beta)$$

67

$$F_{5,10} = -m\,\eta_c\,\Omega^2\,\sin\beta\cos\beta + E_2\,F_{18} - E_1\,F_{58}$$

$$F_{5,11} = m\,\omega^2\left\{(r - r_F + \theta_E\,C_P - \hat{\beta}_D\,e_{DP})\,\sin\beta + (\theta_A + \hat{\beta}_D)(C_P\cos\beta + e_1)\right\}$$

$$- m\,\Omega^2\,r\,\sin\beta$$

$$F_{5,12} = m\,\omega^2\left\{(r - r_D)\cos\beta + e_{DP}(\theta_E\,\sin\beta + \theta_A\,\cos\beta) - \theta_E\,e_1\right\}$$

$$- m\,\Omega^2\,r_D\,\cos\beta$$

$$F_{5,13} = -m\,\omega^2\left\{(r - r_P)(\theta_E\,\cos\beta - \theta_A\,\sin\beta) + e_1\right\}$$

$$- m\,\Omega^2\left\{e_P\,\sin\beta + (\theta_E + \hat{\beta}_F)(r - r_P)\cos\beta\right.$$

$$\left. + (e_2 + \eta_c)\,\sin 2\beta + e_1\,\cos 2\beta\right\}$$

$$F_{68} = F_{24} = -m\,\Omega^2\,r$$

$$F_{6,10} = -E_1\,F_{24}$$

$$F_{94} = -m\,\omega^2(e_2 + \eta_c) - m\,\Omega^2\left\{(e_2 + \eta_c)\cos 2\beta - e_1\,\sin 2\beta\right.$$

$$\left. - (\theta_E + \hat{\beta}_F)\,r\,\sin\beta + (e_P - r_P\,\theta_A - r_D\,\hat{\beta}_D)\cos\beta\right\}$$

$$F_{98} = -m\,\omega^2 e_1 - m\Omega^2 \left\{ (e_2 + \eta_c)\sin 2\beta + e_1 \cos 2\beta \right.$$

$$\left. + (\theta_E + \hat{\beta}_F)\, r \cos\beta + (e_P - r_P\,\theta_A - r_D\,\hat{\beta}_D)\sin\beta \right\}$$

$$F_{9,10} = m\omega^2 (k^2 + \eta_c e_2) - m\Omega^2 \left\{ (e_P - r_P\,\theta_A - r_D\,\hat{\beta}_D)\,\eta_c \cos\beta \right.$$

$$\left. + (k_2^2 - k_1^2)\cos 2\beta + \eta_c\,(e_2 \cos 2\beta - e_1 \sin 2\beta) \right\}$$

$$+ E_2 F_{94} - E_1 F_{98}$$

$$F_{9,11} = m\omega^2 \left\{ (r - r_F + \theta_E\,C_P - \hat{\beta}_D\,e_{DP})\,C_y \right.$$

$$\left. - (\theta_A + \hat{\beta}_D)(K + C_P\,C_y) \right\}$$

$$- m\Omega^2 r\,C_y$$

$$F_{9,12} = -m\omega^2 \left\{ (r - r_D + e_{DP}\,\theta_A)\,C_y \right.$$

$$\left. - \theta_E\,(K + e_{DP}\,C_y) \right\}$$

$$+ m\Omega^2 r_D\,C_y$$

$$F_{9,13} = m\omega^2 \left\{ (r - r_P)(\theta_A\,C_y + \theta_E\,C_y) + K \right\}$$

$$- m\Omega^2 \left\{ K_2 - K_1 + C_P\,C_y - (\theta_E + \hat{\beta}_F)(r - r_P)\,C_y \right\}.$$

The reason for $E_{ii} = 1$ being the only nonzero element in the 3rd, 4th, 7th, 8th, and 10th to 13th rows is that δ_1', δ_1, δ_2', δ_2, ϕ, β_F, β_D, and β_P do not change across a concentrated mass.

The explicit form of the $[F]$ matrix is indicated below:

$$[F] =$$

$$
\begin{bmatrix}
1 & & & F_{1,4} & & & F_{1,8} & & F_{1,10} & F_{1,11} & F_{1,12} & F_{1,13} \\
 & 1 & & F_{2,4} & & & & & F_{2,10} & & & \\
 & & 1 & & & & & & & & & \\
 & & & 1 & & & & & & & & \\
 & & & F_{5,4} & 1 & & F_{5,8} & & F_{5,10} & F_{5,11} & F_{5,12} & F_{5,13} \\
 & & & & & 1 & F_{6,8} & & F_{6,10} & & & \\
 & & & & & & 1 & & & & & \\
 & & & & & & & 1 & & & & \\
 & & & F_{9,4} & & & F_{9,8} & 1 & F_{9,10} & F_{9,11} & F_{9,12} & F_{9,13} \\
 & & & & & & & & 1 & & & \\
 & & & & & & & & & 1 & & \\
 & & & & & & & & & & 1 & \\
 & & & & & & & & & & & 1 \\
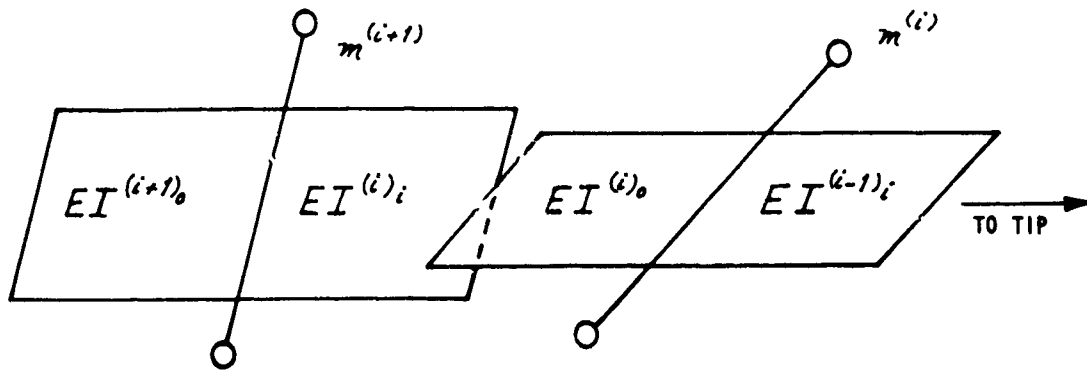\end{bmatrix}
$$

70

METHOD OF SOLUTION

Figure 7. ANALYTICAL REPRESENTATION OF BLADE.

When the blade bays are designated as in the above sketch, the complete matrix equation of the blade is

$$\{\Delta\}^{(root)} = \left(\prod_{tip}^{root} [E]^{(i)}_i \; [R]^{(i)} \; [E]^{(i)}_0 \; [F]^{(i)} \right) \{\Delta\}^{(tip)} . \tag{58}$$

Inasmuch as

$$P_a^{(tip)} = Q_a^{(tip)} = P_b^{(tip)} = Q_b^{(tip)} = Q_x^{(tip)} = 0$$

in the $\{\Delta\}^{(tip)}$ column matrix, only the 3rd, 4th, 7th, 8th, 10th, 11th, 12th, and 13th columns of matrix $[F]^{(1)}$ are carried. Thus $[E]^{(1)}_0$ is multiplied into the 13-x-8 matrix that has replaced $[F]^{(1)}$. This gives another 13-x-8 matrix into which $[R]^{(1)}$ is multiplied. The process is continued until the last inboard matrix is reached. As a result, 13 equations are obtained relating the variables at the blade root and the blade tip. The last three equations merely state that β_F, β_D, and β_P do not change from the tip to the root and need not be retained. The remaining equations can be written in the following matrix form where the $[\alpha]$ matrix is identical to the first 10 rows of the product matrix in Equation (58).

$$
\begin{Bmatrix} P_a \\ Q_a \\ \delta_1' \\ \delta_1 \\ P_b \\ Q_b \\ \delta_2' \\ \delta_2 \\ Q_x \\ \phi \end{Bmatrix}^{(root)} = \begin{bmatrix} \alpha \end{bmatrix} \begin{Bmatrix} \delta_1' \\ \delta_1 \\ \delta_2' \\ \delta_2 \\ \phi \\ \beta_F \\ \beta_D \\ \beta_P \end{Bmatrix}^{(tip)} \qquad \left(\begin{bmatrix} \alpha \end{bmatrix} \text{ is a 10-x-8 matrix} \right)
$$

$$\tag{59}$$

In addition to the five boundary conditions which apply in all cases, namely,

$$
\left(\delta_1' \right)^{(root)} = \delta_1^{(root)} = \left(\delta_2' \right)^{(root)} = \delta_2^{(root)} = \phi^{(root)} = 0 ,
$$

there are three other conditions obtainable by considering the possible constraints at the flapping, lead-lag and pitching hinges of the blade. Take the pitching hinge as an example. If k_P is the spring constant (in inch-pounds per radian) of the pitch control mechanism, then

$$
k_P \, \beta_P = \left(Q_x^{(root)} \cos \theta_E - Q_y^{(root)} \sin \theta_E \right) \cos \theta_A
$$

$$
+ \; Q_y^{(root)} \sin \theta_A
$$

72

or, using $Q_y = Q_a \cos\beta + Q_b \sin\beta$ and $Q_z = Q_b \cos\beta - Q_a \sin\beta$,

$$k_p \beta_p = \left(\cos\beta^{(root)} \sin\theta_A + \sin\beta^{(root)} \sin\theta_E \cos\theta_A\right) Q_a^{(root)}$$

$$+ \left(\sin\beta^{(root)} \sin\theta_A - \cos\beta^{(root)} \sin\theta_E \cos\theta_A\right) Q_b^{(root)}$$

$$+ \left(\cos\theta_E \cos\theta_A\right) Q_x^{(root)}$$

where

$$Q_a^{(root)} = \alpha_{21} (\delta_1')^{(tip)} + \ldots + \alpha_{28} \beta_p$$

$$Q_b^{(root)} = \alpha_{61} (\delta_1')^{(tip)} + \ldots + \alpha_{68} \beta_p$$

$$Q_x^{(root)} = \alpha_{91} (\delta_1')^{(tip)} + \ldots + \alpha_{98} \beta_p$$

Similar equations can be written for the constraints at the flapping and lead-lag hinges. Thus, eight simultaneous linear homogeneous equations in the eight unknowns, $(\delta_1')^{(tip)}, \ldots, \beta_D$, and β_p, can be obtained from matrix Equation (59). The determinant of these equations is plotted versus various trial values of ω for given rotor angular velocity, Ω, and nonoscillatory flapping, lead-lag, and pitching angles $(\hat{\beta}_F, \hat{\beta}_D, \text{and} \hat{\beta}_P)$. The zeros of this curve are the solutions to the vibration problem for the given Ω, $\hat{\beta}_F$, $\hat{\beta}_D$, and $\hat{\beta}_P$. The simplest case is the one with all three hinges rigidly locked, so that $\beta_F = \beta_D = \beta_P = 0$ and the determinant is simply

$$\begin{bmatrix} \alpha_{31} & \alpha_{32} & \alpha_{33} & \alpha_{34} & \alpha_{35} \\ \alpha_{41} & & & & \\ \alpha_{71} & & & & \\ \alpha_{81} & & & & \\ \alpha_{101} & ------- & ------- & ------- & \alpha_{105} \end{bmatrix}$$

This is the case considered in Reference 2.

73

EXPERIMENTAL APPARATUS

GENERAL DESCRIPTION

The purpose of the experimental apparatus is to apply a controlled vibratory force of up to 6 pounds (12 pounds peak to peak) to each blade of a two-bladed rotor system while operating in a vacuum at rotational speeds up to 1900 rpm. The equipment which has been developed has the following capabilities. The vibratory force can be applied to the blades so that either the symmetric or antisymmetric degrees of freedom of the rotor can be excited. The radius at which this force is applied is adjustable with a maximum of 46 inches. A unique feature of this equipment is that the angular orientation of the line of action of the vibratory force relative to the plane of rotation of the blades is adjustable. It can be varied from lying in the plane of rotation to lying normal to the plane of rotation. This feature enables excitation of either the chordwise or the flapwise degrees of freedom and also allows the input generalized force in a specific degree of freedom to be maximized by aligning the applied force with the motion of the blade at the point of application. The vibratory force is measured at the attachment point of the shaker system to the blades with a specially designed force coupling.

The test apparatus is composed of two major assemblies as installed in the 10-foot-diameter vacuum tank (Figure 8). The lower assembly consists of the test rotor, the slipring assembly, the hydraulic drive motor, and the base supporting structure. The upper assembly consists of the rotating shaker system, a 50-pound electromagnetic vibrator and the overhead supporting structure. These two assemblies are joined at their common center of rotation by a flexible drive coupling. This coupling not only transmits the driving torque to the upper system but also fixes the azimuthal alignment of the rotating shaker system relative to the test rotor. The two assemblies are held erect and in axial alignment by a set of four cables and turnbuckles. The hydraulic motor, slipring assembly, and electromagnetic vibrator are in sealed enclosures to allow forced-air cooling while the system is operating in a vacuum. The driving power was supplied by a 7-1/2-hp electric motor and hydraulic pump mounted outside the vacuum tank.

Four energy-absorbing safety barriers fabricated of wood and metal were installed so as to surround the plane of rotation of the blades and the shaker system. An emergency shutdown device was provided which monitored the vibration level of the supporting structure of the lower assembly. If the vibrations exceeded a preset level, the device would bring the rotating system to a stop by shutting off the hydraulic pump and introducing resistance into the hydraulic circuit.

THE ROTOR HUB AND BLADES

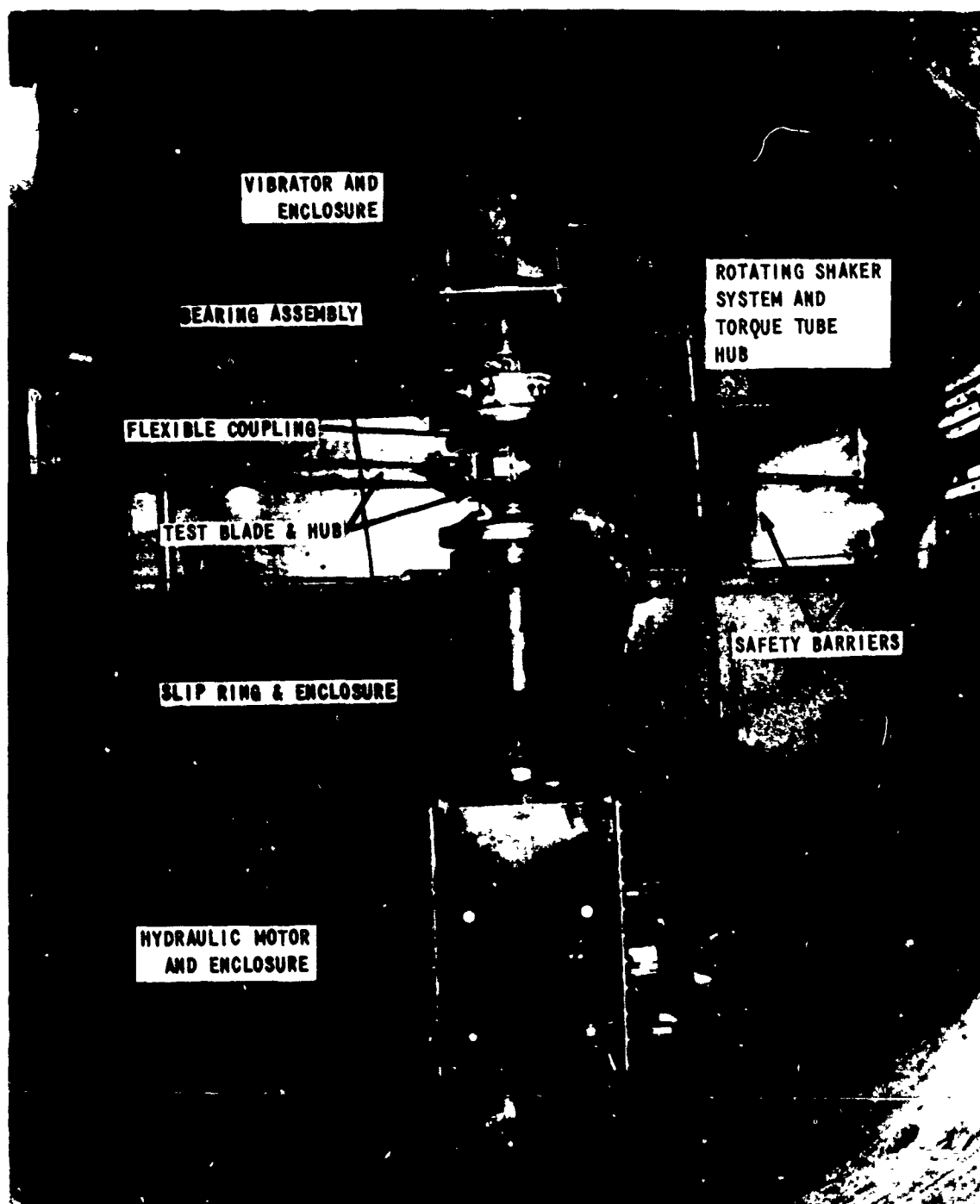An existing rotor hub was used which was designed and

Figure 8. ROTOR TEST APPARATUS INSTALLATION IN VACUUM CHAMBER.

fabricated under the sponsorship of the Air Force Aeronautical Systems Division for use in wind-tunnel tests (Reference 1). The hub can be seen in Figures 8 and 9. The flapping axis for each blade passes through the axis of rotation and normal to it. The lag hinges are parallel to the axis of rotation and offset 5 inches from it. Two steel flexure straps (3.6 inches in length) connect each blade to its lag hinge and provide a pitch degree of freedom. A fixture was fabricated to interlock the two sides of the hub and enable it to be converted to the teetering configuration when desired.

The test blades are uniform beams. They were fabricated as solid aluminum bars with 0.5-x-3.0-inch rectangular cross section, and when installed on the rotor hub they have a tip radius of 44.75 inches. They were mounted so that the effective pitch axis of the rotor hub coincided with the mid-chord of the beams. This placed the blade c.g. on the pitch axis and eliminated the pitch-flap mass coupling. The blade properties for the uniform section outboard of the retention pins are:

Weight	0.1545 lbs./in.
Flapwise EI	0.3125×10^6 lb.-in.^{2}
Chordwise EI	0.1125×10^8 lb.-in.^{2}
Torsional inertia	0.1155 lb.-in.^{2}
Torsional GJ	0.436×10^6 lb.-in.^{2}

Inboard from the retention pins to the lag hinge, the elastic properties of the pitch flexure straps are:

Flapwise EI	0.1795×10^7 lb.-in.^{2}
Chordwise EI	0.529×10^6 lb.-in.^{2}
Torsional GJ	0.135×10^5 lb.-in.^{2}

The flapping inertia of rotor hub per blade is 159 lb.-in.^{2}, and it is considered infinitely stiff relative to the blades.

THE LOWER DRIVE ASSEMBLY

The structure of the lower assembly consists of two large welded box-like enclosures bolted together with their connections sealed using "0" rings and rubber gaskets. The base section encloses the hydraulic motor and has removable access side panels with bulkhead fittings for the hydraulic lines, the air lines, and the instrumentation leads. The top section encloses the slipring assembly. A flexible coupling connects the hydraulic motor to the rotor shaft. A variable reluctance pickup was installed in the lower enclosure section to detect shaft revolutions. Inside the top section of the enclosure, a 44-conductor slipring was mounted on the shaft. Above the slipring assembly, the shaft was hollow with outlets on either side of the top bearing and seals.
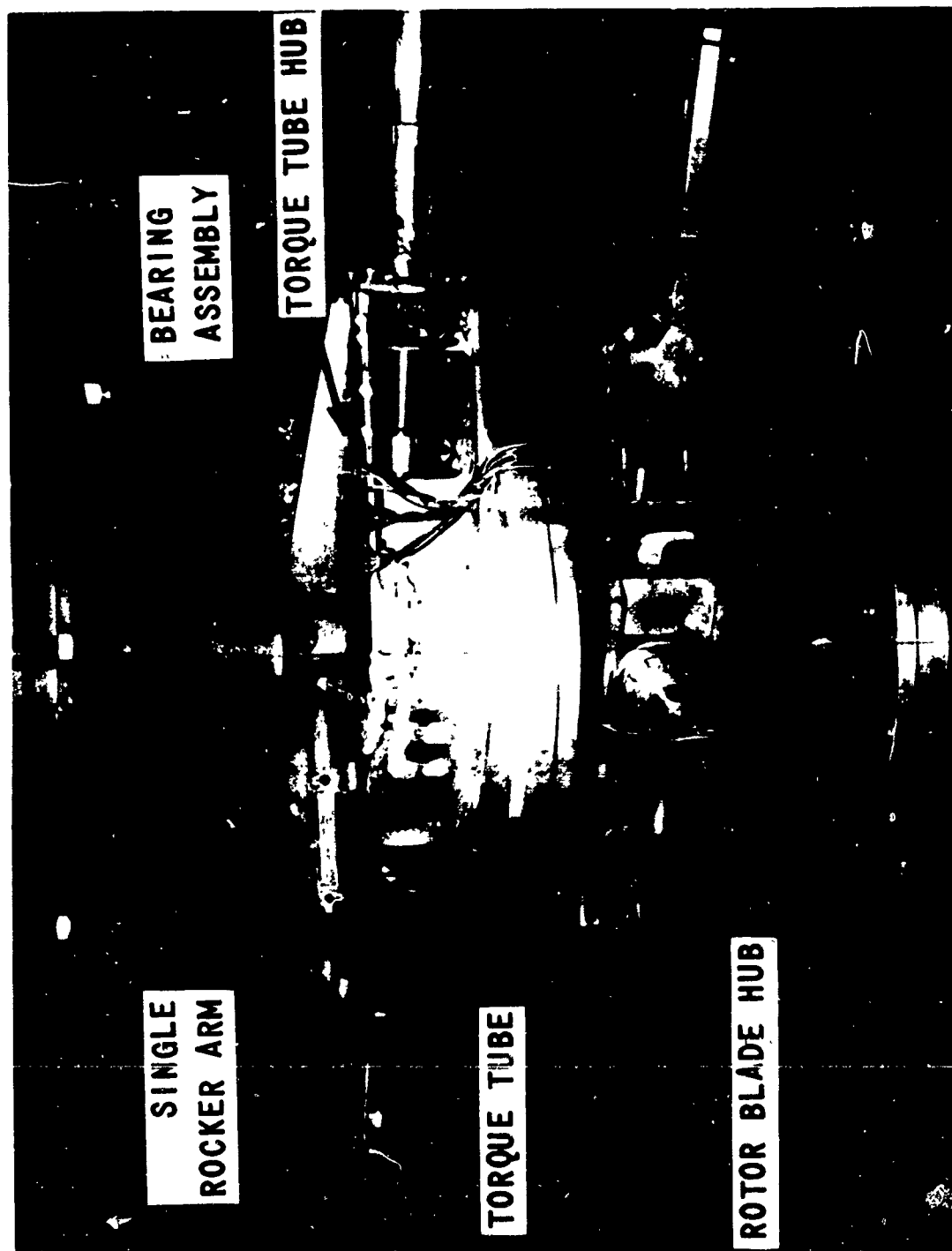
Figure 9. SHAKER SYSTEM AND ROTOR BLADE HUBS.

77

Bulkhead plugs installed on these outlets allowed the instrumentation leads on the rotating side of the sliprings to be passed out of the sealed enclosure through the hollow shaft to a circular terminal board below the test rotor hub. The upper end of the rotor shaft is splined to accept the test rotor hub. This splined section of the shaft is also threaded to permit vertical adjustment of the hub position on the shaft by means of threaded collars on either side of the hub.

THE ROTATING SHAKER SYSTEM AND UPPER ASSEMBLY

The shaker system and upper assembly are suspended overhead on the center line of rotation of the rotor system by a truss structure. The bearing assembly for the rotating shaker system and vibrator mounting are attached to the truss by four threaded rods which allow adjustment of the vertical position of the shaker system and angular adjustment of its axis of rotation. The vibrator is mounted above the bearing assembly and is sealed in an enclosure. The cooling air and electrical lines for the vibrator pass through the enclosure via bulkhead plugs and fittings.

The shaker system consists of a rotating hub and two diametrically opposed torque tubes which oscillate about their longitudinal axes (i. e., pitching oscillation). The pitch oscillation of the torque tubes is driven by the vibrator through a series of push rods, rocker arms and an inboard pitch arm on each torque tube. Each torque tube is connected to a blade through an outboard pitch arm, force rod (push rod), and force coupling. Backlash and friction are minimized by the use of flexures throughout the entire oscillating shaker system except for a bearing at the connection between the rotating and nonrotating sides of the system.

The advantage of this shaking system is the capability of changing the angular orientation of the shaking force relative to the plane of rotation. The line of action of the shaking force can be varied from normal to the plane of rotation (as when forcing the blade flapwise modes) to parallel to the plane of rotation (as when forcing the chordwise modes). This is accomplished by changing the angular orientation (in pitch) of the outboard pitch arms and force rods relative to the torque tube. The radial location of the shaking force can also be changed by changing the radial location of these outboard pitch arms.

The installed torque tube hub can be seen in Figure 9. This hub rotates in and is carried by the bearing assembly below the vibrator. A push rod from the vibrator (which is in the nonrotating system) extends down through the hollow shaft of the hub to a rotating bearing flexure assembly. The bearing of this small assembly is the connection between the rotating and nonrotating sides of the shaker system. Short links connect this bearing assembly to each of the rocker arms (Figure 10) which are mounted on the top surface of the hub. For symmetric shaking of the blades, a single rocker arm is used for each torque tube. Antisymmetric shaking is obtained by replacing one of the single rocker arms
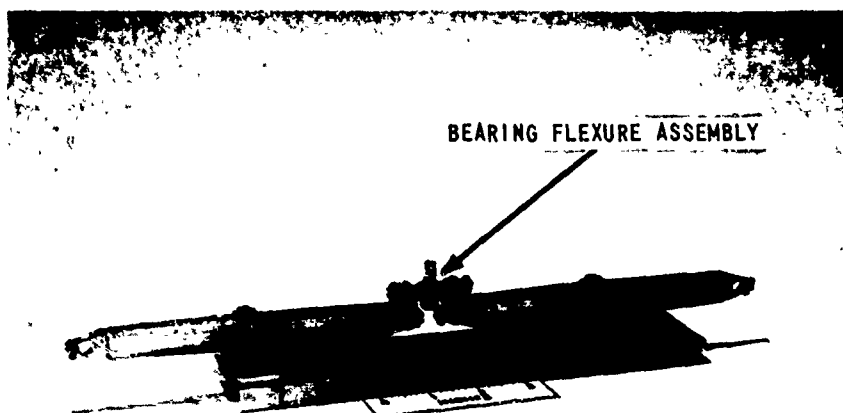
78

BEARING FLEXURE ASSEMBLY

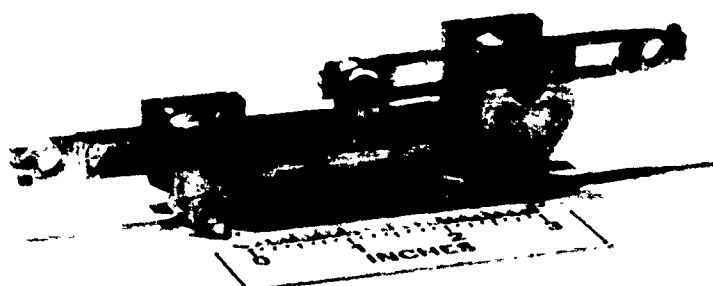Figure 10. ASSEMBLY OF SINGLE ROCKER ARMS WITH BEARING FLEXURE.

Figure 11. DOUBLE ROCKER ARM ASSEMBLY.

79

with a double rocker arm assembly (Figure 11); this reverses the motion of one torque tube. A push rod and inner pitch arm connect each torque tube to the rocker arms, as shown in Figure 12.

Each of the hollow torque tubes is cantilevered from the hub by two pairs of pitch bearings which react the transverse loads on the torque tubes. The two torque tubes are interconnected by a tension strap inside the hub. The axial (centrifugal) loads of the torque tubes are thus reacted against each other through this tension strap.

The outboard pitch arm and force rod are shown in Figure 13. The pitch arm is clamped to the torque tube to facilitate both radial and angular adjustments. The force rod is connected to the outboard pitch arm by a flat flexure designed to carry the centrifugal shear load of the force rod. The force coupling which transmits and measures the shaking force is assembled at the lower end of the force rod.

This force coupling accommodates the relative angular motions of the blade with respect to the force rod without significantly influencing the oscillating shaking force it transmits and measures. The complete assembly and an exploded view of its components are presented in Figure 14. The shaking force is transmitted through a pair of force wires preloaded by a pair of small beams strain gaged to measure the oscillating force. The centrifugal load of the coupling is reacted by the blade through a tension link. A small aluminum fixture clamped to the blade provides an adjustable attachment point for the force wires and tension link. At the attachment point this coupling adds 0.45 oz. of mass to the blade, and at this radial location it adds 0.82 oz. of tension per g of centrifugal acceleration. These small additional loads are included in the analysis, and their effects on the predicted results are found to be small for the test blades of this investigation.
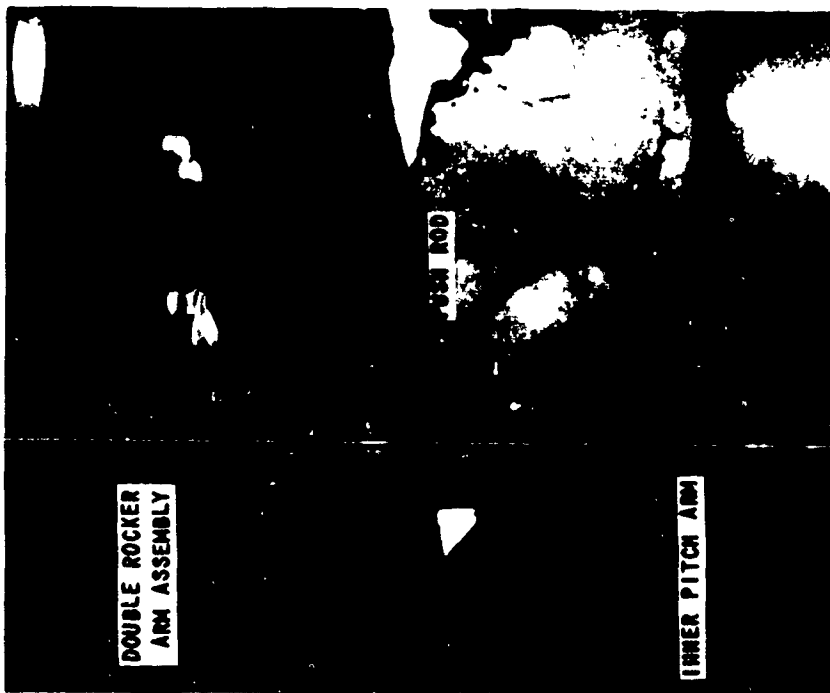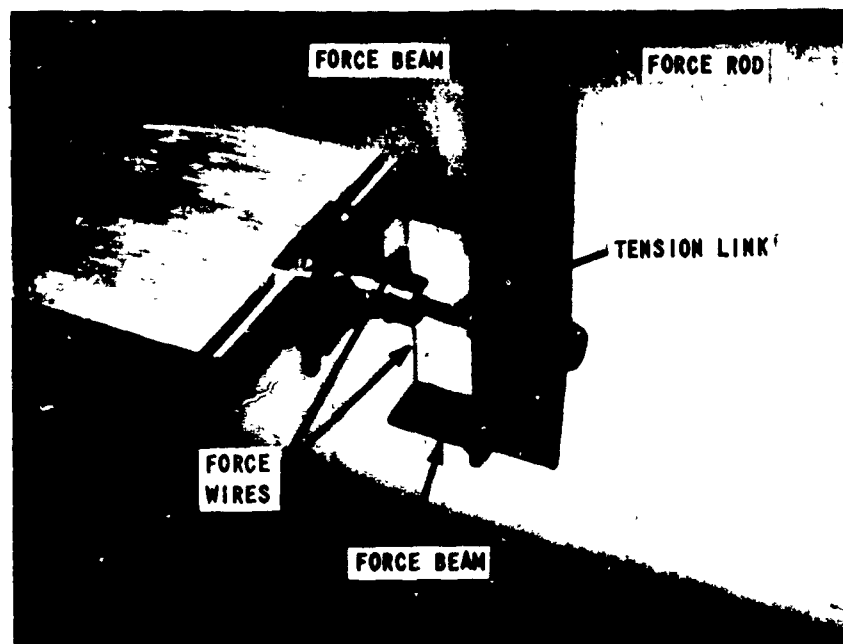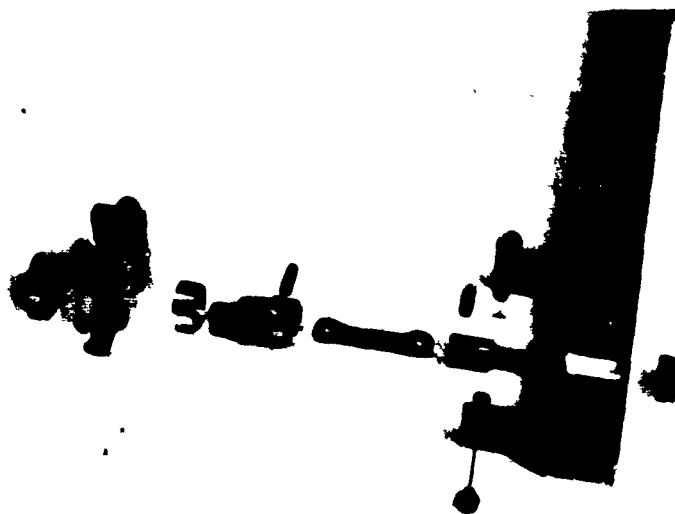
Figure 13. SHAKER SYSTEM OUTBOARD DRIVE LINKAGE.

Figure 12. SHAKER SYSTEM INBOARD DRIVE LINKAGE.

81

a) INSTALLED VIEW

b) EXPLODED VIEW

Figure 14. FORCE COUPLING.

82

INSTRUMENTATION

The test blade was instrumented to determine the spanwise distribution of moments in the flapwise, chordwise, and torsional bending modes by measuring the moments at five radial stations. These were, nominally, r/R = 0.26, 0.40, 0.55, 0.70, and 0.85. As a check on the relative phase and amplitude of the response of the two blades, the moments were measured at r/R = 0.26 on the second blade. The moments were measured using C. E. C. carrier-system "D" and strain-gage bridges with four active arms.

The flap and lag angles of the test blade were measured with calibrated strain-gage beams bridging their respective hinges; a strain-gage bridge installed on the pitch flexure straps was calibrated to measure the blade pitch angle. The shaking force transmitted to each blade was measured with a calibrated four-active-arm, strain-gage bridge installed on the force beams of each force coupling. The rotor shaft speed was determined from a once-per-revolution pulse generated by a variable reluctance pickup and steel pin protruding from the shaft. The oscillating input voltage to the electromagnetic vibrator was recorded as an indication of the total force input to the shaker system and the shaking frequency.

The available slipring assembly limited the rotating instrumentation to 20 channels. Twenty C. E. C. system "D" carrier amplifiers and two power supplies were used. Four power rings on the slipring assembly allowed the instrumentation to be commonly powered in two groups by the two power supplies. The data were recorded on two 6-inch (C. E. C. type 5-114) oscillographs which were slaved together. An internally generated correlation trace was recorded on each, and an accurate timing reference was supplied by recording a 60-Hz signal on each oscillograph.

In addition to the data instrumentation, nine channels of strain-gage instrumentation were required for monitoring the steady and oscillating stresses in the rotating shaker system during these initial tests. The requirement to monitor the nine channels of stresses in the shaker system left only eleven channels for data. The eleven data signals recorded simultaneously were the three blade root angles, the two shaking forces, five of the test blade moments, and one moment from the second blade. The six moments chosen to be recorded simultaneously were either the flapwise, chordwise, or torsional moments, depending on the mode being excited. The switching of signals to be recorded was facilitated by miniature plug-connectors installed in the rotating system. The wiring harnesses, terminal strips, jumpers, plug-connectors, etc., in the rotating system were arranged to provide a flexible data selection-capability, e.g., the nine channels which were used to monitor stresses during these tests could be transferred to record additional blade-moment signals by changing plug connections.

The 50-pound electromagnetic vibrator was driven by a variable oscillator and power supply. A frequency counter monitoring the oscillator provided the operator with an indication of the shaking frequency. The operator monitored the shaking force to the test blade and its response (the moments at one station) on the x and y axes of an oscilloscope. The rotational speed of the system was read on a frequency meter.

EXPERIMENTAL PROGRAM

The objective of the experimental phase of this program was to develop an apparatus and a testing technique for determining the natural vibration modes and frequencies of two-bladed model rotors in the absence of aerodynamic loads. The initial test program which is described herein was designed to determine the adequacy of the apparatus and testing technique. Thus the classical configuration of uniform blades, for which the natural vibration modes and frequencies can be computed accurately, was chosen for this investigation.

The tests were conducted in a vacuum tank with the air density (and thus the aerodynamic loads) reduced to about 1.5 percent of that at sea level; this is equivalent to an altitude of approximately 100,000 feet. The blade vibratory modes were explored at rotor speeds of 300, 600, 900 and 1200 revolutions per minute.

It is noted that the natural vibration modes of a two-bladed teetering rotor include all the modes of a two-bladed rotor with individual blade flapping and zero flap-hinge offset. This assumes that the blades and hub are the same for the two systems and that the rotor shaft impedance as seen by the rotor is infinite. The rotor hub used for these tests is the same in either configuration. It is converted to the teetering configuration by locking together, at the flap hinge, the flapping motion of the two blades. Therefore, the natural vibration modes and frequencies were explored in the teetering configuration. The following six elastic natural vibration modes were investigated:

1. First antisymmetric pin-ended flapwise bending.

2. Second antisymmetric pin-ended flapwise bending.

3. First symmetric cantilever flapwise bending.

4. Second symmetric cantilever flapwise bending.

5. First antisymmetric pin-ended chordwise bending.

6. Second cantilever torsion.

The second torsional mode was investigated instead of the first because the pitch flexure straps at the blade root were torsionally so soft relative to the blade that the first cantilever torsional mode is essentially a rigid body pitch response with virtually no torsional deformation of the blade.

Each mode was investigated by bringing the rotor up to the desired rotational speed and then applying the appropriate vibratory shaking force to the blades (as measured by the force couplings) at a

85

sequence of closely spaced discrete frequencies over a frequency range bracketing the natural frequency. An oscillograph recording of the structural moments and shaking force was obtained at each shaking frequency. The shaking force and the structural moments, at one spanwise station on the blade, were monitored on the x and y axes of an oscilloscope. This facilitated control of the force and response amplitudes. It also helped to nominally locate the natural frequencies by observation of the changing Lissajous pattern due to the phase shift of the blade response relative to the applied force as the shaking frequency passed through the natural frequency. The natural frequencies are determined by the minimums in the shaking force per unit amplitude of response as a function of shaking frequency.

THEORETICAL COMPUTATIONS

As discussed in the preceding sections, the experimental investigation of the natural frequencies and mode shapes was limited, in this particular program, to a rotor system with uniform blades. The conditions of blade uniformity were, therefore, introduced into the general theoretical formulation described in the section titled "Theoretical Development, "and the resulting mass and elastic matrices were obtained for the uniform blade. Two existing computer programs using the matrix method of solution described in the "Theoretical Development" section were modified to use these mass and elastic matrices. The flapwise and chordwise degrees of freedom are analyzed with one program and the torsion degree of freedom with the other program. Both programs are written in FORTRAN IV for use on an IBM 360 computer.

The flapwise-chordwise bending program consists of a main program and 8 subroutines. It has a storage requirement of 162,000 bytes. The blade is represented by a series of concentrated masses separated by massless elastic segments, each of constant stiffness. The maximum allowable number of blade segments in this program is 100. The rotor hub is represented by its inertias. The program computes the flapwise or the chordwise natural frequencies and mode shapes; it also has the capability of computing the coupled flapwise-chordwise modes for a twisted blade. A flow chart of the program logic is presented in Figure 15.

The segmentation of the blade representation is chosen to represent the spanwise blade properties adequately. The inputs are the spanwise mass, elastic, and twist distributions for the mode to be calculated; the hub inertias; root boundary conditions; rotor rotational speed; and initial trial value of the natural frequency. The printed output of the program includes all the inputs in addition to the computed shear, bending moment, slope, and deflection at the spanwise position of each concentrated mass.

The computational scheme used in the torsion program is based on the Holtzer method. The blade is represented by a series of concentrated inertias separated by inertialess elastic segments. A flow chart of the program is presented in Figure 16.
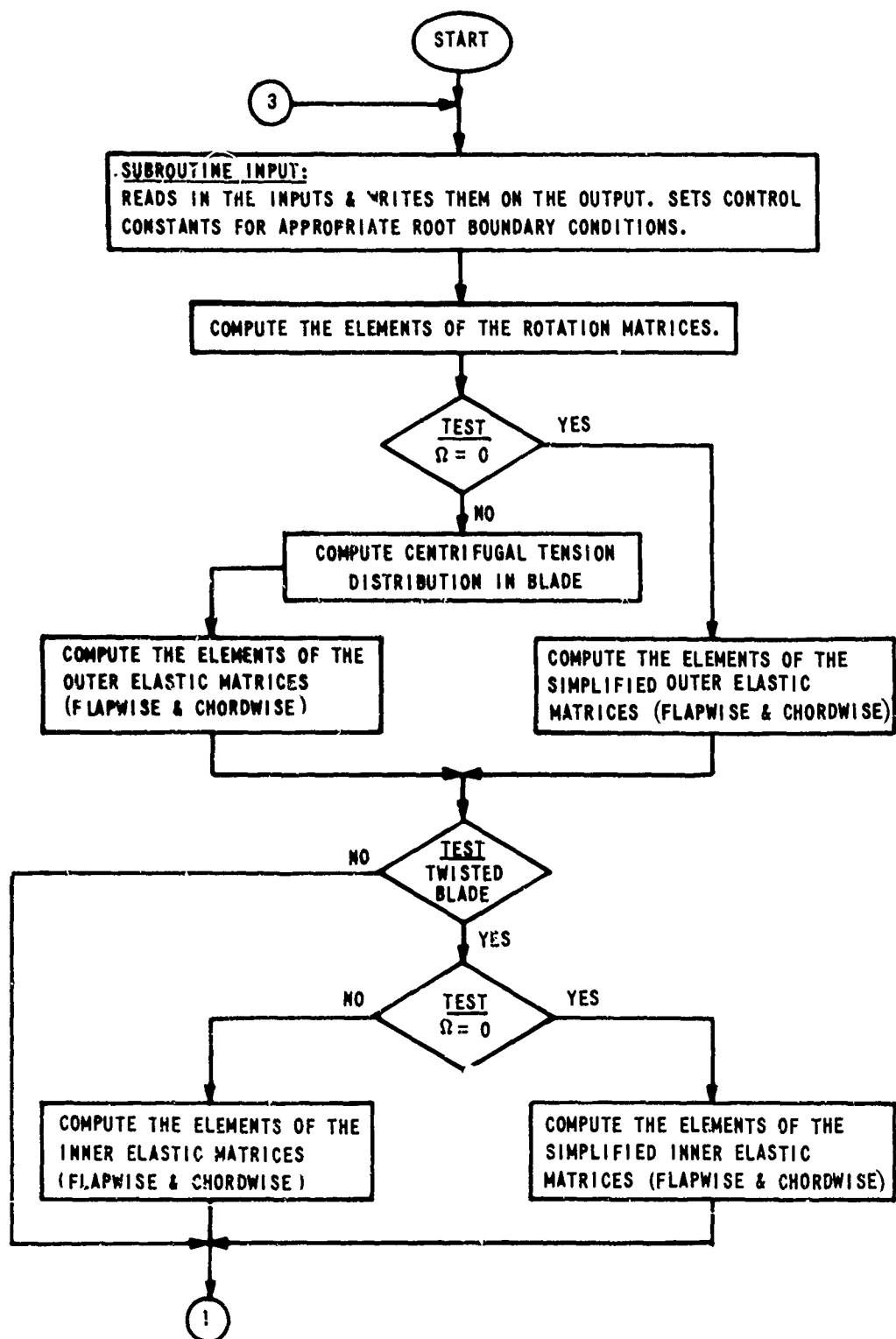
Figure 15. FLOW DIAGRAM FOR THE FLAPWISE-CHORDWISE
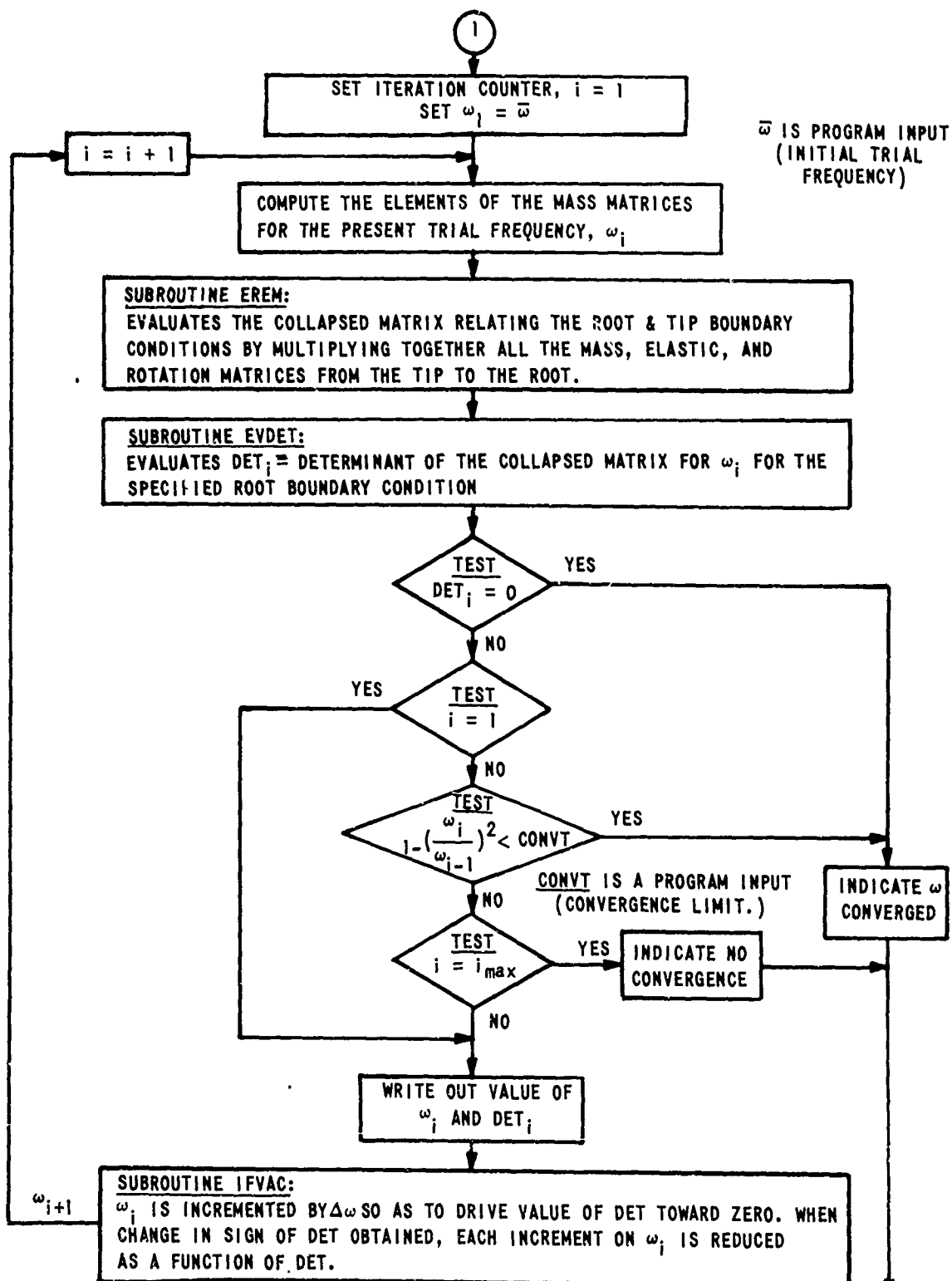BENDING VIBRATION COMPUTER PROGRAM.
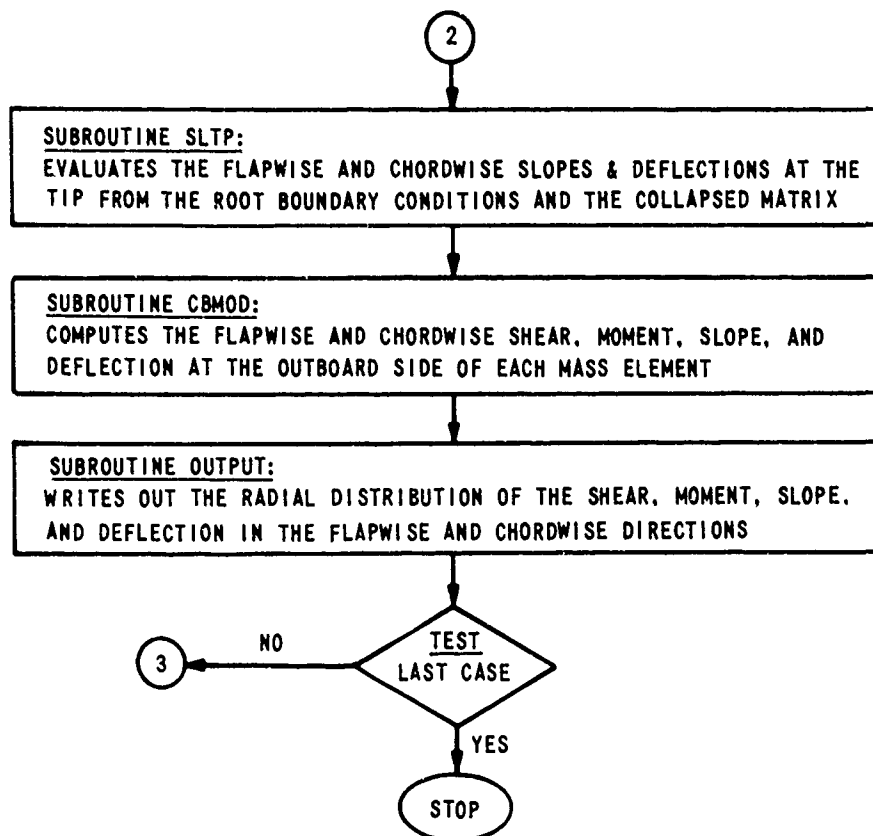
88

Figure 15. (Cont'd)

89

Figure 15. (Cont'd)

START

READ INPUTS

TEST
1

≥ 3

$\phi = (\Delta\theta_{i-1} - \Delta\theta_{i-2})/(\omega_{i-1} - \omega_{i-2})$

$\omega = (\omega_{i-2} - \Delta\theta_{i-2})/\phi$

$K = 0.10225 \times \omega_i{}^2$

$MOM_1 = 0.0$
$\theta_1 = 1.0$

$\overline{\omega_i}$ IS INITIAL TRIAL FREQUENCY
$\Delta\overline{\omega_i}$ IS FIRST FREQUENCY INCREMENT

$j = 1$

$MOM_j = MOM_j + \theta_j \times K \times I_j$

$\theta_{j-1} = \theta_j - (MOM_j \times l_j)/GJ_j$

$j = j + 1$

NO

TEST
$j = N$

N IS INPUT NUMBER
OF RADIAL STATIONS

YES

$\Delta\theta_i = \theta_N + 1$

TEST
$\Delta\theta_i < LIMIT$

YES

NO

TEST
$i = i_{max}$

NO

$i = i + 1$

i_{max} IS INPUT

YES

ITERATION
CONVERGED
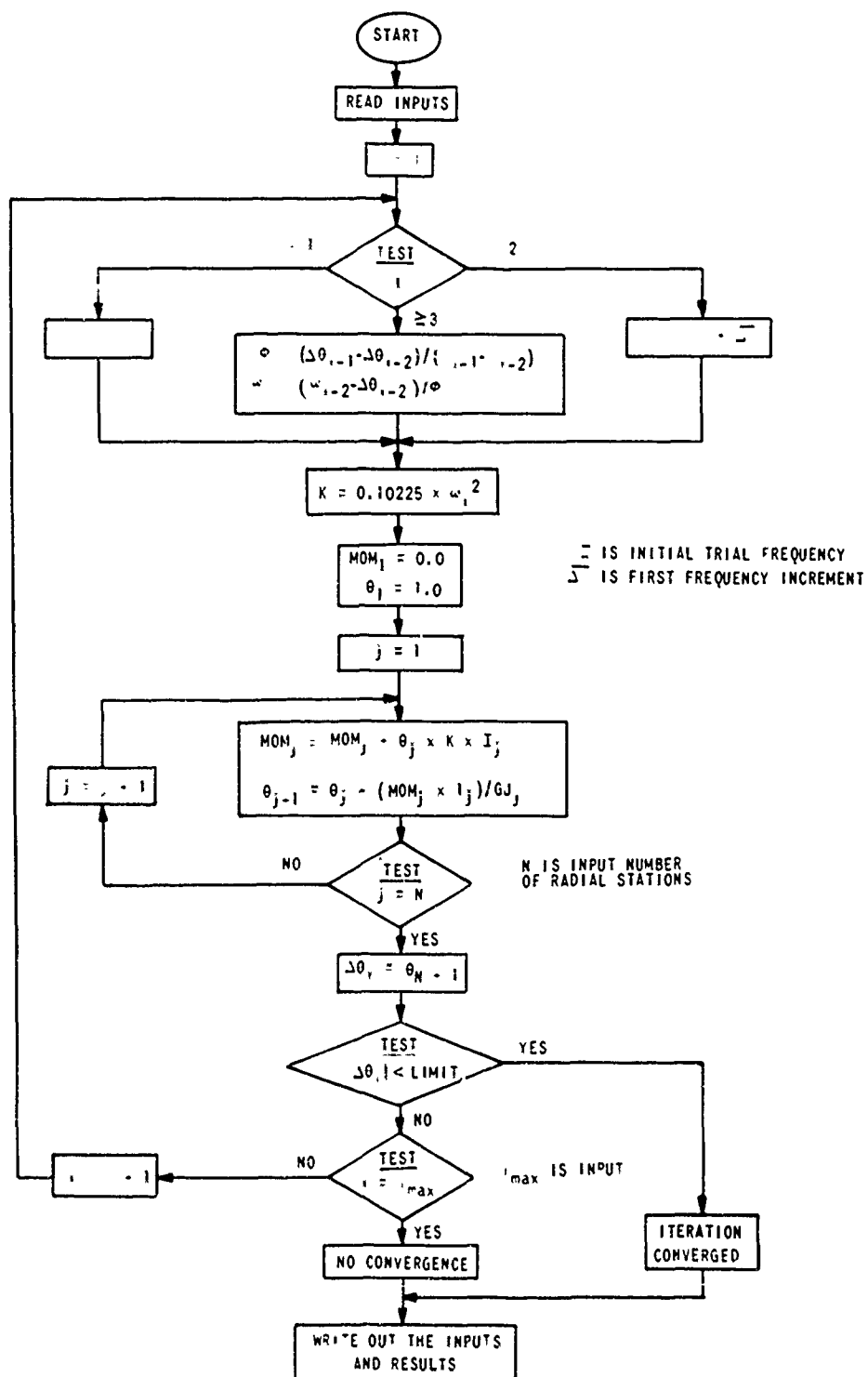
NO CONVERGENCE

WRITE OUT THE INPUTS
AND RESULTS

Figure 16. FLOW DIAGRAM FOR THE TORSIONAL BENDING VIBRATION PROGRAM.

91

DISCUSSION OF TEST RESULTS AND
## COMPARISON WITH COMPUTED RESULTS

The natural frequencies, mode shapes, and corresponding shear and moment distributions were computed for each of the six blade modes corresponding to those of the two-bladed rotor system which was investigated experimentally. Comparisons of the distributions of the measured and computed spanwise moments and the natural frequencies for each of these modes are presented in Figures 17a through 17f. The comparisons are made at rotational speeds of 300 and 600 rpm for all modes and, in addition, at 900 rpm for the first symmetric cantilever flapwise bending mode. The spanwise moment distributions and natural frequencies computed for the nonrotating cases are also presented for reference, although they were not determined experimentally.

The computed spanwise moment distribution for each mode is plotted on a graph as a continuous curve, and the measured moments are plotted at each of the five instrumented stations. The amplitudes of the moment traces were read at three different times within each oscillograph recording (obtained at the experimentally determined natural frequency), and the resulting three sets of moment data are shown in the figures. For identification, a different plotting symbol is used to represent each of these three sets of measured moments. The spread of the measurements at each spanwise station is an indication of the overall accuracy of the reduced data.

The computed moment distributions presented are for the mode shapes normalized to a unit tip deflection-- for the bending modes, one inch of tip deflection was used; for the torsion mode, one radian of tip rotation was used. The measured moments, however, were obtained for tip response amplitudes considerably less than these unit values. Therefore, to enable comparisons of the distributions of the measured and computed moments, the measured moment distribution in each mode was scaled so that the maximum measured moment was made equal to the computed moment at the same radial station.

In general, the measured moment distributions are considered to be in satisfactory agreement with the computed distributions, but there are three exceptions. One exception is the antisymmetric pin-ended flapwise bending mode at 600 rpm (Figure 17a). The other two exceptions are the second torsion mode at 300 rpm and at 600 rpm (Figure 17f).

With one exception, the differences between the measured and computed natural frequencies range from 2 to 14 percent. The exception is the first antisymmetric pin-ended chordwise bending mode for which the difference between the computed and measured natural frequency is about 35 percent.
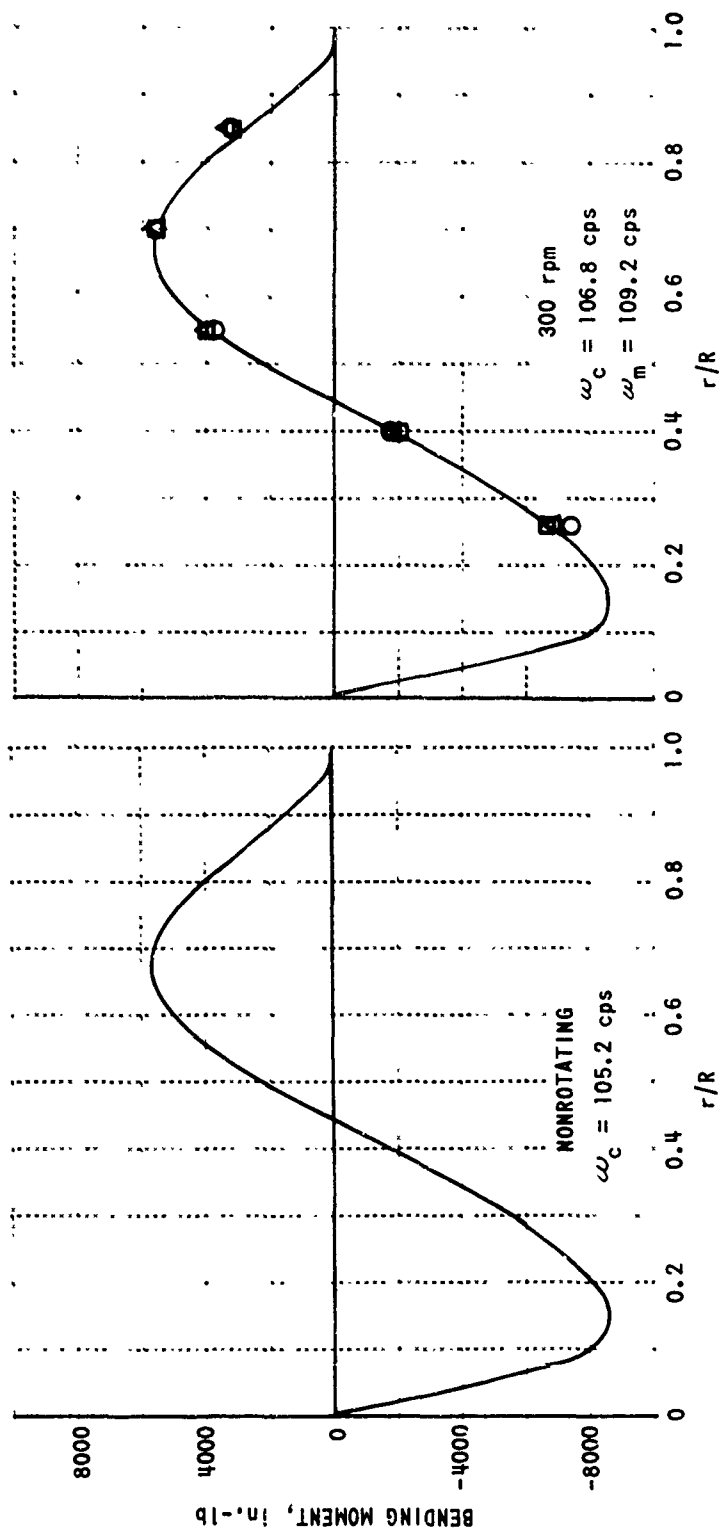
NONROTATING

$\omega_c = 32.2$ cps

300 rpm

$\omega_c = 34.1$ cps
$\omega_m = 38.6$ cps

BENDING MOMENT, in.-lb

r/R

r/R
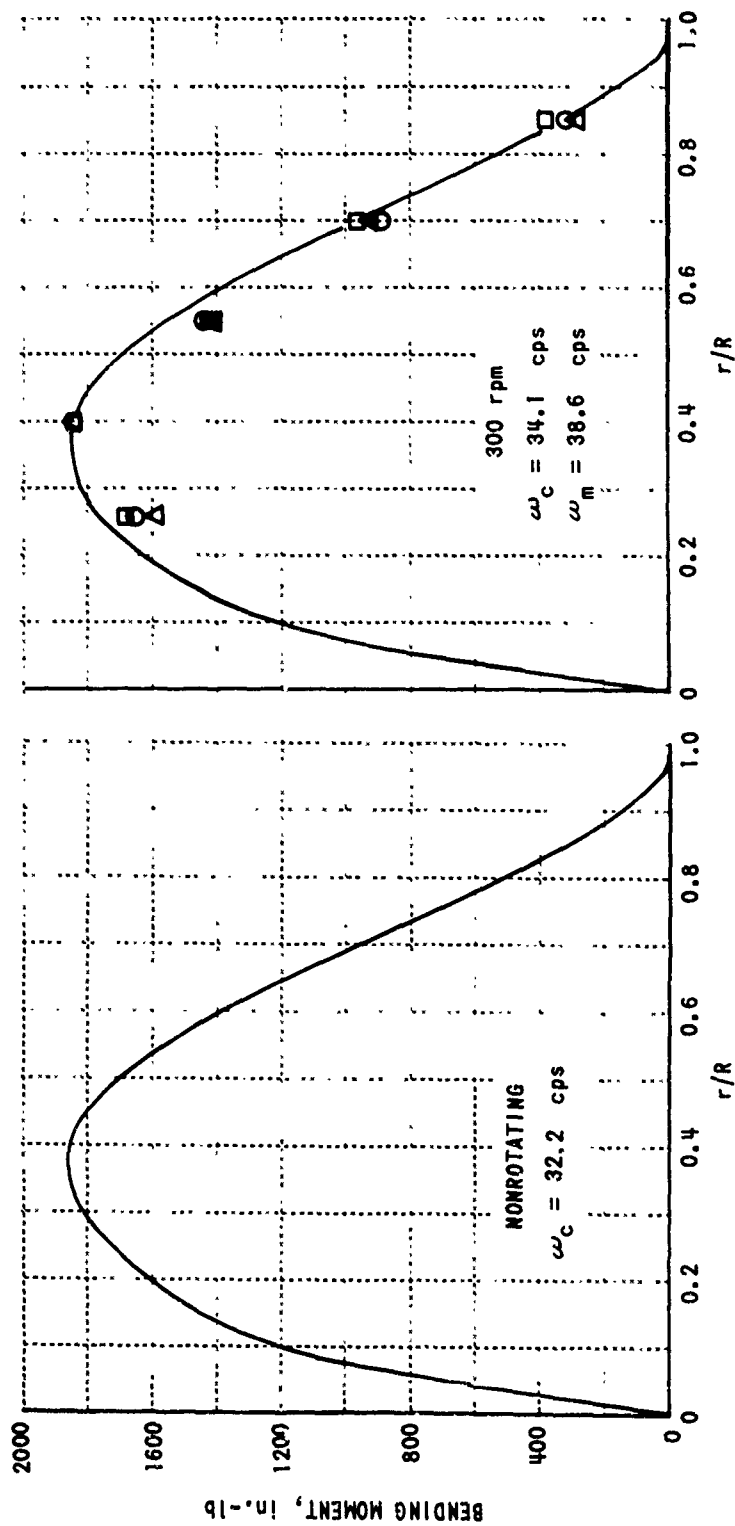
a. FIRST ANTISYMMETRIC PIN-ENDED FLAPWISE BENDING MODE

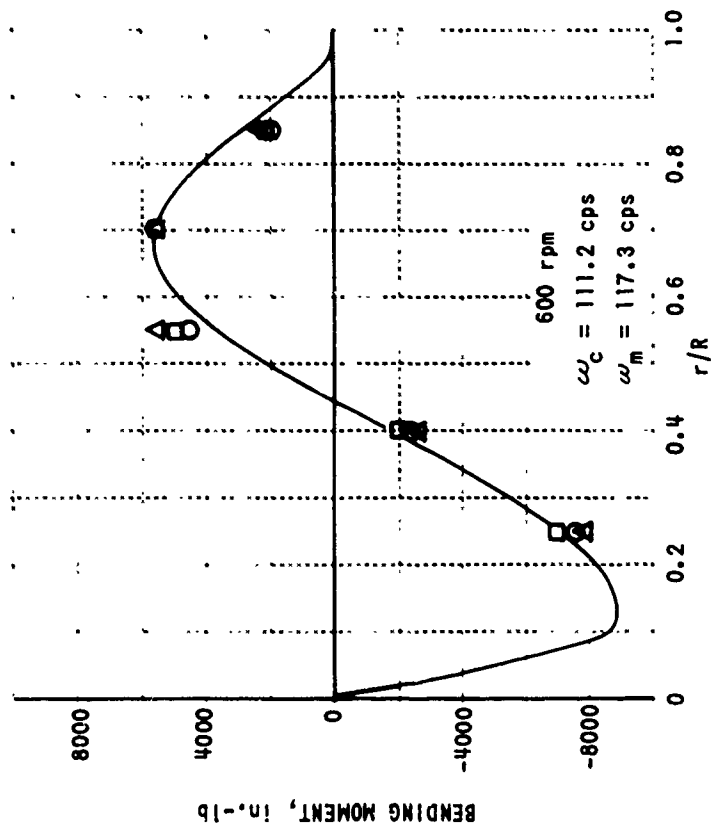Figure 17. COMPARISONS OF MEASURED AND COMPUTED SPANWISE MOMENT DISTRIBUTIONS FOR EACH MODE.
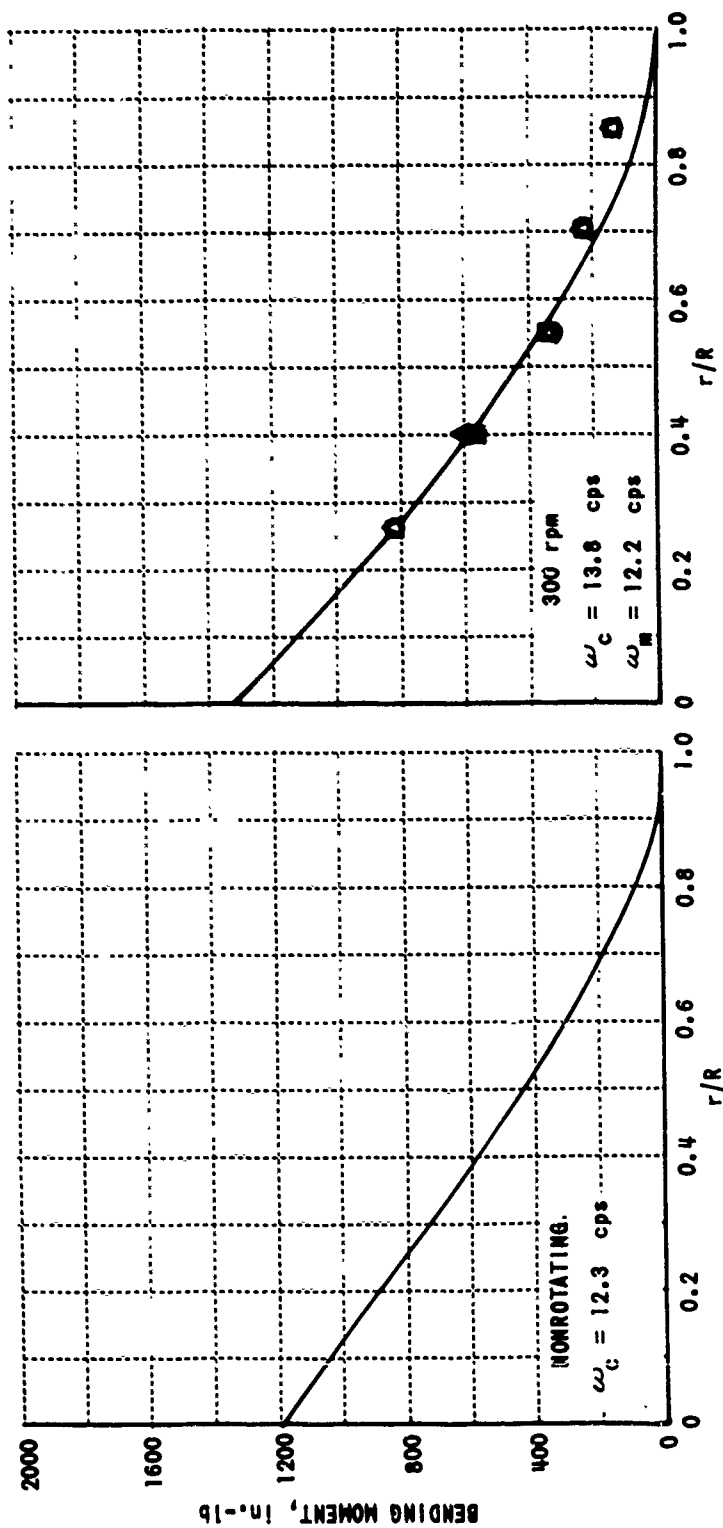
93
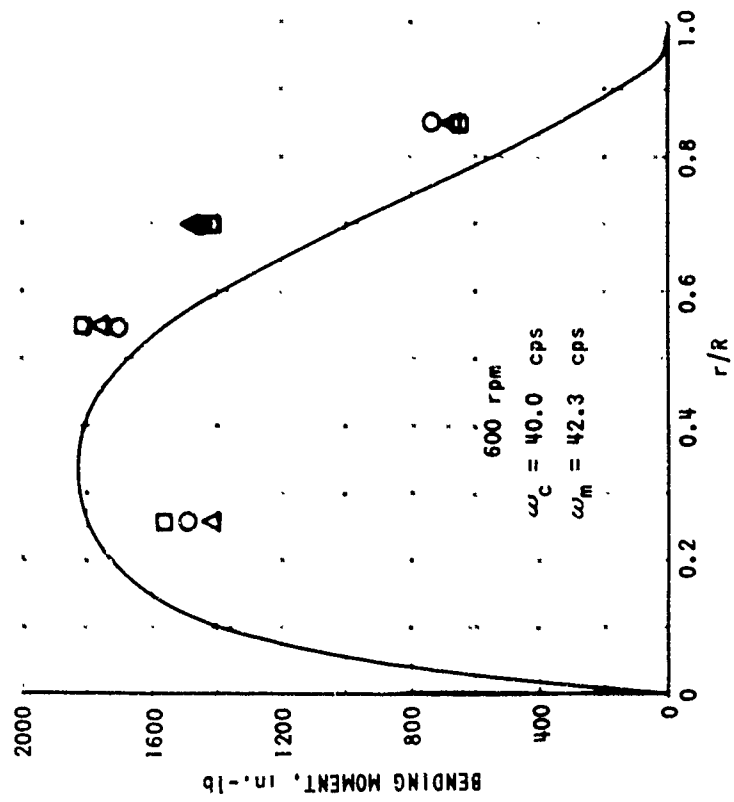
a. (Cont'd)

Figure 17. (Cont'd)

b. SECOND ANTISYMMETRIC PIN-ENDED FLAPWISE BENDING MODE
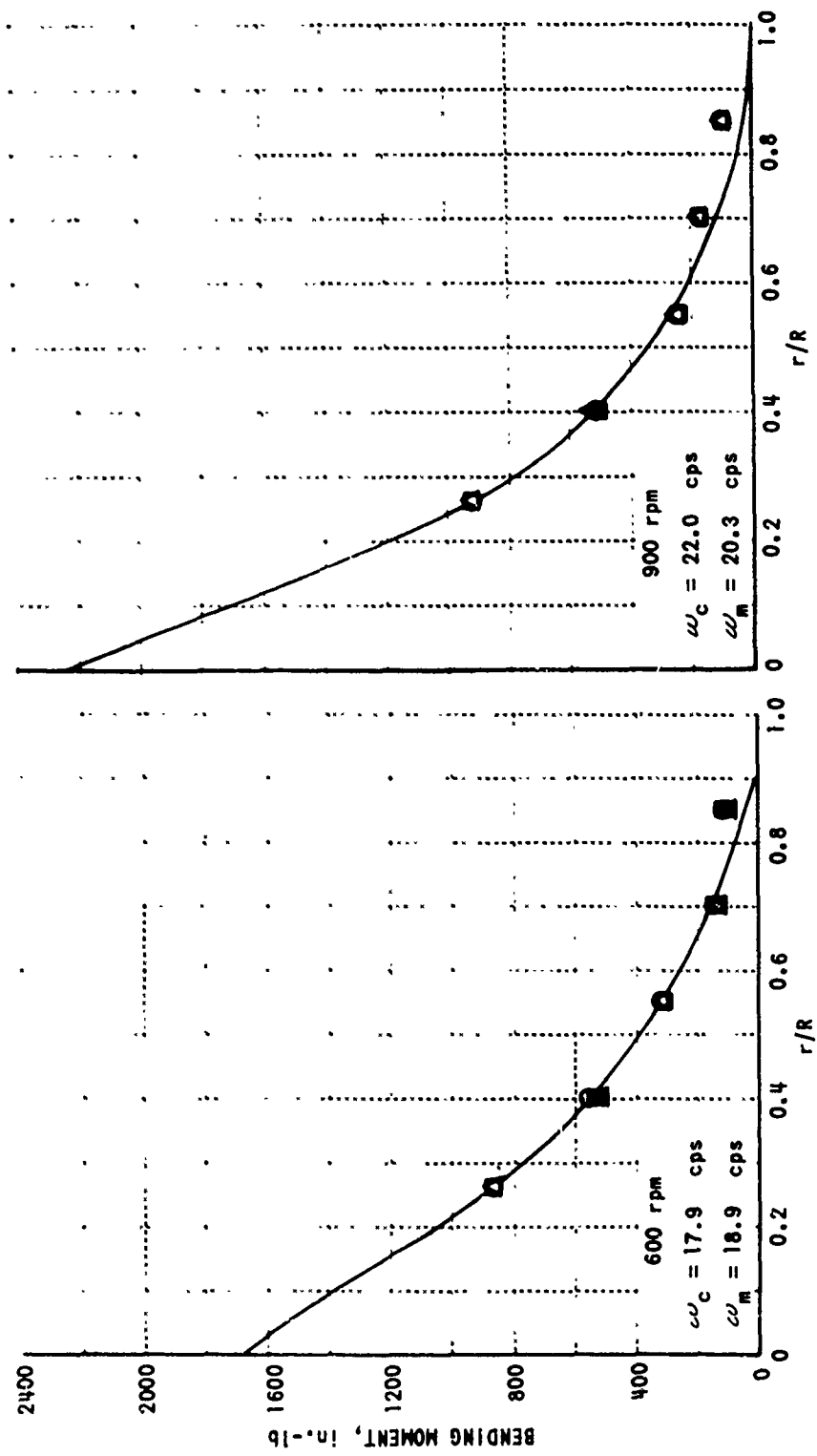
Figure 17. (Cont'd)

600 rpm

$\omega_c = 111.2$ cps

$\omega_m = 117.3$ cps

b. (Cont'd)

Figure 17. (Cont'd)

BENDING MOMENT, in.-lb

96

c. FIRST SYMMETRIC CANTILEVER BENDING MODE

Figure 17. (Cont'd)

97

c. (Cont'd)

Figure 17. (Cont'd)
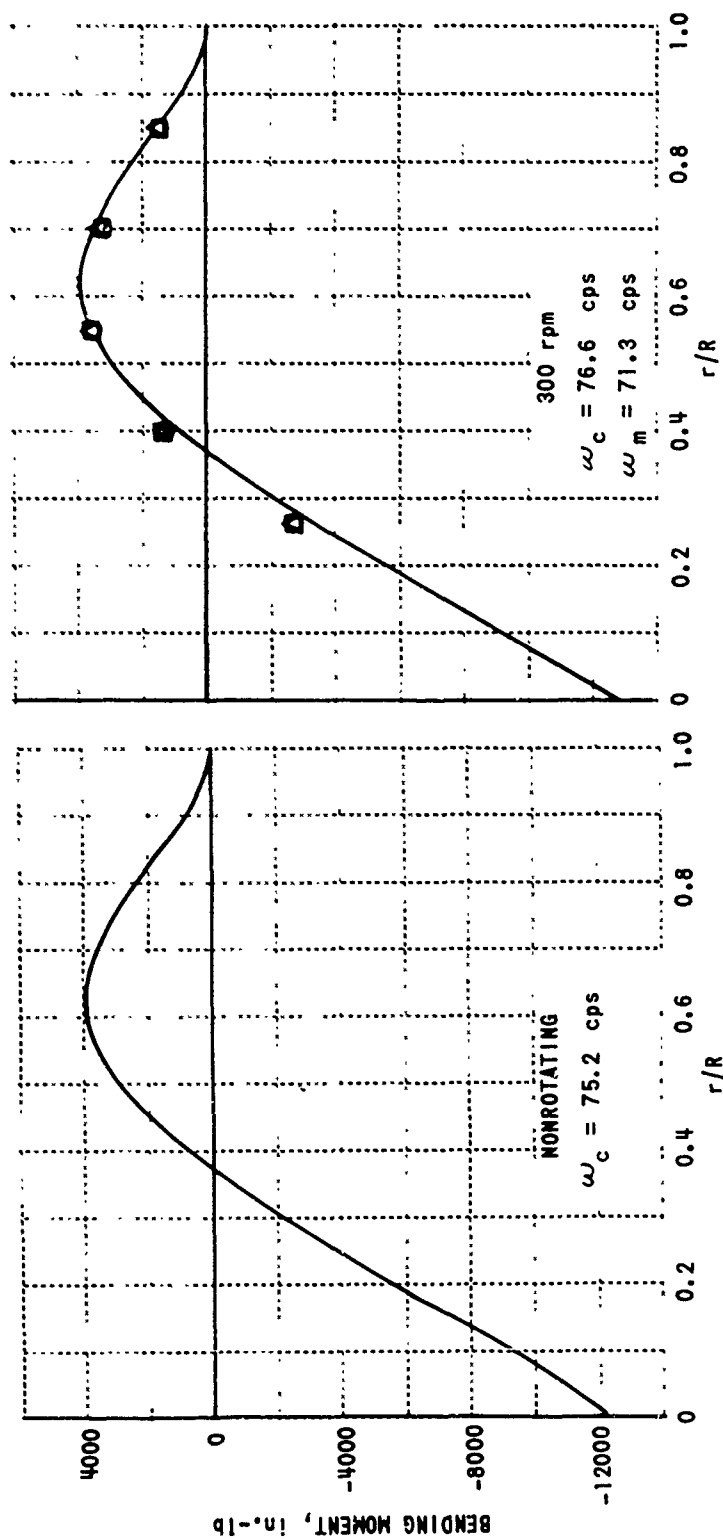
NONROTATING

$\omega_c = 75.2$ cps

300 rpm

$\omega_c = 76.6$ cps

$\omega_m = 71.3$ cps

r/R

r/R

BENDING MOMENT, in.-lb

4000

0

-4000

-8000

-12000

0   0.2   0.4   0.6   0.8   1.0

d. SECOND SYMMETRIC CANTILEVER FLAPWISE BENDING MODE

Figure 17. (Cont'd)

600 rpm

$\omega_c = 80.9$ cps

$\omega_m = 74.8$ cps

r/R

d. (Cont'd)

Figure 17. (Cont'd)

BENDING MOMENT, in.-lb

Figure 17. (Cont'd)

FIRST ANTISYMMETRIC PIN-ENDED CHORDWISE BENDING MODE

300 rpm
$\omega_c = 235.1$ cps
$\omega_a = 170.8$ cps

NONROTATING
$\omega_c = 234.7$ cps

BENDING MOMENT, in.-lb

r/R
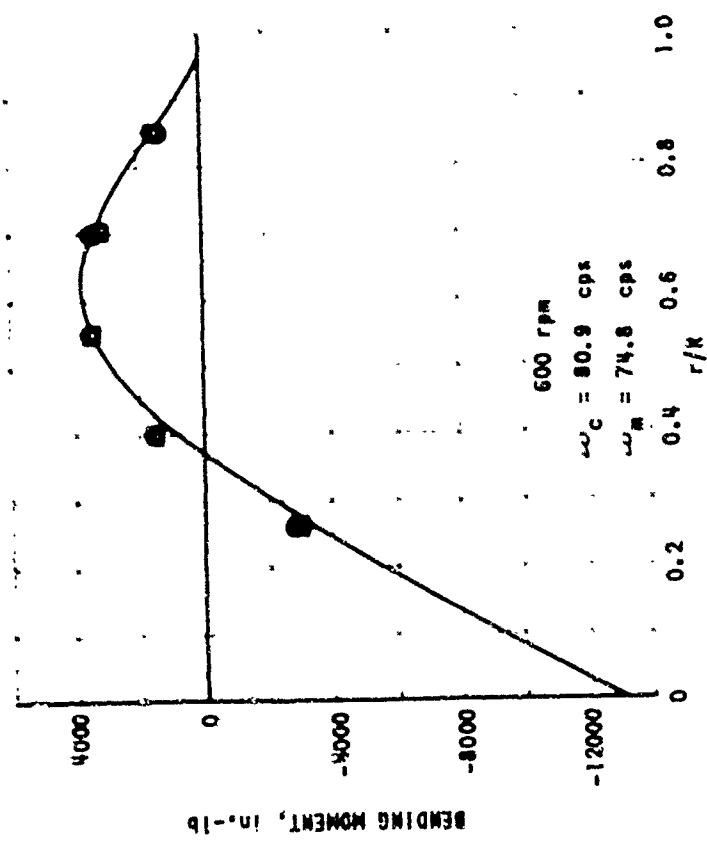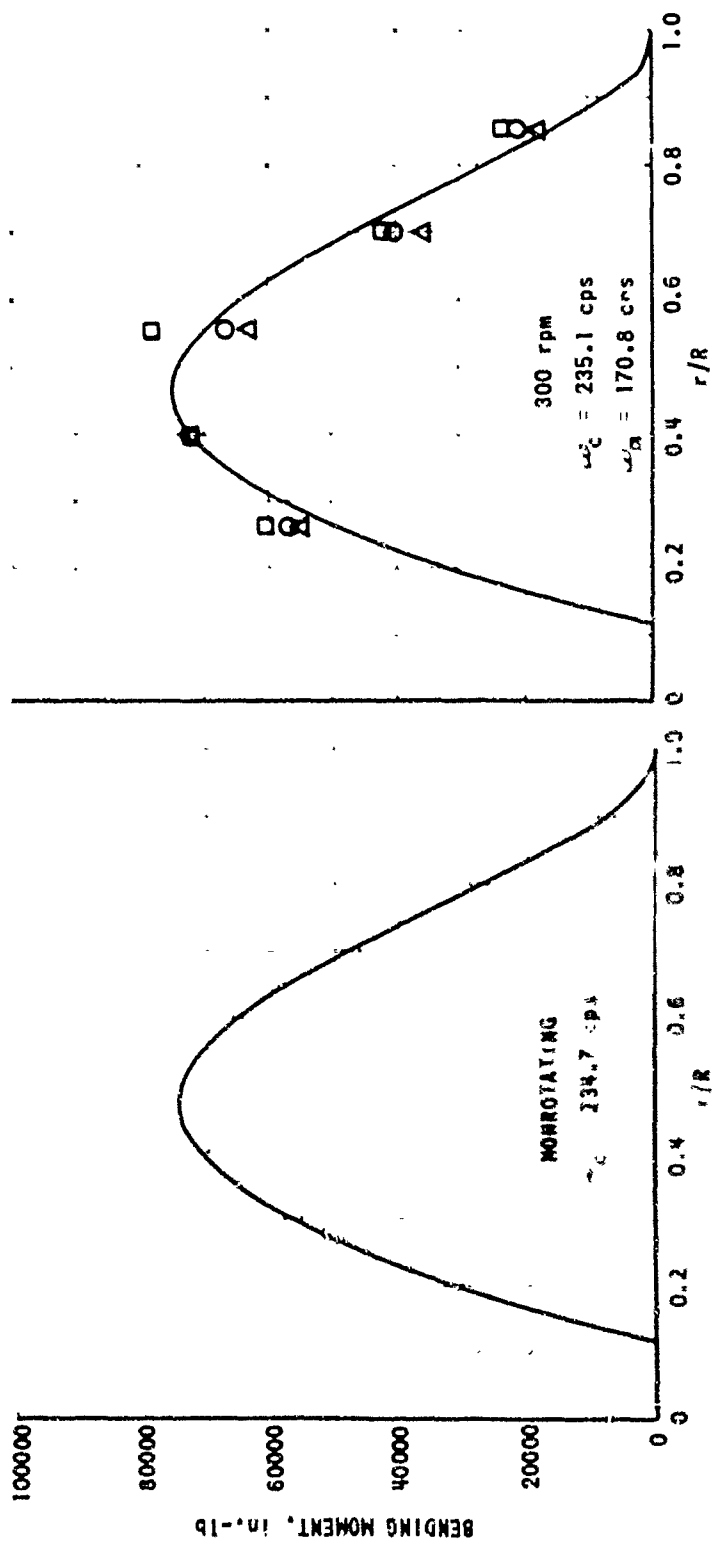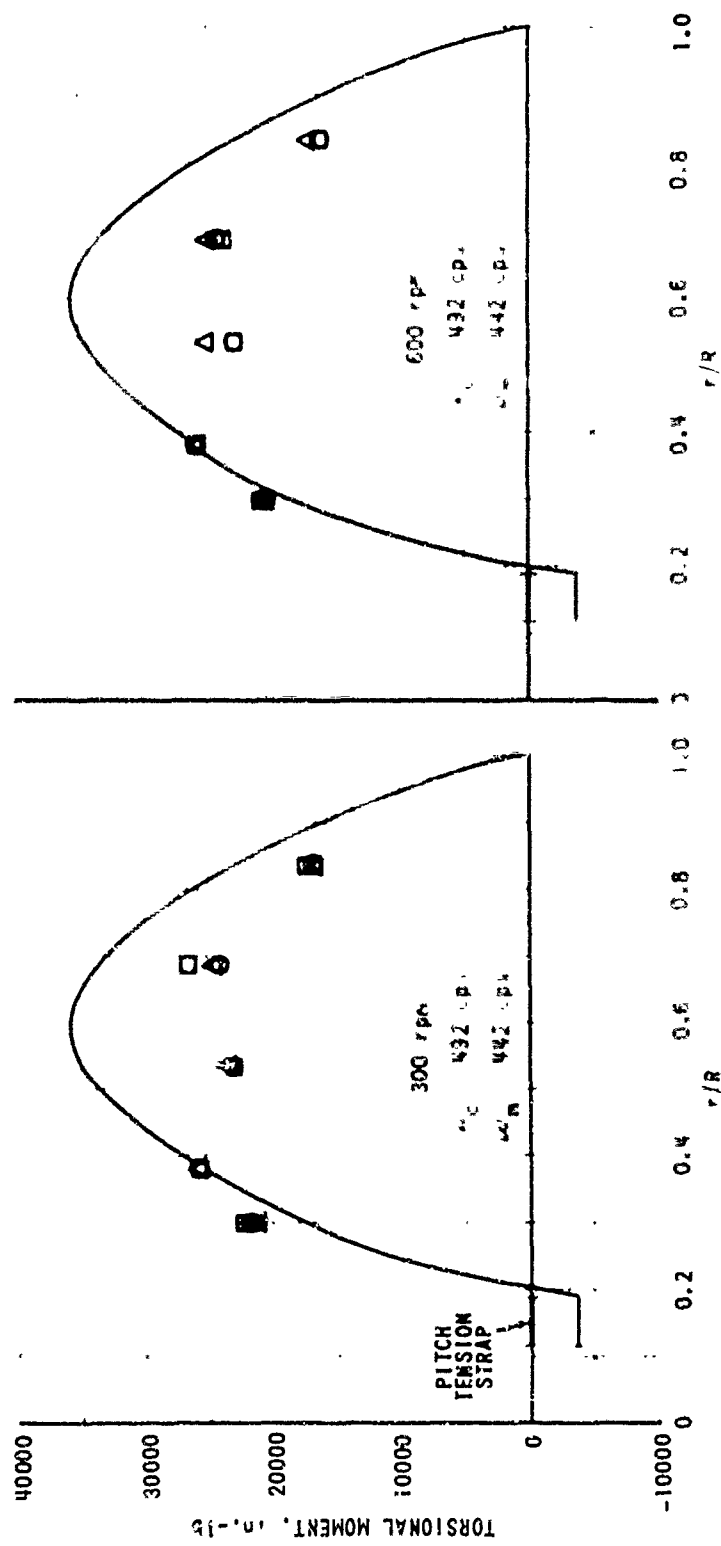
f. SECOND ANTISYMMETRIC CANTILEVER TORSION MODE
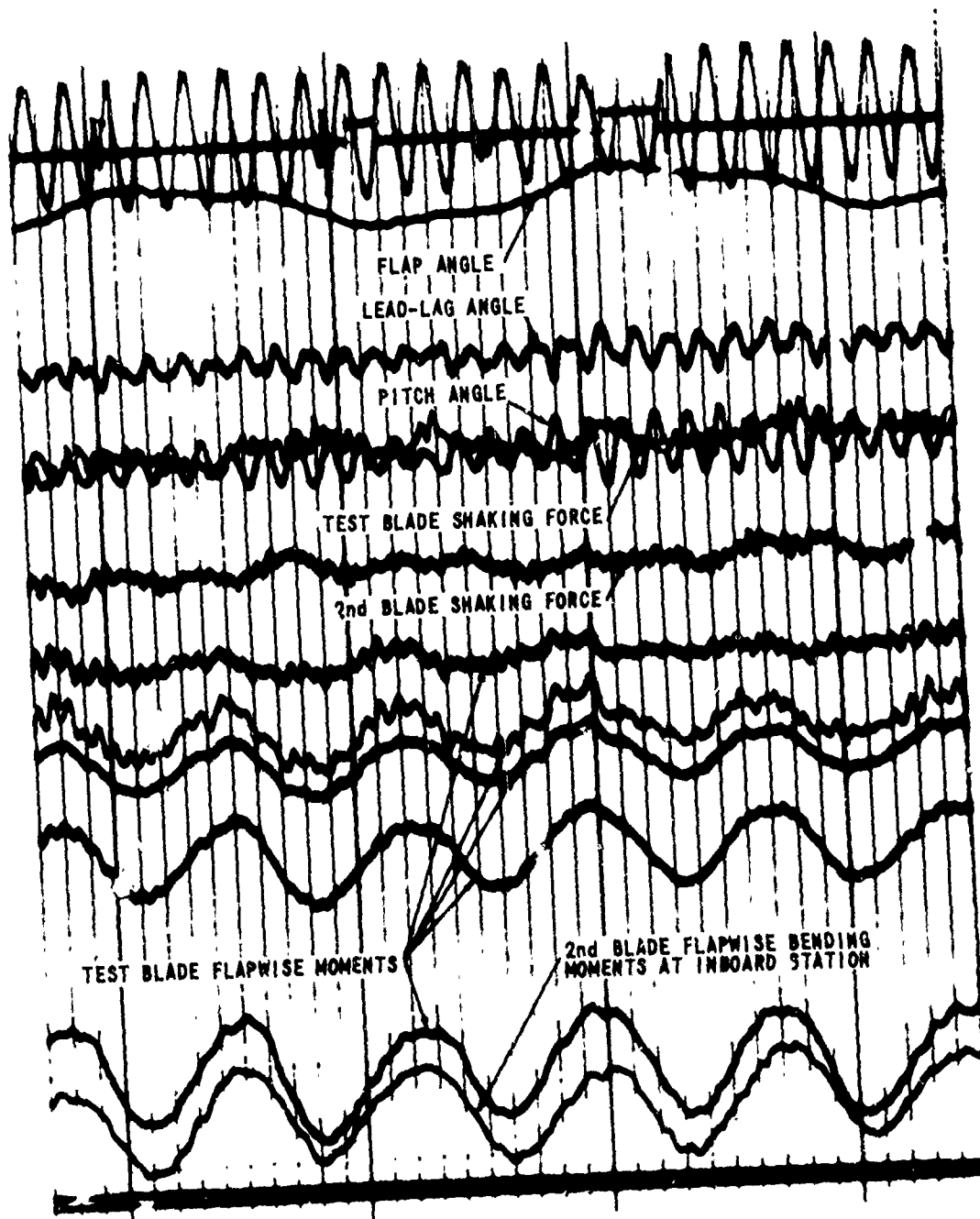
Figure 17. (Cont'd)

103

Analyses of the theoretical and experimental results have indicated that the differences can be attributed to both experimental inaccuracies and limitations in the assumed mathematical model.

As a precautionary measure, the shaking force during these initial tests was restricted to a rather low level. This factor, together with the high stiffness of the test blades, resulted in low amplitude response of the blade at the fundamental shaking frequency. Consequently, the signal levels were very low, in general, and the instrumentation was operated at maximum gain. Internal electronic noise was, therefore, amplified as well. Furthermore, excitations extrinsic to the fundamental shaking force were apparently being introduced to the system. Sources of the extrinsic excitations are such things as the rotating shaker system itself, small misalignments of the rotating shaker system with respect to the test rotor system, the hydraulic drive motor, and other mechanical equipment operating in the building (via the vacuum tank structure). These extraneous excitations and the very low structural damping of the solid test blades resulted in significant responses at other frequencies in addition to the fundamental shaking frequency. These effects superimposed a "noise" on the signal corresponding to the response to the fundamental shaking force. As a result of these factors, the signal-to-noise levels on the records were quite low and became worse with increasing rotational speed.

Sample oscillograph records are presented in Figure 18. Both of these sample records were obtained for the first symmetric cantilever flapwise bending mode being forced very close to its natural frequency. One record was taken at a rotational speed of 300 rpm and the other at 500 rpm; the noise level and its increase with rotational speed are evident.
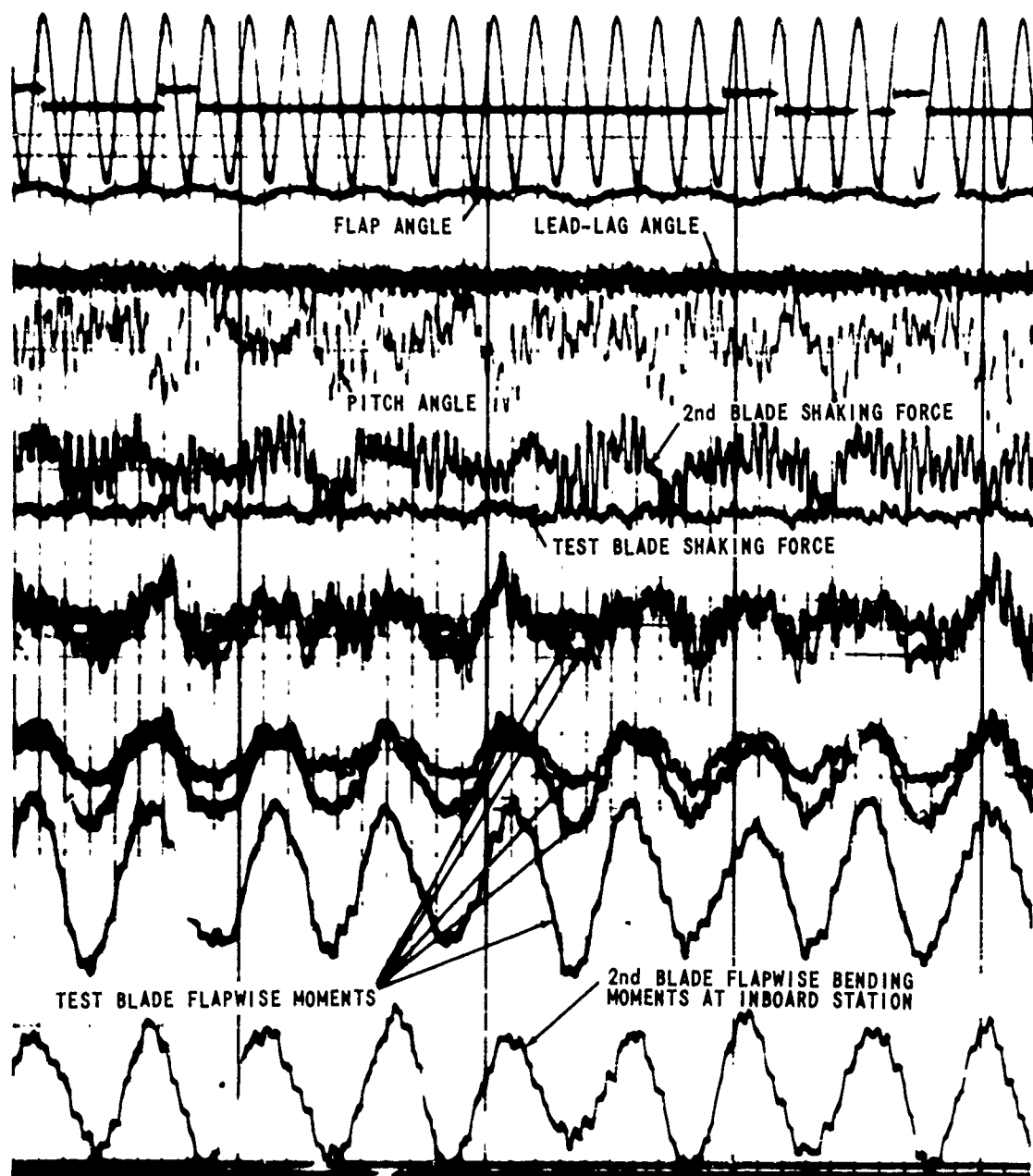
Without any filtering of the data signals, the low signal-to-noise levels resulted in readout errors, particularly in the measurement of the natural frequencies. The measured natural frequency was determined by the minimum in the variation with fundamental shaking frequency of the shaking force per unit amplitude of response (i. e., at the peak response). The precise definition of this minimum was obscured by the noise level in the data.

Nevertheless, while there are limitations on the experimental accuracy associated with problems such as those discussed above, the probable errors in the measurements are not sufficiently large to account for the differences between the computed and measured results in general. The major reason for the differences that have been observed in this investigation is that the analytical representation does not correspond to the actual physical system that was tested. It was intended that the model configuration and conditions designed for these initial tests should be so simple as to be representable by a uniform beam having negligible intermodel coupling. This objective apparently

FLAP ANGLE

LEAD-LAG ANGLE

PITCH ANGLE

TEST BLADE SHAKING FORCE

2nd BLADE SHAKING FORCE

TEST BLADE FLAPWISE MOMENTS

2nd BLADE FLAPWISE BENDING
MOMENTS AT INBOARD STATION

a. 300 rpm

Figure 18. SAMPLE OSCILLOGRAPH RECORD.

FLAP ANGLE   LEAD-LAG ANGLE

PITCH ANGLE   2nd BLADE SHAKING FORCE

TEST BLADE SHAKING FORCE

TEST BLADE FLAPWISE MOMENTS   2nd BLADE FLAPWISE BENDING MOMENTS AT INBOARD STATION

b. 900 rpm

Figure 18. (Cont'd)

was not achieved, and significant effects were introduced due to coupling and the simultaneous excitation of several degrees of freedom. For example, the exceptionally large discrepancy noted previously between the measured and computed natural frequency for the pin-ended chordwise bending mode is due to the fact that the measured resonance was actually that of a coupled-mode response whereas the analysis assumes no coupling. Indications are that the measured response in this case was a coupled mode involving not only pin-ended chordwise bending but significant amounts of torsion and motion of the rotor shaft and drive system as well. In addition to this usual type of linear coupling, there can be a nonlinear coupling, such as a change (and/or periodic variation) of the generalized mass in the pitch and torsion modes proportional to the simultaneous response in one of the bending modes. This intermodal coupling due to multimode forced response can have a significant influence on the measured resonant frequencies of the system, depending on the modes and their amplitudes. The simple analytical representation which was assumed does not account for the response of the rotor on its shaft and drive system. In the computations for the pin-ended modes, the blade moments and deflections have been assumed to be zero at the pin; this is not necessarily true for the test rotor system. For example, the torsional response of the rotor shaft and drive system will allow an oscillating displacement of the radially offset lead-lag hinge. Also, the relatively complex tension-torsion straps used in the hub in place of pitch bearings and a pitch spring apparently introduced coupling in the system which is not accounted for in the analytical representation.

107

CONCLUDING REMARKS

An analysis and computational technique has been developed for predicting the natural vibration modes and frequencies of rotor blades which are of a general configuration including the combined rigid body and elastic motions of the blades. This was programed for the special case of the uniform blade used in the experimental phase of this effort.

An experimental apparatus and a testing technique have been developed for determining the natural vibration modes and frequencies of two-bladed rotor systems in all degrees of freedom while operating in the absence of aerodynamic loads. Initial tests to establish the capabilities of this experimental apparatus were conducted by measuring the natural vibration modes and frequencies of a relatively simple two-bladed rotor system.

The experimental phase of this effort has demonstrated the capability of the experimental apparatus for applying controllable oscillating shaking forces in the plane of rotation or normal to the plane of rotation at the tip of each blade of a two-bladed rotor while rotating in a near vacuum. This program has also demonstrated the feasibility of the experimental technique for the use of this apparatus to determine the natural vibration modes and frequencies of a two-bladed rotor system while rotating in a near vacuum.

The tests performed with the system during this initial program have indicated that, with some small improvements, sufficiently accurate measurements of natural vibration modes and frequencies can be made. Satisfactory measurements have been extracted from the experimental data even though the signal-to-noise levels were quite low and no special measures were taken during data processing to minimize the resultant errors. Some elementary mathematical filtering of the data might have improved the results substantially.

It appears that the extrinsic excitations constitute the primary limitation on the adequacy of the experimental apparatus. The simultaneous excitation of the rotor at frequencies other than the fundamental test frequency and the corresponding response can have a significant influence on the measured resonant frequencies. The coupling effects (which can be linear or nonlinear) associated with such simultaneous excitations are normally neglected but could be important depending on the particular modes and their amplitudes. Some effort must be applied to reducing the levels of these undesirable shaking forces or to isolating the rotor system from them.

A major cause of the differences between the measured and computed natural frequencies appears to be that the assumed mathematical model does not correspond to the actual system tested. Some of the complexities in the test model were introduced as a result of making use of an available rotor hub. For example, the pitch-tension

straps used in this hub (in place of a pitch bearing and pitch spring) are believed to have produced unexpectedly large coupling effects. However, the model rotor system used in these tests was designed on the basis of standard procedures in which effects such as those described above and in the previous section have normally been assumed negligible. Indications are that these assumptions are not valid for the high-frequency modes. Consequently, although these initial tests were intended primarily to establish the capability of the experimental system, they have, in fact, already demonstrated the inadequacy of structural analysis methods in current use.

RECOMMENDATIONS

The present effort has developed an analysis capable of predicting the dynamic characteristics of rotor systems of a very general configuration and has developed, fabricated, and performed initial tests with the experimental apparatus required to verify the analysis. While the feasibility of using the developed apparatus and test technique has been demonstrated, there is a problem with extrinsic excitation of the test rotor which must be attenuated. Also, because of the need for verifying the analytical procedure which has been developed, it is recommended that the test apparatus and technique developed in this program be used to obtain the validating data. Specifically, it is recommended that:

1. An effort should be made to attenuate the spurious excitation reaching the test rotor by isolating the experimental apparatus from the vacuum tank and from the hydraulic drive motor.

2. For any further tests, relays shall be incorporated on the rotating side of the slipring assembly to switch from stress-monitoring signals to data signals. This would permit simultaneous recording of flapwise, chordwise, and torsional moments.

3. The analytical technique developed for the general rotor configuration should be programed for digital computation.

4. Several model rotor configurations should be designed, fabricated, and tested to obtain the experimental data necessary to verify the general analytical method that has been developed.

LITERATURE CITED

1. Targoff, W. P., THE ASSOCIATED MATRICES OF BENDING AND COUPLED BENDING-TORSION VIBRATIONS, Journal of the Aeronautical Sciences, Vol. 14, No. 10, October 1947.

2. Targoff, W. P., THE BENDING VIBRATIONS OF A TWISTED ROTATING BEAM, WADC Technical Report 56-27, Wright Air Development Center, Wright-Patterson Air Force Base, Ohio, December 1955.

3. Houbolt, J. C., and Brooks, G. W., DIFFERENTIAL EQUATIONS OF MOTION FOR COMBINED FLAPWISE BENDING, CHORDWISE BENDING AND TORSION OF TWISTED NONUNIFORM ROTOR BLADES, NACA Technical Report 1346, National Aeronautics and Space Administration, Washington, D. C., 1957.

4. Amer, K. B., PRELIMINARY RESULTS OF PERFORMANCE AND BLADE LOAD TESTS CONDUCTED ON A HIGH-SPEED HELICOPTER ROTOR MODEL, Report BB-1-13, Hughes Tool Company, Culver City, California, 31 March 1958.

DOCUMENT CONTROL DATA - R & D

(Security classification of title, body of abstract and indexing annotation must be entered when the overall report is classified)

1. ORIGINATING ACTIVITY *(Corporate author)*	2a. REPORT SECURITY CLASSIFICATION
Cornell Aeronautical Laboratory, Inc. Buffalo, New York	Unclassified
	2b. GROUP

3. REPORT TITLE

INVESTIGATION OF THE STRUCTURAL DYNAMICS OF HELICOPTER ROTORS

4. DESCRIPTIVE NOTES *(Type of report and inclusive dates)*

Final Report - June 1967 - October 1969

5. AUTHOR(S) *(First name, middle initial, last name)*

Raymond A. Piziali

6. REPORT DATE	7a. TOTAL NO. OF PAGES	7b. NO. OF REFS
April 1970	128	4

8a. CONTRACT OR GRANT NO. DAAJ02-67-C-0099	9a. ORIGINATOR'S REPORT NUMBER(S)
b. PROJECT NO. 1F162204A13904	USAAVLABS Technical Report 70-24
c.	9b. OTHER REPORT NO(S) *(Any other numbers that may be assigned this report)*
d.	CAL Report No. BB-2487-S-1

10. DISTRIBUTION STATEMENT

This document is subject to special export controls, and each transmittal to foreign governments or foreign nationals may be made only with prior approval of U. S. Army Aviation Materiel Laboratories, Fort Eustis, Virginia 23604.

11. SUPPLEMENTARY NOTES	12. SPONSORING MILITARY ACTIVITY
	U. S. Army Aviation Materiel Laboratories, Fort Eustis, Virginia

13. ABSTRACT

    An analysis and computational procedure has been developed for predicting the natural vibration modes and frequencies of rotor blade and hub systems. This method is capable of treating rotor systems which are of a general configuration and of including configuration variables which are normally neglected.

    An experimental apparatus and a testing technique have been developed for obtaining the experimental data necessary to verify the analytical procedure. This apparatus and the technique are capable of determining the natural vibration modes and frequencies of two-bladed rotor systems of a very general configuration while operating in the absence of aerodynamic loads. An initial test program with the apparatus was conducted to determine the adequacy of the equipment. The tests not only demonstrated the capability of the equipment and test procedure but also revealed a problem with extrinsic excitation of the test rotor at frequencies other than the shaking frequency. Recommendations are made for modifications to the system and the techniques in order to reduce the levels of these extraneous excitations and to minimize their effects.

    The computed and measured spanwise moment distributions and the corresponding natural frequencies are presented for six of the natural vibration modes of the test rotor at several rotational speeds. The theoretical and experimental results are compared and their differences are discussed.

14. KEY WORDS	LINK A		LINK B		LINK C	
	ROLE	WT	ROLE	WT	ROLE	WT
Helicopters						
Rotor Blades						
Dynamics						